SISSA
Scuola
Internazionale
Superiore di
Studi Avanzati

Neuroscience Area – PhD course in

Cognitive Neuroscience

Perception of the intensity and duration of a stimulus within a unified framework: psychophysics and underlying neuronal processing

Candidate:

Alessandro Toso

Advisor:

Mathew E. Diamond

Academic Year 2018-19

Table of Contents

General Introduction

When presented with a stimulus, our brain is able to generate parallel percepts from it. For instance, when we see a bird darting across the sky, we can at the same time perceive its color and the direction and speed of its motion. This is possible because the same stream of visual input is processed in parallel by separate pathways: the magnocellular pathway processes input coming from the M-cells in the retina, going through magnocellular cells in LGN, and then to MT area, and is mostly involved in motion perception. On the other hand, the parvocellular pathway processes input from P-cells in the retina going through parvocellular cells in the LGN, and then encodes color in area V4 (1). Parallel processing becomes more complex when one of the features to be processed is time. No specific receptors or neuronal pathways for the processing of time are known. It is a sense without its own sensory system. This means that the perception of the duration of a sensory stimulus could be either encoded within a dedicated neural circuit that behaves as a biological clock or pacemaker and receives external time markers (2), or could be extracted from the neural activity coming from sensory receptors sensitive to other features of the same stimulus. The aim of this work is to explore how the brain generates both the perception of stimulus features (in our case, vibration intensity) and the perception of the duration of the same stimulus.

All the experiments that are shown in the next chapters were inspired by previous work done in the Tactile Perception & Learning Lab. After developing a novel working memory task for rats (3), Fassihi et al. (4) discovered an intriguing effect of time on vibration perception. In rats trained to judge the relative intensities of two sequential vibrations (approximated by their amplitudes in units of mean speed), manipulation of vibration duration systematically and robustly affected perceived intensity – a vibration

that was extended in time (e.g. from 400 to 600 ms) was felt as stronger in intensity; a vibration that was contracted in time (e.g. from 400 to 200 ms) was felt as weaker in intensity. The effect held whether the first or second vibration of the pair was manipulated, or both. These experiments led our research group to realize, first hand, that there is not an invariance of perceived intensity. Rather, there is a time confound. Because the longer vibration feels stronger and the shorter feels weaker, one can imagine that a single value of perceived intensity could arise from a (theoretically) infinite combination of vibration amplitude and duration. In other words, in the two-dimensional space of vibration speed (abscissa)/duration (ordinate), a single quantity of perceived intensity does not arise as a vertical line associated with one value of speed, but is instead a curving contour through speed/duration space.

The confound between perceived intensity and stimulus duration, outlined above, seemed to uncover a real "uncertainty principle" governing that percept: the brain cannot be certain of actual vibration amplitude unless the vibration's duration is known. We speculated that the interaction between the two parameters might be symmetric – perhaps the perceived duration of a vibration is confounded by its actual amplitude.

The work shown in this thesis explores the relationship between the perception of duration and the perception of intensity of a vibration, and the brain mechanisms that lie behind it. Chapter I works out the details of the interaction between vibration amplitude and duration, showing (as speculated) that the confound is symmetric: perceived duration of a vibration depends on its speed, just as perceived intensity depends on its duration. This interaction is found both in rats and human subjects, suggesting that it is a fundamental characteristic of the mammalian somatosensory system. Quantification of their interaction allowed us to formulate a testable

computational model for the generation of both percepts, which we present in the chapter. Chapter II addresses the effect of stimulus history. Systems neuroscience has given considerable attention in recent years to the effects of preceding stimuli on the perception of the current stimulus. We now ask whether the interaction found in Chapter I extends to an interaction in the memory trace of recent stimuli: are the perceptual priors for vibration amplitude and duration mixed or separate? Chapter III begins to look for neuronal correlates of perceived duration, and its interaction with stimulus speed, in rats.

Overall, these results revealed a fundamental limit of our sensory system: the inability to generate independent representations of the duration and the intensity of a vibrotactile stimulus. This limit turned out to be an opportunity for understanding the neural coding of stimulus properties, and their durations.

Chapter I: A sensory integration account for time perception

Abstract

Sensory experiences are embedded within a feeling of the passage of time, yet the connection between stimulus perception and time perception remains unknown. The present study examines perceived time in sense of touch, with vibration intensity as the stimulus feature. We performed psychophysical tests in humans and rats, with the two species coinciding in all key findings. When the subject judged the duration of a vibration applied to the fingertip (human) or whiskers (rat), increasing intensity led to increasing perceived duration. Symmetrically, increasing vibration duration led to increasing perceived intensity. We reproduced the experimental results through a computational model where common sensory input is integrated by dual leaky integrators, an intensity integrator with short time constant and a duration integrator with long time constant. Experiment plus model offer a unified, quantitative framework wherein time is perceived through distinct, sequential operations – sensory coding and subsequent accumulation of sensory drive.

Introduction

Every sensory experience is embedded in time, and is accompanied by the perception of the passage of time. The coupling of the perception of the content of a sensory event and the time occupied by that event raises a number of questions: Do these percepts interact with each other? Do they emerge within separate neural populations? At which processing stage does the divergence occur? Which neuronal mechanism underlies the generation of two distinct percepts? The present study addresses these questions, focusing on stimuli in the range of < 1s. By comparing and contrasting human and rat psychophysics, we aim to uncover generalized mechanisms through which the brain represents the passage of time.

Two principal frameworks have been proposed to explain the neuronal bases of the feeling of time in short time scales: one framework posits a central clock, not connected with any specific sensory modality (2) while a second framework posits that the cortical circuit associated with each modality intrinsically encodes the passage of time for events within that modality (5, 6). There are also mixed models that argue for the existence of a core timing structure that integrates cortical activity in a context-dependent way (7, 8). To determine to what extent time perception is embedded within the coding of the stimulus itself, here we examine the relationship between the perceived features of a sensory event and the perceived duration of that same sensory event. As a stimulus feature, we focus on intensity. By assembling the remarkably similar results obtained in humans and rats, we propose a computational framework to account for the experimental findings.

Results

We carried out four experiments to investigate the effect of two tactile vibration features – intensity and duration – on the two percepts directly connected to those features. The experiments involved both human subjects, to whom stimuli were delivered to the left index fingertip, and rats, to whom the same vibrations were delivered to the whiskers on the right side of the snout (Fig 1A). Next, we embedded the experimental findings in a computational framework. This framework pointed, in turn, to candidate mechanisms for the integration of the vibration which we tested in a final set of experiments.

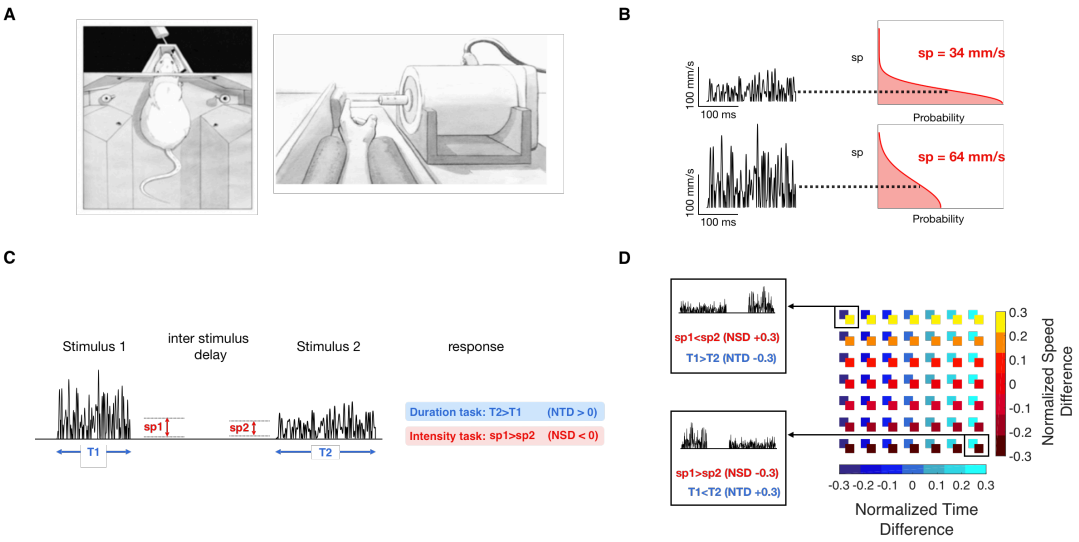

Figure 1. Experiment conditions and stimulus parameters.
A) Left: experiment setup for the rat, with its whiskers in contact with the vibrating plate. Right: Experiment setup for the human, with the left index fingertip in contact with the vibrating probe.
B) Schematic representation of the noisy vibration stimulations delivered by the motor. The left side shows two traces of sampled speed over time, and the right side shows the folded half Gaussian distribution to which each sample corresponds. The distribution's expected value is shown for each trace.
C) Representation of delayed comparison trial structure. Each trial consisted of the presentation of two noisy stimuli, with specified durations and mean speeds, separated by an interstimulus delay. The response was deemed correct according to the task rule: compare the relative durations (blue-shaded rule) or relative intensities of Stimulus 1 and 2 (red-shaded rule).
D) Representation of all possible stimulus intensities and durations presented to the subjects in the delayed comparison task. Each square in the matrix is color coded according to the NTD and NSD of the two vibrations presented. Selected NSD/NTD combinations from the top left and bottom right of the matrix are illustrated.

Experiment 1: Interaction of vibration speed and duration in a delayed comparison task

In Experiment 1 and all further experiments, each vibration was constructed by stringing together over time a sequence of velocity values, v_t, sampled from a Gaussian distribution. We consider the stimuli as speed rather than velocity since earlier work has shown that perceived intensity is mapped directly from vibration mean speed (4, 9). The distribution then took the form of a folded half-Gaussian (right side of Fig 1B) and the vibration can be considered a sequence of speed values, sp_t (left side of Fig 1B). A single vibration was thus defined by its nominal mean speed in mm/s, denoted sp (equivalent to the standard deviation of the Gaussian multiplied by $\sqrt{(2/\pi)}$). We consider *perceived intensity* to be the subjective experience related to objective intensity, or *sp*. Each stimulus was also defined by its duration in ms, T.

Experiment 1 employed a delayed comparison task (Fig1C). On each trial, subjects received two vibrations (Stimulus 1, Stimulus 2), separated by a fixed delay (500 ms for human subjects, 2 s for rats). The experiment was comprised of two distinct tasks: for *duration delayed comparison*, the subject had to judge which of the two stimuli was longer according to the relative *T* values ($T1 > T2$ or $T2 > T1$). For *intensity delayed comparison*, the subject had to judge which of the two stimuli was of greater intensity according to the relative mean speeds ($sp1 > sp2$ or $sp2 > sp1$). On trials when the parameter of interest was equal, the correct answer was assigned randomly. Each of 10 human subjects carried out both tasks, on different days, while individual rats were trained on a single task: 7 were *intensity rats* and 7 *duration rats*.

To constrain subjects to rely on working memory, we used a set of stimulus pairs

referred to as the stimulus generalization matrix (SGM; Figure 2) in which any value of $sp1$ could be followed by a larger or smaller $sp2$ and any value of $T1$ could be followed by a larger or smaller $T2$ (3, 10). Since neither stimulus alone provided the information necessary for a correct choice, both stimuli had to be attended to and utilized to solve the task.

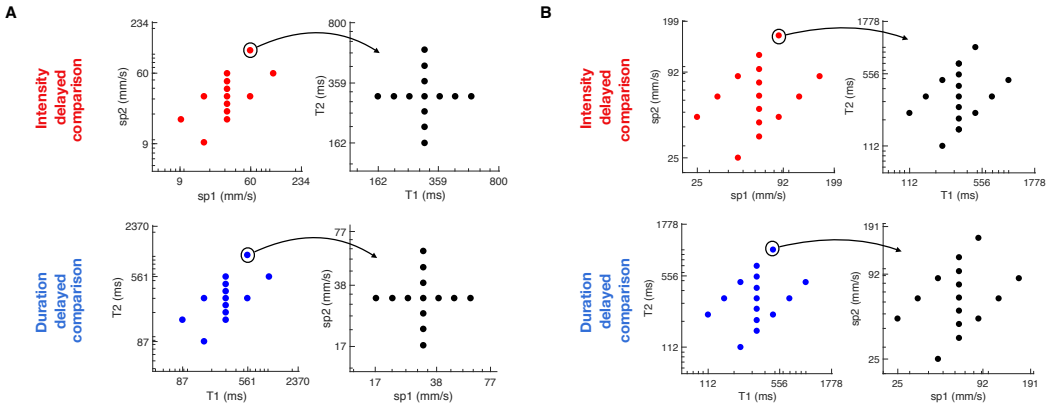

Figure 2. Stimulus generation matrix.
A) The upper row shows the matrices used for the intensity delayed comparison task, while the lower row was used for the duration delayed comparison task, for human subjects. Each trial's pair of task relevant feature values (sp in the intensity task, T in the duration task) was drawn uniform randomly from the set of pairs scattered in the leftmost plots. Each trial's pair of task irrelevant feature values (T in the intensity task, sp in the duration task) was drawn uniform randomly from the set of pairs scattered in the rightmost plots.
B) Same as A, for rat subjects.

In each trial, the two stimuli could differ in sp, in T, or both. To quantify stimulus differences, we designated two indices. The normalized speed difference (NSD), defined as $(sp2 - sp1)/(sp2 + sp1)$, ranged from -0.3 to 0.3 for both humans and rats, while the normalized time difference (NTD), $(T2 - T1)/(T2 + T1)$, ranged from -0.3 to 0.3 for humans and from -0.35 to 0.35 for rats. The stimulus set was constructed to present every possible combination of NTD/NSD values during the session (Fig 1D). Subjects received the same stimuli whether the task was to judge intensity or duration (see Figure 2 for the set of speed and duration values). Thus, any resulting difference in performance of the tasks could not be attributed to differences in tactile input.

To assess the effect of vibration speed on perceived duration, the upper panel of Fig 3A shows results from the duration delayed comparison sessions, with separate psychometric curves plotted for each value of NSD. In both species, there was a pronounced shift of the duration psychometric curves as NSD grows from negative to positive (dark red to yellow), signifying that a greater value of $sp2$ relative to $sp1$ increased the likelihood of the subject judging $T2 > T1$. The lower panel reveals the effect of vibration duration on perceived intensity. The substantial shift of the psychometric curves as NTD grows from negative to positive (dark blue to cyan) signifies that, in both species, a greater value of $T2$ relative to $T1$ increased the likelihood of the subject judging $sp2 > sp1$. We quantified the bias in perception as the slope of the linear correlation relating the change in the non-relevant feature to the change in the NTD or NSD value at which the subject judged Stimulus 1 and Stimulus 2 as equivalent – that is, the point of subjective equality (PSE).

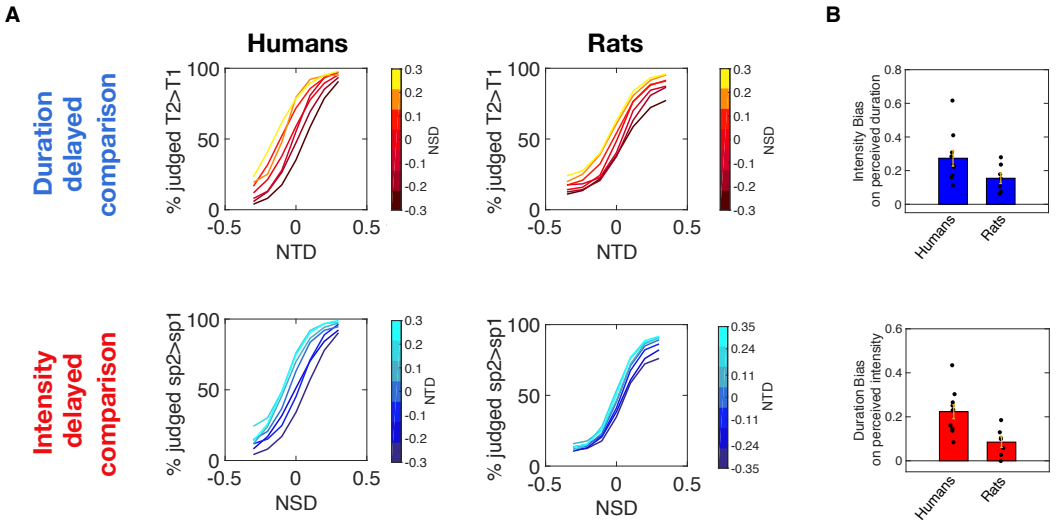

Figure 3. Interacting stimulus features in delayed comparison.
A) Psychometric curves for 10 humans (left) and 7 rats (right) in the duration (top) and intensity (bottom) delayed comparison tasks.
B) Upper plot: bias caused by the non-relevant stimulus feature, intensity, in duration comparison. Lower plot: bias caused by the non-relevant stimulus feature, duration, in intensity comparison. In all plots, dots represent single subjects, bars represent mean of biases across subjects, while error bars represent the standard error of the mean across all subjects. The median value of each bias was significantly different from zero (humans: $p = 0.002$ for both intensity and duration bias, rats: $p = 0.0156$ for intensity bias, $p = 0.032$ for duration bias, Wilcoxon signed rank test).

The sign of the bias was consistent across subjects both in the duration task (Fig 3B, upper panel) and in the intensity task (Fig 3B, lower panel). The median value of each bias was significantly different from zero (humans: $p = 0.002$ for both intensity and duration bias, rats: $p = 0.0156$ for intensity bias, $p = 0.032$ for duration bias, Wilcoxon signed rank test, Figure 4).

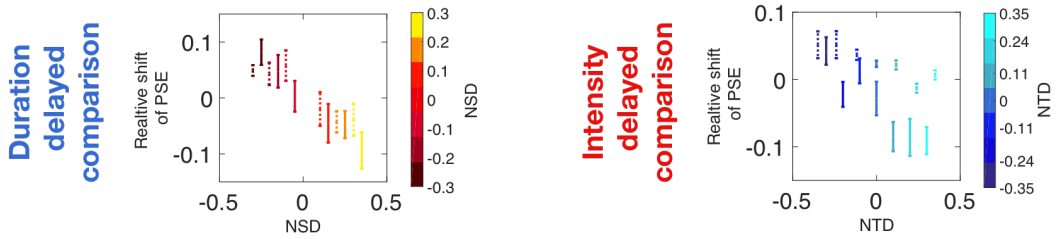

Figure 4. Quantification of the perceptual biases.
Left panel: Duration delayed comparison task. Each bar is the standard error, centered on the mean, of the psychometric curve PSE for each NSD value across all 10 human subjects (solid) and all 7 rats (dashed), relative to the PSE for the $NSD = 0$ condition. Right panel: same analysis for intensity delayed comparison task. The downward slanting distribution of data indicates that, for the duration task, PSE shifted to the left as NSD grew while, for the intensity task, PSE shifted to the left as NTD grew.

In our experimental design, the perception of Stimulus 1 is dissociated from any decisional process since the choice can be generated only after presentation of Stimulus 2. Variations in the non-relevant feature affected choices in the same way whether applied to Stimulus 1 or Stimulus 2 (Figure 5).

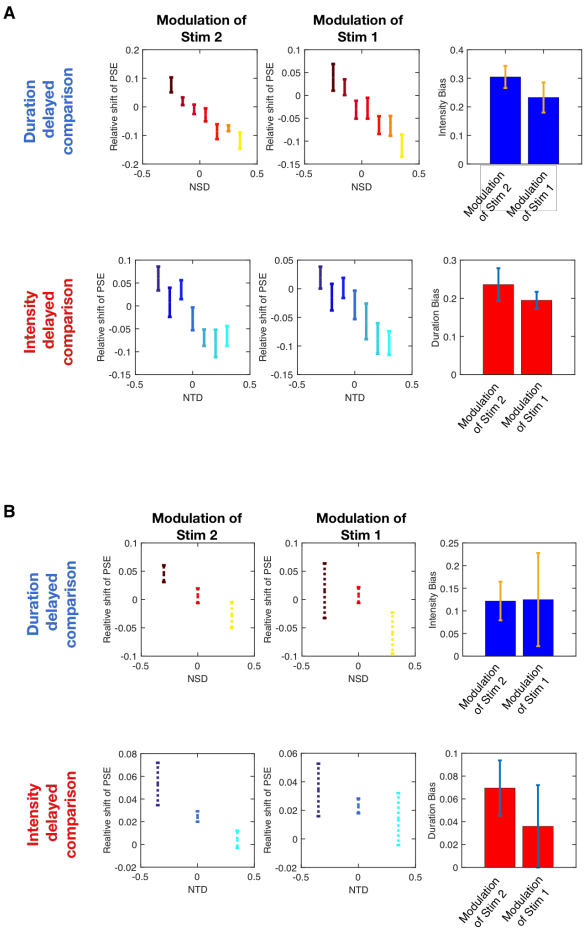

Figure 5. Effect of variations in the non-relevant feature whether applied to Stimulus 1 or Stimulus 2

A) Upper row: Each bar is the standard error, centered on the mean, of the psychometric curve PSE for each NSD value across all 10 human subjects, relative to the PSE for the $NSD = 0$ condition, when varying the non-relevant feature of Stimulus 2 (left panel) or Stimulus 1 (middle panel), for the duration delayed comparison task. Right panel shows bias caused by the non-relevant stimulus feature, intensity, in duration comparison, for both conditions. Dots represent single subjects, while error bars represent the standard error of the mean across all subjects. Lower row: symmetrical analysis for intensity delayed comparison task.

B) Same analysis as in B, for 7 rats doing duration delayed comparison (upper plots), and 7 doing intensity delayed comparison (lower plots).

The biases were better explained as a horizontal psychometric curve shift than a vertical shift (Figure 6 and Methods). On this basis, we interpret the observed shift of psychometric curves as a perceptual phenomenon, not a decisional bias.

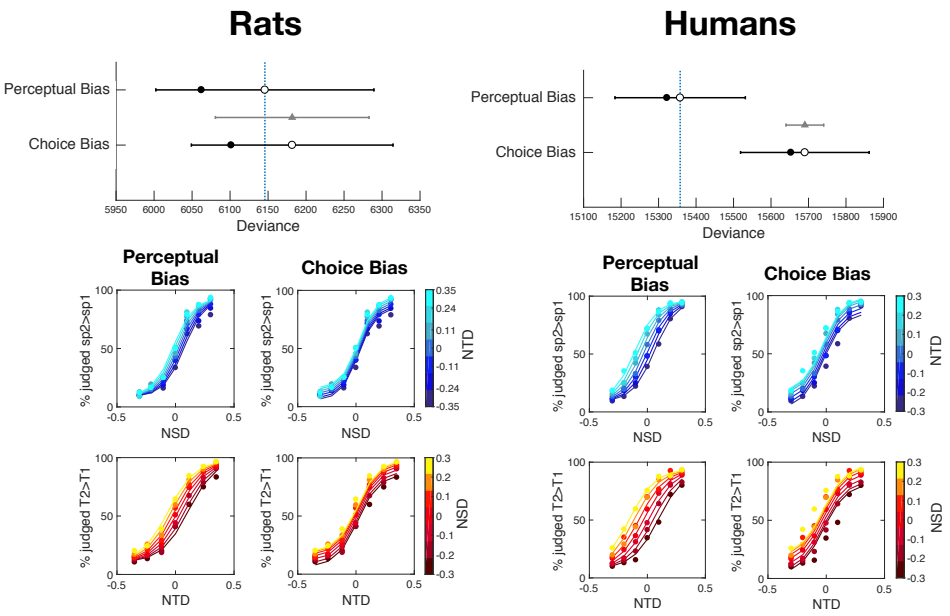

Figure 6. Characterization of the observed bias as horizontal versus vertical curve shifts. The left column shows the analysis of the rat data; right column human data. The uppermost plot shows the in and out of sample deviance estimated by WAIC using the perceptual (horizontal) and choice (vertical) biasing models. Empty dots show the out-of-sample deviance (WAIC) of each model, the filled dots show the in-sample deviance (WAIC - 2 pWAIC) of each model. The black bars show the WAIC standard deviation of each model. The gray triangle shows the model's WAIC difference, and the bar represents the WAIC difference's standard deviation. Standard deviation is smaller, due to correlations between the computations of WAIC for each model. The middle row shows the data in the duration delayed comparison task (dashed lines) along with each model's prediction (solid curves). The bottom row shows the data in the intensity delayed comparison task (dashed lines) along with each model's prediction (solid curves). The columns correspond to either the perceptual or choice bias models. Much better fit is obtained in all cases by the perceptual (horizontal) shift model.

In short, the main finding of Figure 2 is that subjects (humans and rats) readily extracted the stimulus feature required by the task, be it duration or intensity, but were biased by the non-relevant feature (speed or duration, respectively).

Experiment 2: Interaction of vibration speed and duration in a direct estimation task

In the second experiment, perception was measured through "*direct intensity estimation*" and "*direct duration estimation*". On a given trial, the subject received a single vibration, defined (as before) by *sp* and *T*. A slider image appeared on the monitor 500 ms after the end of the vibration (Fig 7A). By choosing the mouse-click

position along the slider, the subject reported the perceived intensity of the vibration or else the perceived duration of the vibration. Delayed comparison (Experiment 1) involves a number of steps: Stimulus 1 encoding, storage in working memory, Stimulus 2 encoding, and comparison of current Stimulus 2 to the memory of Stimulus 1. The persistence of an intensity/duration confound in direct estimation would strengthen the argument that mixing emerges within the initial percept, before the percept is committed to or retrieved from working memory. Moreover, the brevity of direct estimation trials enabled more trials per session and thus a wider-range coverage of *sp* and T, addressing the consistency of the confound across different stimulus values.

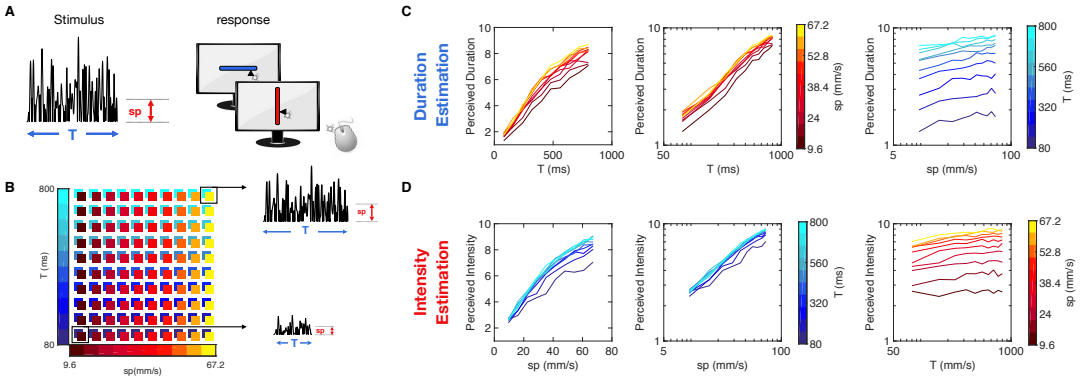

Figure 7. Interacting stimulus features in direct estimation.
A) Experimental setup. 10 Human subjects received a single noisy vibration and reported perceived duration or intensity by mouse-clicking on a computer screen.
B) Stimulation matrix. The vibration duration and mean speed was randomly picked from the set of (*T, sp*) combinations represented by the colored squares. Two sample stimuli from the upper right and lower left of the matrix are illustrated.
C) Duration estimation results. The left and middle plots show the median perceived duration as a function of true duration, first in a linear-linear scale and then in a log-log scale. The right plot shows the median perceived duration as a function of stimulus intensity in a log-log scale, with each color denoting one actual duration.
D) Intensity estimation results, following the same convention as panel C).

The slider did not display any landmarks, numbers, or ticks. To help subjects create two separate subjective scales, the orientation of the slider was specific to the task (e.g. horizontal for the intensity session and vertical for duration session), with

task/orientation association randomized among subjects. The test stimulus set was comprised of 10 durations (linearly spaced from 80 to 800 ms in 80 ms steps) and 10 mean speed values (linearly spaced from 9.6 mm/s to 67.2 mm/s in 6.4 mm/s steps). All 100 possible combinations of speed and duration were presented in each session (Fig 7B).

Figure 3C, left panel, shows the results of direct duration estimation, averaged across subjects. Perceived duration increased not only with *T*, as expected, but also with *sp* (designated by colors from dark red to yellow), confirming the main result from Experiment 1. By plotting the same data in a log-log scale (Fig 7C, middle panel), the relationship between objective and perceived duration becomes linear, with each step in *sp* causing an upward shift of the line.

Within the same data set, the speed-induced bias is highlighted by plotting reported duration as a function of *sp* separately for each stimulus duration (Fig 7C, right panel, and Figure 8). With log-log axes, the result is a linear relationship, with a nearly invariant slope across durations. The fact that the plots are linearized by converting to log-log axes confirms the nonlinear relationship between perceived duration and *sp*.

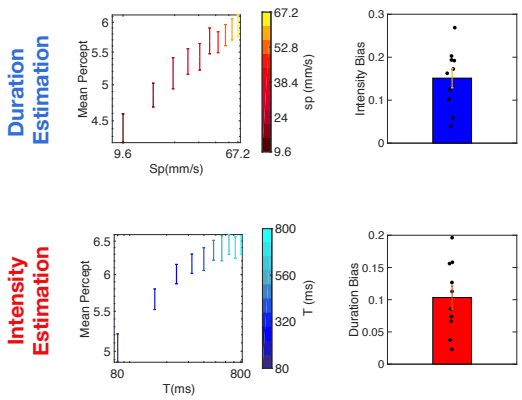

Figure 8. Quantification of the perceptual biases in direct estimation.
Panels on the left show how the mean percept, averaged across all values of the relevant feature, changes with increasing values of the non-relevant feature in log scale, for the duration and intensity estimation sessions. On the right, the Intensity bias and the Duration bias, calculated as the linear coefficient between mean perception and different values of the non-relevant feature of stimuli in log scale, across all 10 subjects. The distribution of biases is significantly different from zero (Wilcoxon signed rank test, $p = 0.002$ for both tasks).

Figure 7D, left panel, shows the results of direct intensity estimation, averaged across subjects. Perceived intensity increased not only with *sp*, as expected, but also with *T* (from dark blue to cyan). Thus, longer stimuli were perceived as stronger in direct estimation, as found earlier in delayed comparison. Again, in a log-log scale (Fig 7D, middle and right panels), the data reveal a nonlinear relationship between *sp* and perceived intensity, and between *T* and perceived intensity.

Experiments 3 and 4: Candidate models to explain duration/intensity interaction

Next, we asked which computations the brain might use to construct the two percepts from a common stream of sensory input. Neurons in rat somatosensory cortex precisely encode instantaneous speed (4), and analogous coding mechanisms exist in primates (11). Because the vibration was stochastic, no instantaneous value could provide an intensity estimate for the entire vibration. A subject could, in theory, achieve optimal

performance in the intensity task by linearly integrating the output of speed-coding neurons over the entire vibration and then normalizing the integrated value by elapsed time. The denominator of this normalizing operation – elapsed time – could itself be the basis of the estimate of stimulus duration. But this computation would not explain the observed perceptual confound between the relevant and the irrelevant stimulus features, inasmuch as the time counter in the normalization is conceived of as an independent term.

As an alternative, we posit that the brain constructs the percept of both stimulus duration and stimulus intensity by nonlinear accumulation of the sensory signal over time. A renowned model of accumulation in perceptual decision-making is the leaky integrator, in which some form of input is summated across time (12).

Leaky integration of sensory input can be formulated as:

$$C\frac{d\Upsilon}{dt} = -\lambda\Upsilon + f(sp_t, t) \quad (1)$$

where Υ is the percept, $f(sp_t, t)$ is the external drive to the integrator, λ is the leak rate and $\frac{C}{\lambda} = \tau$ specifies a time constant of integration.

We assume that the external drive to the integrator is made up of the tactile sensory input and added noise. We also assume the sensory signal follows a power law with instantaneous speed input raised to exponent α (see below). Furthermore, we assume additive normally distributed noise, ξ, that is independent of the stimulus and might

even originate through a different sensory modality. Thus, external drive can be specified as:

$$f(sp_t, t) = sp_t^{\alpha} + \xi \quad (2)$$

Inclusion of the exponent α is based on the nonlinear effect of sp on both perceived duration and perceived intensity, as can be observed in Figure 7C-D. Furthermore, a power law relationship between sp and perceived intensity is consistent with the classical work of Stevens (13)

It can be readily appreciated that a leaky integrator of this general form will account for the main findings in a qualitative sense: both percepts will increase monotonically with sp and with T, thus causing a confounding perceptual crosstalk between the two stimulus features.

In order to constrain the model before setting out to fit the results of humans and rats, we posed two questions. First, is a single integrator at work, one which operates with parameters tuned on each trial according to the current task (Model 1: Fig 9A, left panel)? Or do two integrators, characterized by different parameter values, operate in parallel, with the subject retrieving the percept from the task-specified integrator (Model 2: Fig 9A, right panel)?

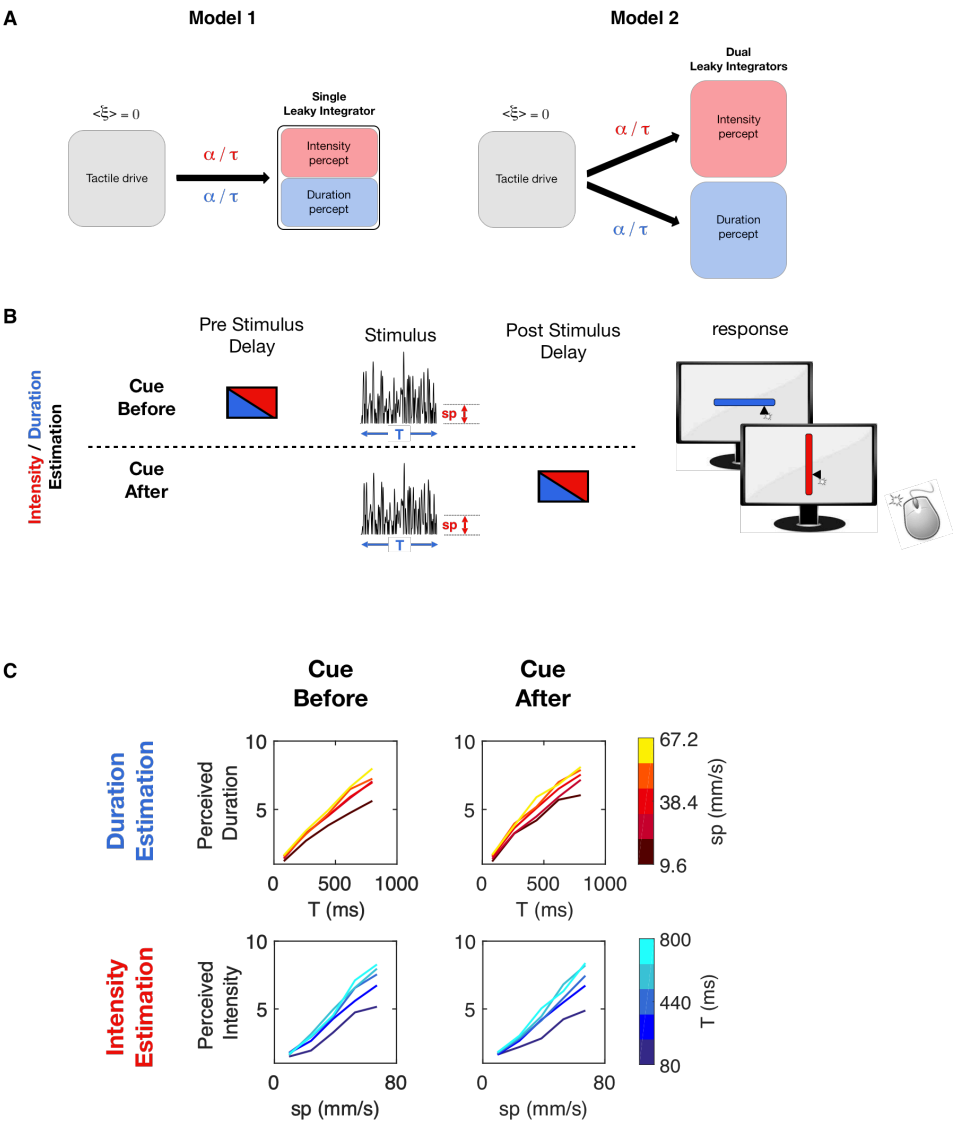

Figure 9. Test of single versus dual integrators.
A) Alternative hypotheses for the leaky integration process underlying the construction of both intensity and duration perception. Model 1 is represented by a single integrator that receives tactile drive but switches between task-specific values for the parameters α and τ. Model 2 is represented by dual integrators that receive the same tactile drive. Each integrator has task-specific values for the parameters α and τ.
B) Schematic representation of cue-before versus cue-after direct estimation experiment. On half the trials, the cue providing trial instruction (symbolized by red or blue box) was provided before the vibration (above dashed line), and on the remaining half, the cue was presented after the vibration (below dashed line).
C) Comparison of median perceived duration (upper row) and median perceived intensity (lower row) when the cue was presented before (left column) versus after (right column) the vibration, for 8 human subjects. Time of cue did not affect estimation.

To select between the two models, we designed Experiment 3, in which human subjects performed direct stimulus estimation, however the instruction cue indicating which

stimulus feature to report was given to the subject either before or after stimulus delivery (Fig 9B). According to the single integrator model of Fig 9A, performance would be good on trials with cue delivery prior to vibration onset, inasmuch as the integration parameters could be correctly tuned for the relevant feature. Performance would be lower with cue delivery after the conclusion of the stimulus inasmuch as the integration parameters could not be optimally "pretuned" prior to stimulus presentation. According to the dual integrator model of Fig 9A, performance would be nearly the same on trials with cue delivery prior to vibration onset versus cue delivery after vibration conclusion. This is because the two integrators operate in parallel, each with optimized parameters. The results, illustrated in Fig 9C, show that performance was not significantly affected by cue delivery time (Kruskal Wallis test: for duration estimation $p = 0.83$; for intensity estimation $p = 0.75$; see Figure10). Experiment 3 thus supports the dual integrator model.

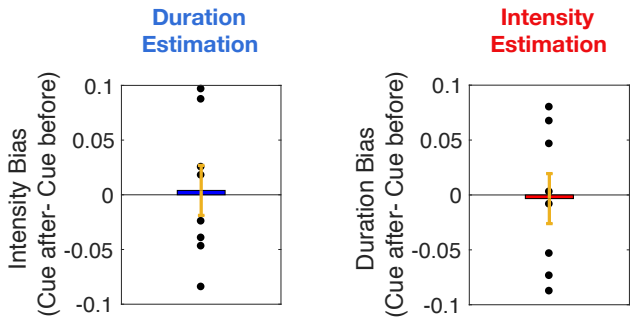

Figure 10. Observed bias in Experiment 3.
Left plot: Bias caused by the irrelevant feature (sp) in the duration estimation task. Each dot corresponds to a single subject, while the bar is the mean across subjects. Right plot: Bias caused by the irrelevant feature (T) in the intensity estimation task. Each dot corresponds to a single subject; the bar is the mean across all 8 subjects. In both plots, orange error bars are standard error of the mean across subjects. Cue delivery did not affect the bias of the non-relevant feature (Kruskal Wallis test: for duration estimation $p = 0.83$; for intensity estimation $p = 0.75$).

If two integrators are at work, in what way do they differ? It is simplest to envisage the integrator underlying the intensity percept as highly sensitive to sp by virtue of large α and minimally affected by temporal accumulation by virtue of small τ (Model 2A: Fig 11A, left panel).

The integrator underlying the duration percept would be expected to operate with the parameters tuned in the opposite direction (small α, large τ). However, as an alternative, the parameter α may be an intrinsic property of the sensory representation, reflecting task-independent coding of vibration speed in primary sensory cortex (Model 2B: Fig 11A, right panel).

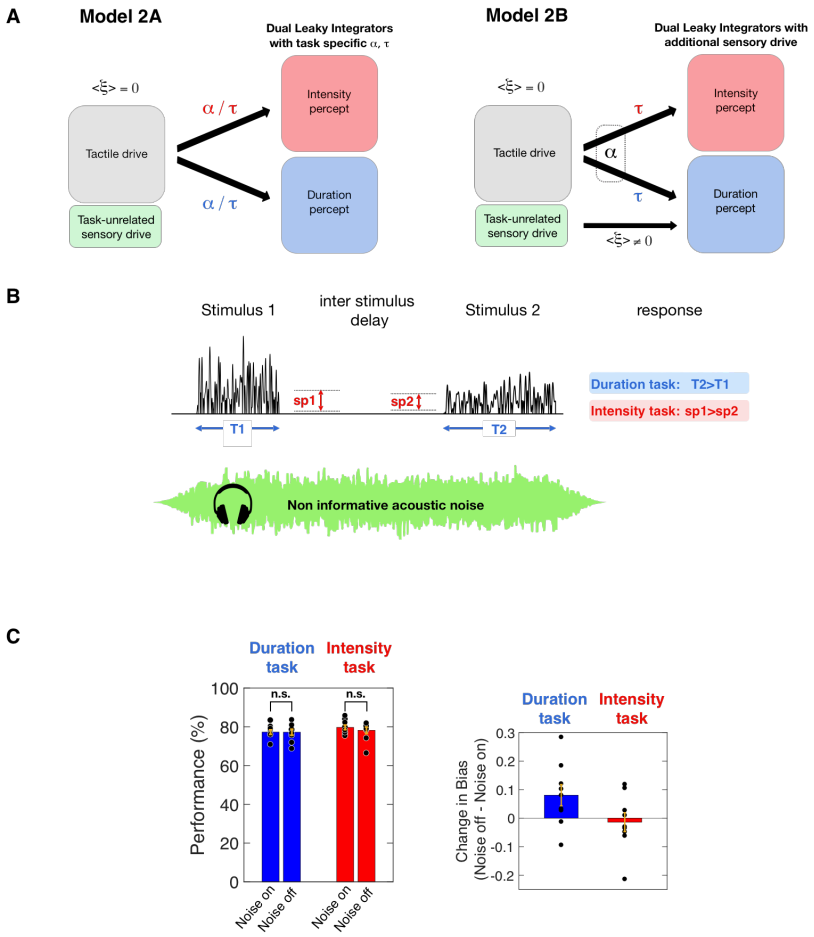

Figure 11. Test for integration of task-unrelated sensory drive.
A) Alternative hypotheses for the leaky integration process underlying construction of both intensity and duration perception. Model 2A is represented by dual integrators with task-specific values for the parameters α and τ and no input from task-unrelated sensory drive. Model 2B is represented by dual integrators that share α but have task-specific values for τ. This model also posits input from task-unrelated sensory drive.
B) Schematic representation of a trial with non-informative acoustic noise delivered through headphones.
C) Upper plot: bars denote mean performance on the duration and intensity tasks for trials with noise on and off, across 9 human subjects. Each dot represents a single subject's mean performance. Orange error bars are standard error of the mean across subjects. The presence or absence of noise did not affect accuracy (Kruskal-Wallis test, $p = 0.72$ for the duration task, $p = 0.66$ for the intensity task) Lower plot: Effect of acoustic noise on the bias caused by the task-irrelevant feature. For the duration task, the presence of noise reduced the bias normally caused by intensity (one sample, one-tailed Wilcoxon signed rank test, $p = 0.0273$). For the intensity task, noise did not affect the bias caused by duration (one sample, one-tailed Wilcoxon signed rank test, $p = 0.5$). Each dot represents a single subject's bias difference, whilst the bar represents the average across subjects. Orange error bars are standard error of the mean across subjects.

If α resides in a common input and assumes the same value for the two integrators, how can separate percepts be formed? The basic framework (Equations 1-2) includes a noise term, ξ, as one component of the external drive. In Model 2B, the two integrators differ

in their sensitivity to task-irrelevant noise: the percept of duration (but not intensity) could be affected by noise carried within a sensory modality other than that whose duration must be judged. This hypothesis is motivated by the fact that time perception is a supramodal process; all sensory channels are connected with the same sense of time (14). To select between the two models of Figure 11A, in Experiment 4 human subjects again performed the delayed comparison task; in half the trials, the tactile stimuli to be judged were accompanied by non-informative acoustic noise played through headphones (Fig 11B). Each session tested one percept, either intensity or duration.

According to Model 2A, task dependence originates in the readout of the appropriate integrator, with its specific value of τ, and the presence of irrelevant acoustic noise would have no effect on psychometric curves. According to Model 2B, acoustic noise would selectively affect the percept of duration. Because the total, integrated external drive (Equation 2) includes sp raised to the power α plus noise, ξ, the addition of acoustic noise would increase the relative contribution of ξ compared to that of sp. The final effect would be to dilute the *sp*-dependent bias in duration perception.

The presence or absence of noise did not affect accuracy (Fig 11C upper panel; Kruskal-Wallis test, $p = 0.72$ for the duration task, $p = 0.66$ for the intensity task). To quantify the bias induced by the non-relevant feature on the perception of the relevant feature, as before we measured the shift of the PSE of psychometric curves caused by the value of the non-relevant feature (see Methods). The lower panel of Figure 11C, shows that in the duration comparison task, the bias induced by intensity was significantly different between the "noise on" and "noise off" conditions (one sample, one-tailed Wilcoxon signed rank test, $p = 0.0273$), whereas in the intensity comparison task the bias

induced by duration was *not* significantly different between the "noise on" and "noise off" conditions (one sample, one-tailed Wilcoxon signed rank test, $p = 0.5$). These results are consistent with the predictions made by Model 2B (Fig 11A).

Parameter values in the model

From the constraints uncovered through Experiments 3 and 4, the working model of Equations 1-2 can now be better specified. The perception of intensity is based on the accumulation of sp_t^{α} with a task-specific decay time constant, τ_I. Task non-specific noise, ξ_I, is assumed to be white, zero mean, and to have a variance equal to σ_I^2. Thus

$$C_I \frac{dY_I}{dt} = -\lambda_I Y_I + f_I(sp_t, t) \tag{3}$$

$$f_I(sp_t, t) = sp_t^{\alpha} + \xi_I \tag{4}$$

The perception of duration is based on the accumulation of sp_t^{α} with task-specific decay time constant τ_D, and a non-specific noise term, ξ_D, whose mean, μ_D, may be non-zero; noise variance is σ_D^2. The sensitivity to sp and α is equivalent to that underlying intensity perception, while τ_D is specific to the duration integrator. Thus

$$C_D \frac{dY_D}{dt} = -\lambda_D Y_D + f_D(sp_t, t) \tag{5}$$

$$f_D(sp_t, t) = sp_t^{\alpha} + \xi_D \tag{6}$$

Except for α, all model parameters are independent between intensity and duration sessions. To test its validity, the model was fit to the results of humans (Fig 12A-B left panels) and rats (Fig 12C left panels). Points are experimental data and the curves are simulations after parameter setting. Figure 12A shows the fit on the human data for the delayed comparison task, Figure 12B shows the fit for the human direct estimation task data and Figure 12C shows the fit for the rat delayed comparison task data. In every panel, the left plot shows the aggregated data across all subjects (points) and the mean across the predictions of the corresponding fits (curves). In all three sets of plots, the model's simulations closely overlie the data points.

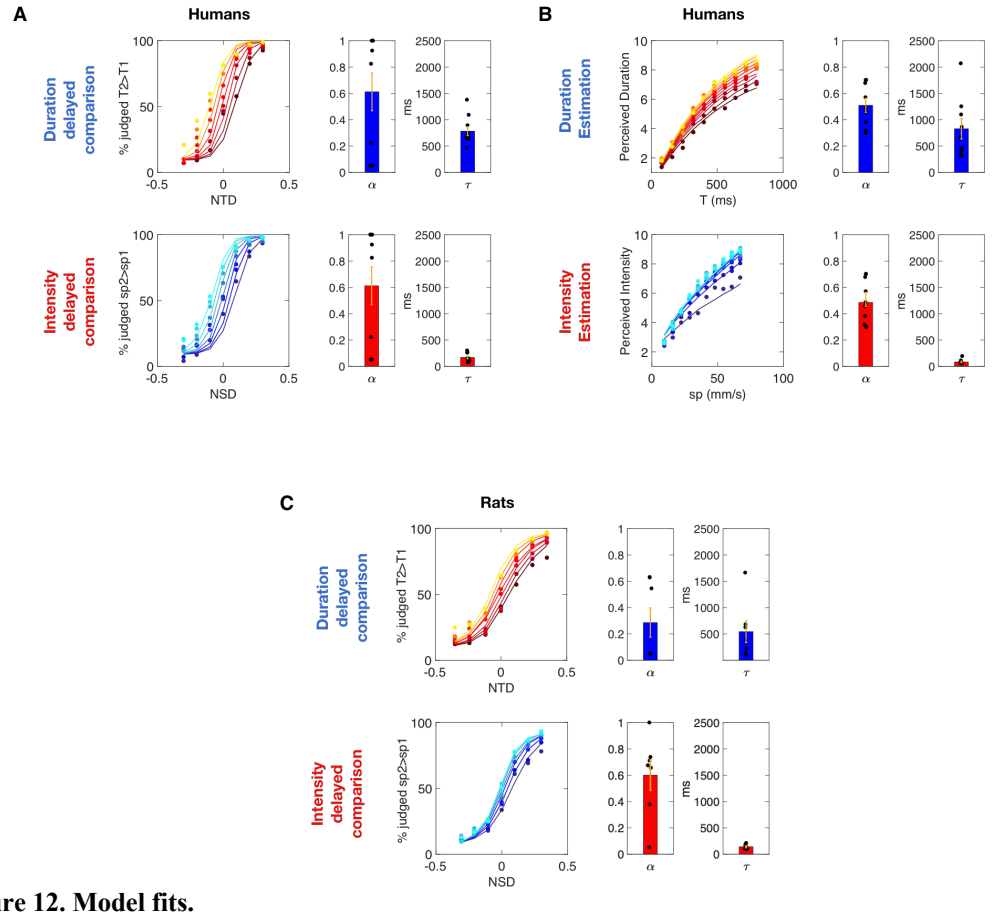

Figure 12. Model fits.
In all panels the upper plots correspond to duration delayed comparison or estimation tasks, while lower plots correspond to the intensity delayed comparison or estimation tasks. The right plot of each panel gives the parameter values of α and τ. Dots correspond to the parameter values of an individual subject, and the bar indicates the mean across subjects. Orange error bars are standard error of the mean across subjects.
A) Fit for the human delayed comparison task.
B) Fit for the human direct estimation task.
C) Fit for the rat delayed comparison task. The color codes in A and C are the same as in Figure 2; the color code in B is the same as in Figure 3.

The plots on the right of each panel show the fitted values of the parameters α and τ for the duration (top) and intensity (bottom) sessions. The points are individual subjects and the bars are the group means. For the human data, the parameter fits were done independently on the delayed comparison and direct estimation tasks; the fitted values of α and τ were comparable for the two tasks. The larger is the time constant of integration, the greater will be the effect of the overall duration of the input onto the final output. As expected, the time constant of integration, τ, is greater for the extraction of duration than for the extraction of intensity for both tasks and both species.

Furthermore, the model captures the observed confound between intensity and stimulus duration for both tasks and both species. These results show that by tuning the leakiness of the integration ($1/\tau$), the same mechanism could account for duration perception and intensity perception.

As individual rats only performed a single delayed comparison task (either duration or intensity), it is impossible to fit α and μ_D simultaneously. Thus, we chose to fix $\mu_D = 0$ and leave α as a free effective parameter, whose value was fitted (equivalent to Model 1 of Fig 9). For human data, the quality of the fit for the model using distinct α values for intensity and duration tasks is the same as the model where α is shared (Figure 13).

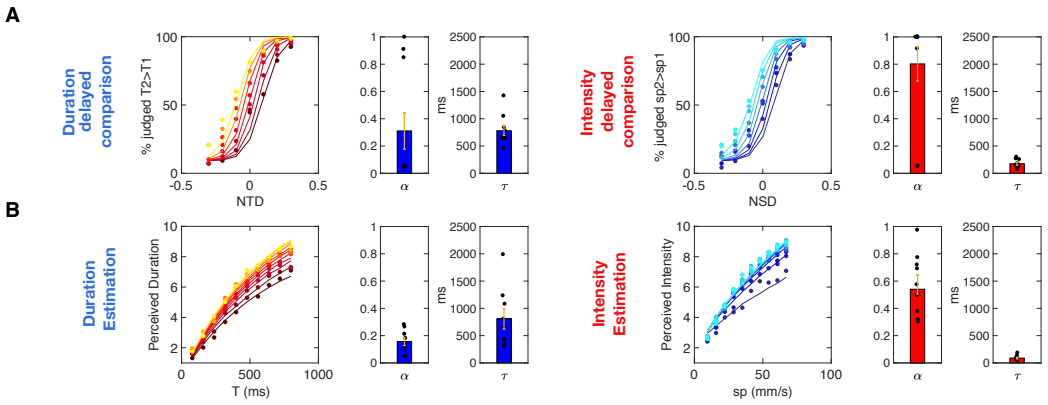

Figure 13. Fits obtained using Model 2A.
In this model, depicted in Figure 5, α values are set separately for duration and intensity perception. The figure layout and color codes match those used in Figure 6.
A) Delayed comparison experiment; on the left, duration delayed comparison and on the right, intensity delayed comparison.
B) Direct estimation experiment; on the left, duration estimation and on the right, intensity estimation.

The τ values are comparable across the two models but the α values are not. The model with shared α on average has a value in between the α_D and α_I of the model with two separate α parameters. Thus, it is not possible to make a direct comparison between the fitted α for humans and rats. However, we can risk a comparison of the τ values. In both species, τ_D (386 ± 205 ms for rats, 669 ± 91 ms for humans) is about 3 to 4 times

larger than τ_I (131 ± 17 ms for rats, 148 ± 68 ms for humans). The fact that the same form of model, with a similar ratio of task-dependent time constants, has explanatory power leads us to propose that the mechanism underlying the formation of the two percepts is shared across both species.

The two integrators are not a literal portrayal of a physiological mechanism, but are a characterization of some network property that participates in the conversion of the vibration sensory code to the conscious experience of intensity and duration. The dual integrators constitute a unified framework inasmuch as both key features of the stimulus representation – the coding of vibration speed and its distribution through time – contribute to both integrators. The main features that distinguish the two integrators are: (i) the leak time constant, τ, by which sensory input is accumulated over time – leakiness is lower for duration perception compared to intensity perception, and (ii) the degree to which stimulus-unrelated input, ξ, is integrated – task-irrelevant stimulation contributes to duration perception but not to intensity perception.

Discussion

A single vibration presented to the sensory system generates two parallel percepts: the perception of its intensity and the perception of the time it occupies. The study was motivated by a number of questions. Do these percepts interact? Experiment 1 and Experiment 2 show that neither rats nor humans are able to generate independent representations of stimulus intensity and stimulus duration.

In earlier work based on human psychophysics, an increase in perceived intensity with increased stimulus duration has been reported in touch (4, 15), audition (16–18) and vision (16). Separately, an increase in perceived duration with intensity has been reported in touch (19), audition (20) and vision (21). The dependence of perceived intensity on stimulus duration was thought to arise from a temporal integration process: the sensory system summates input over time linearly, following Bloch's Law (22), or else as a nonlinear weighted sum (4, 18, 23). On the other hand, the dependence of perceived duration on stimulus intensity has been interpreted in a separate framework, that of internal clock models, which posit that a central clock keeps track of time (2). In this framework, the increase of perceived duration with increasing stimulus intensity is an attentional phenomenon, where a stronger stimulus leads to an increase in arousal, resulting in augmented speed of the central clock (24, 25). Opposing the view of two independent confounds, our experiments show that the influence of stimulus duration on perceived intensity and the influence of vibration intensity on perceived duration are inextricable phenomena. Furthermore, by uncovering both perceptual confounds from a single set of stimuli, our experiments made it possible to configure perceived intensity and perceived duration within a unified framework.

A further question was, do the percepts emerge within separate neural populations? Experiment 3 argues that the two percepts are generated through two computations that operate in parallel. We speculate that two different neuronal populations receive a common input, and the final state of these populations can be interrogated separately in order to produce the required judgment (Model 2 of Figures 9 and 11).

At which stage of processing do the neuronal representations of the sensation and its duration diverge? Our results suggest that neurons in the common input to the two integrators encode vibration by a power function (13) of speed raised to an exponent, α. From the properties of sensory coding of vibration amplitude in primary and secondary somatosensory cortex in primates (10) and rats (26, 27), we suggest that they constitute the common input to downstream regions at which distinct percepts emerge.

Next, we asked which neuronal mechanism underlies this divergence. On the basis of the model's robustness in simulating psychophysical results, we propose that leaky integration of sensory drive is the underlying mechanism. Specifically, we posit that two separate integrators operate in parallel (Experiment 3), and that they differ not only in their leak time constant, but also in their permeability to stimulus-unrelated input (Experiment 4). Our results derive from the case in which the time that must be measured is the sensory stimulus itself. In conditions where the time to be judged lies between two discrete events — a start and stop signal, for example — the integration mechanisms remain to be worked out. Of course, leaky integration is not equivalent to specifying a physiological process, but it can serve to alert us as to which network properties should be sought in future physiological work. For instance, the model makes

the straightforward prediction that the neuronal population implementing the readout of stimulus duration must be modulated by stimulus intensity.

The hypothesis that perceived duration is achieved through leaky integration of stimulus-related and stimulus-unrelated sensory input is particularly relevant to the debate on models for the perception of time in the scale that ranges from tens of milliseconds up to a few seconds. Our results are in accordance with the idea that sensory-specific areas contribute to time perception (6, 28), but are harder to reconcile with the amodal central clock theory (2). However, in our framework primary sensory areas do not encode time by themselves, but serve instead as the drive to downstream areas that accumulate input with the appropriate time constant. Primary somatosensory cortex is characterized by a short intrinsic timescale, and does not show temporal integration (4, 29, 30). Our hypothesis is in line with other work that assume temporal integration processes behind the encoding of the passage of time (31, 32).

The “state-dependent networks” model (33) and the “striatal beat frequency” model (34) have not yet been challenged as to the dependence of time perception on stimulus intensity. In the first type of model, time is encoded by the evolving temporal pattern of activity of a recurrent neural network, so that almost any network could in principle represent the elapsed time without the need of an explicit representation of duration (33, 35). In the second type of model, time is encoded by a pattern of relative phases of different oscillators, thought to be present in both thalamic and cortical neural activity, and is read out by striatal neurons, which act as coincidence detectors. Both models would explain the influence of stimulus intensity on perceived duration as an increase or decrease of the speed by which the activity of the connected neuronal population

evolves in time or else by which the oscillators follow the pattern of their relative phases. Whether intensity-dependent modulation could be reliably implemented in these models is not known.

Temporal leaky integration of sensory information can be performed by a recurrent neural circuit (36–39). Recurrent neural circuits have been widely used to explain decision-related neuronal activity in areas of the brain such as lateral intraparietal cortex (LIP) (40), premotor cortex (41), prefrontal cortex (42), and dorsal striatum (43, 44). The different level of leakiness for intensity versus duration could be achieved by a difference in the strength of recurrent connections in the network, and also on the different levels of background input (36, 45, 46). The finding of a hierarchical ordering in the timescales of intrinsic fluctuations in the cortex (29), growing from posterior to anterior, opens the possibility that circuits with longer intrinsic timescales (greater τ in the terms of the present work) could subserve as a time readout because they would accumulate sensory information more slowly than circuits with shorter intrinsic timescales.

Overall, through both psychophysical experiments and computational modeling, we argue that the perception of stimulus intensity and stimulus duration are closely related one to another, and are generated by parallel and overlapping computations. Our study replicates this perceptual confound in non-humans for the first time, to our knowledge, opening the way for direct neurophysiological measures and manipulations.

Methods

Human and rat subjects

Thirteen healthy human subjects (age range 22–35 yrs) were tested in the delayed comparison task, after giving their informed consent. Only subjects that reached better than 70% performance in both intensity and duration delayed comparison (10 out of 13) were included in the analysis. The same 10 subjects were then recruited for the direct estimation tasks. All subjects were recruited on-line through the SISSA Sona System. (https://sissa-cns.sona-systems.com/). The number of subjects was 8 in Experiment 3 and 9 in Experiment 4. Protocols conformed to international norms and were approved by the Ethics Committee of SISSA (protocol number 6948-II/7).

14 male Wistar rats (Harlan, San Pietro al Natisone, Italy) were housed individually or with one cage mate and maintained on a 14/10 light/dark cycle. Daily access to water was restricted to promote motivation in the behavioral task, yet weight gain followed a standard Wistar-specific curve, indicating that the quantity of water obtained during training and testing was comparable to the ad lib quantity. After each session, rats were placed for several hours in a large, multistory enriched environment with other rats. Protocols conformed to international norms and were approved by the Ethics Committee of SISSA and the Italian Health Ministry (license numbers 569/2015-PR and 570/2015-PR).

Stimulus generation

Vibrations were generated by stringing together sequential velocity values (v_t) at 10,000 samples/s, taken from a normal distribution. In all analyses we treat the stimuli as a sequence of discrete samples, although the motor moved through space continuously. The velocity time series for a given trial was taken randomly from among 50 unique sequences of pseudo-random values. Because stimuli were built by sampling a normal distribution, the statistical properties of an individual vibration did not perfectly replicate those of the distribution from which it was constructed. Converting v_t to its absolute value, sp_t, the distribution takes the form of a folded, half-Gaussian (see Figure 1B).

The acoustic noise used for Experiment 4 was generated by stringing together sequential amplitude values at 10,000 samples/s, taken from a normal distribution. The signal was then filtered using a Tukey (also known as tapered cosine) window and delivered through headphones. The rising phase of acoustic noise amplitude was initiated 0.1-0.5 seconds (taken randomly) before Stimulus 1 vibration onset, and the falling phase occurred at a random time interval between 0.1 and 0.5 seconds, after the conclusion of Stimulus 2; in this manner, overall duration of the acoustic stimulus changed on each "*Noise on*" trial and provided no information about the vibration duration or intensity.

Delayed comparison task for rats

Each delayed comparison trial began when the rat positioned its nose in the nose-poke (equipped with optic sensor) and placed its whiskers on the plate (Figure 1A). After a

short delay (500 ms), Stimulus 1 was presented, characterized by nominal mean speed, $sp1$, and duration, $T1$ (Figure 1B). After the inter-stimulus delay of 2 s, Stimulus 2 (with $sp2$ and $T2$) was presented (Figure 1C). The rat remained in the nose-poke throughout both stimuli and could withdraw only when the "go" cue sounded at the end of the post-stimulus delay of 500 ms. Early withdrawal was considered an aborted trial and went unrewarded; it was not scored as correct or incorrect. At the go cue, the rat selected the left or right spout; reward location depended on the relative values of $sp1$ and $sp2$, for rats doing the intensity delayed comparison task, while it depended on the relative values of $T1$ and $T2$ for rats doing the duration delayed comparison task. Incorrect choices went unrewarded. Trials with $sp1 = sp2$ or $T1 = T2$, according to the task, were rewarded randomly.

Rats learned the delayed comparison task by generalizing the comparison rule across the entire stimulus range, referred to as the stimulus generalization matrix (SGM; Figure 2), whereby neither stimulus alone provided the information necessary for a correct choice (1,2). Seven rats were trained to discriminate $T1$ vs $T2$, and another 7 were trained to discriminate $sp1$ vs $sp2$.

The training of duration delayed comparison rats progressed through a sequence of stages:

- In the first stage of the training, rats were given vibration pairs with fixed sp values of 64 mm/s, and with NTD of +/- 0.35.
- When they reached 70% correct performance on the above condition, vibration pairs with lower NTD values (+/- 0.24, +/-0.11, 0) were introduced.

- When rats reached 70% correct performance with the full set of SGM pairs, unbalanced values of $sp1$ and $sp2$ were introduced (with small NSD values of +/-0.1) were included in the stimulus set.
- When they reached an overall performance of 70% correct in the above condition, the complete set of NSD values was introduced gradually, so that all the NTD and NSD values were presented.
- Only sessions when rats achieved at least 70% correct performance on the $NSD = 0$ pairs were used for the analysis.

The training of intensity delayed comparison rats progressed through a similar sequence of stages:

- In the first stage of the training, rats were given vibration pairs with fixed T values of 300 ms, and with a NSD of +/- 0.30.
- When they reached 70% correct performance on the above condition, vibration pairs with lower NSD values (+/- 0.2, +/-0.1, 0) were introduced.
- When rats reached 70% correct performance on the full set of SGM pairs, new values of $T1$ and $T2$ were introduced in a "balanced" way, meaning that $T1$ was always equal to $T2$. The durations used were 100, 200, 400, 600 ms.
- When rats reached 70% correct performance on the above condition, unbalanced values of $T1$ and $T2$ were gradually introduced, beginning with small NTD and concluding with the complete set of NTD and NSD combinations.
- Only sessions when rats achieved at least 70% correct performance on the $NTD = 0$ pairs were used for the analysis.

Delayed comparison task for human subjects

Experiments 1 and 4 employed a delayed comparison design. Stimulus 1 was characterized by nominal mean speed $sp1$ and duration $T1$. After the interstimulus delay of 1 s, Stimulus 2 (with $sp2$ and $T2$) was presented. Stimuli delivered to human subjects on the fingertip were the same as those used in rats except that the velocity values were halved. Each subject went through both an intensity and a duration delayed comparison session on different days. Subjects were verbally instructed to report which of the two stimuli was perceived as longer in duration or stronger in intensity, according to the behavioral task, by pressing the left (for Stimulus 1) or right (for Stimulus 2) arrow on the computer keyboard. They received visual feedback (correct/incorrect) on each trial through a monitor. A total of 1,456 trials were presented at each session.

Each subject went through both an intensity and a duration delayed comparison session, in different days. The trial structure was the same as the previous delayed comparison tasks, except for the fact that in half the trials, the tactile stimuli to be judged were accompanied by non-informative acoustic noise played through headphones. Moreover, no visual feedback was presented to subjects after their response. A total of 1,020 trials were presented at each session.

Direct estimation task

The same human subjects that went through the duration and intensity delayed comparison task participated in the estimation task. Each subject went through both a duration estimation and an intensity estimation session, held on different days. Each session began with a training phase. In this phase, subjects received 40 stimuli, sampled

randomly from the 100 possible stimuli (10 possible sp values from 9.6 mm/s to 67.2 mm/s and 10 possible T values from 80 to 800 ms, linearly spaced), to become confident with the task and to sample the stimulus range. In the test phase, a single stimulus was presented, characterized by nominal mean speed, $sp1$, and duration, $T1$. After a post-stimulus delay of 500 ms, a slider appeared on the screen. The slider did not present any landmark, ticks or numbers. The orientation of the slider was different between the two sessions, either vertical or horizontal. Subjects were instructed to report the perceived intensity or else the perceived duration of the vibration on a subjective scale, in which the extreme left/bottom position indicated a very weak or a very short stimulus, and the extreme right/top position indicated a very strong or a very long stimulus. The report was done by mouse-clicking on the chosen position along the slider. A total of 1,300 trials was presented at each session.

Five durations linearly spaced from 80 to 800 ms, and 5 sp values from 9.6 to 67.2 mm/s were used. A visual cue, either a blue or a red square, was presented for 1 second, either before or after the delivery of the vibration. The orientation of the slider was kept horizontal for both intensity and duration estimation trials, so that the orientation could not be used as a cue for the trial type and subjects were forced to attend to the visual cue. A total of 1,300 trials was presented at each session.

Analysis of human and rat delayed comparison data

To characterize the performance of the intensity delayed comparison task, we computed the proportion of trials in which subjects judged Stimulus 2 greater than Stimulus 1 on stimulus pairs characterized by a fixed $sp1$ ($sp1 = 32$ mm/s for human subjects, $sp1 = 64$ mm/s for rats) and different *sp2* values, separately for each normalized time

difference (NTD) value, defined as $(T2 - T1)/\,(T2 + T1)$. We fit the data with a four-parameter logistic function using the nonlinear least-squares fit in MATLAB (MathWorks, Natick, MA):

$$P(Stim2 > Stim1) = \gamma + (1 - \gamma - \lambda)\frac{1}{1 + e^{\left(-\frac{NSD-\mu}{\nu}\right)}} \quad (7)$$

where *NSD* is normalized speed difference, (*sp2-sp1*) / (*sp2+sp1*), γ is the lower asymptote, λ is the upper asymptote, *1/ν* is the maximum slope of the curve and μ is the *NSD* at the curve's inflection point.

For the duration delayed comparison task we computed the proportion of trials in which subjects judged $Stimulus\ 2\ >\ Stimulus\ 1$ on stimulus pairs characterized by a fixed $T1$ ($T1 = 300$ ms for human subjects, $T1 = 334$ ms for rats) and different $T2$ values, separately for each NTD value, by fitting:

$$P(Stim2 > Stim1) = \gamma + (1 - \gamma - \lambda)\frac{1}{1 + e^{\left(-\frac{NTD-\mu}{\nu}\right)}} \quad (8)$$

where γ is the lower asymptote, λ is the upper asymptote, *1/ν* is the maximum slope of the curve and μ is the NTD at the curve's inflection point.

In order to quantifying the bias of stimulus duration on the percept of stimulus intensity in the intensity delayed comparison task, we then computed a linear correlation between

the *PSE* values fitted for different NTD values, and the actual NTD values. The additive inverse of the regression coefficient, was defined as *duration bias*. Symmetrically for the duration delayed comparison task, we computed a linear correlation between the *PSE* values fitted for different NSD values, and the actual NSD values. The additive inverse of the regression coefficient, was defined as *intensity bias*.

Delayed comparison task: perceptual versus choice bias

Figure 3A reveals that both species show a pronounced shift in their psychometric curves on both duration and intensity discrimination tasks due to the task irrelevant feature, *NSD* and *NTD* respectively. Horizontal and vertical shifts of the psychometric curve are frequently attributed to different steps in the cognitive process, a perceptual shift and a choice shift, respectively (47). To quantify whether the shifts are better explained as purely horizontal or vertical we fit the following two models of decision probabilities:

$$P(Stim2 > Stim1) = (1 - p_L)s\big(\beta_p \Delta p + \beta_b \Delta b + \varepsilon_p\big) + p_L\, s(\varepsilon_L) \qquad (9)$$

$$P(Stim2 > Stim1) = (1 - p_L)s\big(\beta_p \Delta p + \varepsilon_p\big) + p_L\, s(\beta_b \Delta b + \varepsilon_L) \qquad (10)$$

where $P(Stim2 > Stim1)$ is the probability of choosing Stimulus 2 greater than Stimulus 1, Δp and Δb are the normalized differences of the relevant and irrelevant task features, respectively (i.e. NTD and NSD for the duration delayed comparison task, and NSD and NTD for the intensity delayed comparison task). p_L is the probability of a lapse trial, β_p is the linear weight that the task relevant feature has on choice, β_b is

the linear weight that the task irrelevant feature has on choice, and $s(x)$ is a logistic function, ε_p is the constant perceptual bias, and ε_L is the lapse trial constant choice bias. Both models in Equations 9 and 10 assume that on each trial there is a probability p_L that the choice will not be determined by the task relevant features. A non-sensory error is called a lapse. On the remaining trials, choice is determined by a generalized linear model (GLM), specifically the logit link function, of the task relevant feature Δp. The two models differ in the role of the task irrelevant feature. In the model of Equation 9, Δb is linearly combined with Δp on the non lapsed trials, whilst in the model of Equation 10, Δb goes through a separate GLM that determines the choice on lapsed trials. This means that the model of Equation 9 assumes that the task irrelevant feature biases the effective percept yielding only a horizontal shift, whilst the model of Equation 10 assumes that the task irrelevant feature biases choice on lapsed trials, yielding only a vertical shift.

We fit both models to the human and rat data using a Python software package PyMC3 (48). In both cases, we pooled all the subjects together. We then compared the goodness of fit of both models using the Widely Applicable Information Criteria (WAIC, (49)). We find that the entire dataset is better explained by a perceptual bias (Equation 9) as compared to a choice bias (Equation 10). In the case of the humans, the normalized WAIC difference (ndWAIC which is equal to WAIC divided by its standard deviation) was equal to 6.62. In the case of the rats, ndWAIC = 0.34 (Figure 6). A detailed comparison can be found in Table 1

Subject	Model Type	WAIC	pWAIC	dWAIC
Human	Perceptual bias	15357±174	17	0
	Choice bias	15690±172	19	333±50
Rat	Perceptual bias	6146±143	42	0
	Choice bias	6181±133	39	35±101

Table 1: Model comparison for the human and rat data. The WAIC column shows the model's WAIC value with its corresponding standard deviation. The pWAIC column shows the model's effective number of parameters given the dataset. The dWAIC column shows the WAIC difference across each model and the one with the lowest WAIC value. The standard deviation of the dWAIC is smaller than that of each WAIC value, because each model's WAICs are correlated, as they are fit to the same dataset.

Analysis of estimation task data

Results from the estimation task were analyzed taking into account two main factors. First is that the subjects tended to be more variable in their responses at the beginning of the session before setting a consistent subjective scale. In order to keep this variability from affecting our results, we calculated the mean response for each of the possible combinations of sp and T, and excluded outlier responses, those more than 1.5 SD displaced from the mean. Second was that not all subjects used the whole range of the slider; every participant set their minimum and maximum responses at a different position in the scale. In order to make each subject's subjective scale comparable, we used a min-max normalization algorithm:

$$Normalized\ x_n = 9\frac{x_n - min(x)}{max(x)\ - min(x)} + 1 \qquad (11)$$

where x_n is the non-normalized response on trial n, x is the range of total responses, and $Normalized\ x_n$ is the normalized response. We then multiplied by 9 and added 1, so that the normalized responses range from 1 to 10.

In order to estimate *duration bias* for intensity estimation trials in Experiment 3, we first computed the average normalized response across all possible sp, for each T. We then computed a linear regression between the average normalized responses and stimulus T, and defined the regression slope as *duration bias*.

Similarly, in order to estimate *intensity bias* for intensity estimation trials in Experiment 3, we first computed the average normalized response across all possible T, for each sp. We then computed a linear regression between the average normalized responses and stimulus sp, and defined the regression slope as *intensity bias*.

Analysis of data from delayed comparison task with supplementary auditory noise

We first characterized the behavior by using the same procedure as in the purely tactile delayed comparison task. For the intensity delayed comparison task, we then computed a linear correlation between the *PSE* values fitted for different NTD values, and the actual NTD values. The additive inverse of the regression coefficient, was defined as *duration bias*. Symmetrically for the duration delayed comparison task, we computed a linear correlation between the *PSE* values fitted for different NSD values, and the actual NSD values. The additive inverse of the regression coefficient, was defined as *intensity bias*.

Leaky integrator models

The models posit that percepts are constructed by the leaky integration of an external "drive", both task relevant and task-irrelevant drive. The general form of the dynamics is given by Equations 1 and 2. The assumed distribution of sp_t is a half Gaussian over positive values, whereas ξ is assumed to be normally distributed with a mean and variance denoted as μ_b and variance σ_b^2. Given that we assume $\alpha \in [0, 1]$, sp_t^α will have a narrower distribution than sp_t. This implies that the time integral of sp_t^α will converge to a Gaussian due to the central limit theorem. Thus, we can approximate the distribution of sp_t^α within the differential equation (1) by a Gaussian with mean and variance equal to $E[sp_t^\alpha]$ and $Var[sp_t^\alpha]$, leading to the following Itô stochastic differential equation which guides percept formation:

$$C\,\mathrm{d}Y = (-\lambda Y + a(t))\mathrm{d}t + g(\mathrm{t})\mathrm{d}W \tag{15}$$

where $$a(t) = \mathrm{E}[sp^\alpha] + \mathrm{E}[\xi] = \sqrt{\pi^{\alpha-1} sp^{2\alpha}}\,\Gamma\left(\frac{1+\alpha}{2}\right) + \mu_b$$

and $$g(t) = \sqrt{\mathrm{Var}[sp^\alpha] + \mathrm{Var}[\xi]}$$

$$= \sqrt{\pi^{\alpha-1} sp^{2\alpha}\left[\sqrt{\pi}\,\Gamma\left(\frac{1}{2}+\alpha\right) - \Gamma\left(\frac{1+\alpha}{2}\right)^2\right] + \sigma_b^2}$$

Further, sp is the nominal mean speed of the half Gaussian from which sp_t is sampled and Γ is the gamma function. The resulting stochastic differential equation for $Y(t)$ leads to an Ornstein-Ulhenbeck process, whose general solution is

$$\Upsilon(t) = \mathrm{e}^{-\frac{t}{\tau}}\left[\Upsilon(0) + \int_0^t \frac{\lambda \mathrm{a}(t')}{\tau}\mathrm{e}^{\frac{t'}{\tau}}\mathrm{d}t' + \int_0^t \frac{\lambda g(\mathrm{t}')}{\tau}\mathrm{e}^{\frac{t'}{\tau}}\mathrm{d}W\right] \quad (16)$$

where $\tau = C/\lambda$ (50). Given the functional form of $a(t)$ and $g(t)$, the resulting percept, $\Upsilon(t)$, will follow a normal distribution with the following mean and variance

$$E[\Upsilon(t)] = E[\Upsilon(0)]e^{-\frac{t}{\tau}} + \frac{\lambda}{\tau}\left(1 - e^{-\frac{t}{\tau}}\right)\left[\sqrt{\pi^{\alpha-1}sp^{2\alpha}}\Gamma\left(\frac{1+\alpha}{2}\right) + \mu_b\right] \quad (17)$$

$$\mathrm{Var}[\Upsilon(t)] = \mathrm{Var}[\Upsilon(0)]e^{-\frac{2t}{\tau}} + \frac{\lambda^2}{\tau^2}\left(1 - e^{-\frac{2t}{\tau}}\right)\left\{\pi^{\alpha-1}sp^{2\alpha}\left[\sqrt{\pi}\Gamma\left(\frac{1}{2}+\alpha\right) - \Gamma\left(\frac{1+\alpha}{2}\right)^2\right] + \sigma_b^2\right\} \quad (18)$$

We assume that subject directly reports the value of $\Upsilon(t)$ at the end of the stimulus in the direct estimation experiment, whereas they compare the two percepts associated with Stimulus 1 and Stimulus 2, $\Upsilon_1(T1)$ and $\Upsilon_2(T2)$ respectively, in the delayed comparison task. The probability that $\Upsilon_2(T2) > \Upsilon_1(T1)$ can be calculated, given that both percepts are normally distributed and their mean and variance are known. Thus

$$P\big(\Upsilon_2(T_2) > \Upsilon_1(T_1)\big) = \int_{-\infty}^{+\infty}\int_{\Upsilon_1}^{+\infty} P(\Upsilon_2, \Upsilon_1)\mathrm{d}\Upsilon_2\,\mathrm{d}\Upsilon_1 = \frac{1}{2} + \frac{1}{2}\mathrm{erf}(d') \quad (19)$$

$$d' = \frac{\mathrm{E}[\Upsilon_2(T_2)] - \mathrm{E}[\Upsilon_1(T_1)]}{\sqrt{2(\mathrm{Var}[\Upsilon_2(T_2)] + \mathrm{Var}[\Upsilon_1(T_1)])}} \quad (20)$$

where $\mathrm{erf}(x)$ is the normal error function. Given that on some trials, the subject may lapse (that is, make a non sensory error), we assume that the probability of reporting that the second percept is larger than the first is:

$$P\big(\text{choice}(2>1)\big) = \mathrm{p_{low}} + \big(1 - \mathrm{p_{low}} - \mathrm{p_{high}}\big)\left[\frac{1}{2} + \frac{1}{2}\mathrm{erf}(d')\right] \qquad (21)$$

Where $\mathrm{p_{high}}$ ($\mathrm{p_{low}}$) is the probability of making an incorrect decision due to a lapse at a trial with large positive (negative) mean $\Upsilon(T)$ difference.

We model two independent percepts, Υ_D and Υ_I, for the perceived duration and intensity, respectively, as detailed in Equations 3-6. Each percept evolves through time following Equation 15, with different parameter values which were fitted to the experimental data through the procedure described below.

The fitted parameters are summarized in Table 2.

Parameter name	Fitting range	Observations
τ_I	$[2\ 10^{-4}, 10^4]$ms	
λ_I	$[10^{-6}, 100]$	In delayed comparison data, λ_I was fixed to 1
$\Upsilon_I(0)$	$[-10^3, 10^3]$	
$\sigma_{b\,I}^2$	$[0, 10^5]$	In direct estimation data, $\sigma_{b\,I}^2$ was fixed to 0
$\mathrm{p_{high}}_I$	$[0, 0.5]$	In direct estimation data, $\mathrm{p_{high}}_I$ was fixed to 0
$\mathrm{p_{low}}_I$	$[0, 0.5]$	In direct estimation data, $\mathrm{p_{low}}_I$ was fixed to 0
τ_D	$[2\ 10^{-4}, 10^4]$ms	L1 regularization applied on τ_D fits
λ_D	$[10^{-6}, 100]$	In delayed comparison data, λ_D was fixed to 1
$\Upsilon_D(0)$	$[-10^3, 10^3]$	

$\sigma_{b_D}^2$	$[0, 10^5]$	In direct estimation data, $\sigma_{b_D}^2$ was fixed to 0
$\mathrm{p_{high}}_D$	$[0, 0.5]$	In direct estimation data, $\mathrm{p_{high}}_D$ was fixed to 0
$\mathrm{p_{low}}_D$	$[0, 0.5]$	In direct estimation data, $\mathrm{p_{low}}_D$ was fixed to 0
μ_{b_D}	$[0, 100]$	For rat data, μ_{b_D} was fixed to 0
α	$[0.05, 1]$ms	For rat data, two separate α values were fitted, one for duration and the other for intensity tasks

Table 2. Fitted model parameters, range of allowed values and observations of different treatment for the parameters during fitting.

We assume that $\mathrm{Var}[Y(0)]$ is always equal to zero. The scale of the response is adjustable by the leak, λ, and is only relevant for the direct estimation data. The target function that guided the parameter fits of the direct estimation data was a least squared difference between the mean response given by the subjects and the $\mathrm{E}[Y(T)]$ predicted by the model (Equation 17) for each $\{T, sp\}$ stimulation pair. Thus, the model's predicted variance was ignored in these fits.

In the delayed comparison experiment, the target function that guides the parameter fits was the least squared difference between the observed fraction of choices Stimulus 2 > Stimulus1 and the model predicted choice probability (Equation 21) for each $\{T, sp\}$ pair of the vertical psychometric stimulation protocol.

The reported fitted parameter values were obtained by using a Covariance Matrix Adaptation Evolutionary Strategy to find the set of values that yielded the minimum least squared difference in the target function.

All codes used for computing model predictions and performing the fits were written in Python and are freely available (GitHub repository will be provided). For fitting we used the pyCMA package (50).

Chapter II: History effects on the perceived intensity and the perceived duration of a vibration

Introduction

Ongoing sensory events are experienced not as "snapshots" but as a smooth continuation of the past and as a predictor of the future. It follows that perception is not dependent only on the currently available sensory information but is also shaped by the sensory inputs that were processed in the past (51). When the influence of the past on the present is quantified in the laboratory, two opposing effects are reported: (i) a positive effect, by which the current percept tends to resemble, or is attracted towards, the percepts evoked by previously presented stimuli, and (ii) a negative effect, by which the current percept is pushed away from, or repulsed by, those evoked by past stimuli (52, 53). What might be the functional roles of these effects? The first phenomenon, it is reasoned, helps the brain build a stable percept, exploiting temporal regularities in a noisy environment: if the world changes with a long time constant (seconds to minutes), then instantaneous differences in the sensory signal might be noise, and biasing the current percept towards recent history would constitute the most accurate representation of the world. The second phenomenon, called adaptation, makes the perceptual system sensitive to changes in the environment. It is reasoned that static sensory signals provide little useful information; thus, it is efficient to encode changes in the environment. While the neurophysiological substrates of adaptation for simple oriented visual stimuli are well studied and are thought to be confined in low level sensory areas (54, 55), it is debated if the neural mechanism behind perceptual positive serial dependence using the same type stimuli, is localized in the same low-level sensory cortex (52, 56), or in higher-level areas (57).

Chapter I showed that the percept of intensity and the percept of duration can be simulated as two leaky integrators of sensory input. This computation makes the magnitude of the final percept dependent on both the magnitude of the stimulus speed and the stimulus duration. We can represent this interaction in a 3-dimensional space, where the *x*- and *y*-axes represent the stimulus duration and mean speed, respectively, while the *z*-axis represents the final percept, which grows non-linearly with both physical dimensions of the stimuli. Depending on the characteristics of the leaky integrator at work, we can build a duration "perceptual space" (Figure 1, upper panels) or an intensity "perceptual space" (Figure 1, lower panels). A single vibration, characterized by a mean speed *sp* and a duration *T*, can be represented as a single point lying on the surface of all possible perceptual values.

From these findings, various questions relevant to history effects of intensity and duration perception arise. First, is the perceived intensity and the perceived duration of vibrations attracted or repulsed from the previously presented stimuli? All experiments presented in this chapter, show that the perception of the current stimulus is attracted toward previously presented ones. Second, is the magnitude of the final percept of the current stimulus biased toward the magnitude of the feature that had to be extracted (Figure 1A) or by the magnitude of both low-level physical features (speed and duration) of previously received stimuli (Figure 1B)?

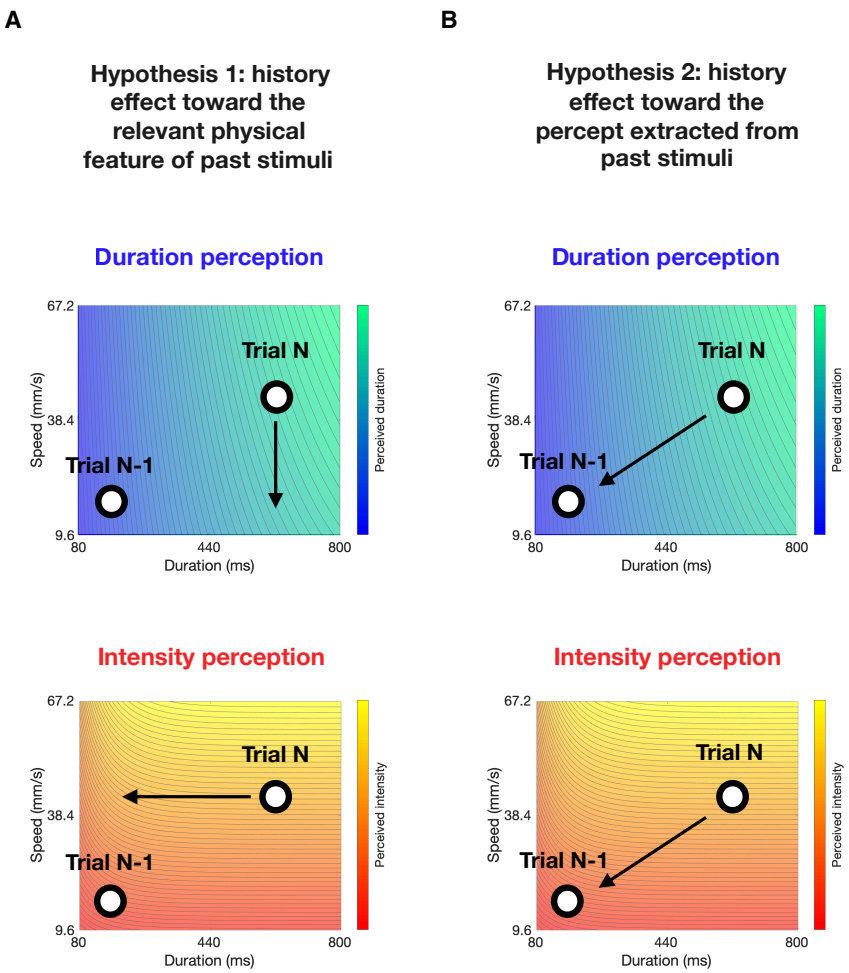

Figure 1. Alternative hypotheses for how stimulus history could influence intensity and duration perception.
A) Vibrations presented on trial *N-1* and trial *N* are depicted in 3-dimensional space. The perceived durations extracted by the subject are represented as single points in a perceptual space whose *x*- and *y*-axes are defined by the possible stimulus durations and mean speeds, and whose *z*-axis quantifies the percept extracted from the stimulus (represented by the colored gradient in the upper panel). Hypothesis 1 posits that the perceived duration on trial *N* is attracted towards the duration of the stimulus presented at trial *N-1* (black arrow), and not its final percept. The lower panel represents the same hypothesis in an intensity perceptual space, where the colored gradient quantifies the final perceived intensity extracted from each possible stimulus duration/speed combination.
B) Hypothesis 2 posits that both the perceived duration (upper panel) and the perceived intensity (lower panel) of the vibration of trial *N* are attracted towards the final percept extracted on trial *N-1* (black arrow), which is itself dependent on both the physical speed and duration of the vibration.

Results from a delayed comparison task in both humans and rats will be shown to support the second Hypothesis (Figure 1B). Moreover, results from both a delayed comparison task and a direct estimation task will reveal that the history effect is prevalent towards the feature that has to be extracted (the "relevant" feature) as compared to the feature that should be ignored (the "non-relevant" one). In other words,

the magnitude of the current percept is attracted towards the magnitude of the previously integrated value, and not towards the low-level physical features of stimuli.

A third question was then investigated: are there two separate priors for intensity and duration perception (Figure 2A), or else a unique prior updated with the task-relevant feature (duration or intensity) or with some mapping of the physical features of the stimulus (Figure 2B)?

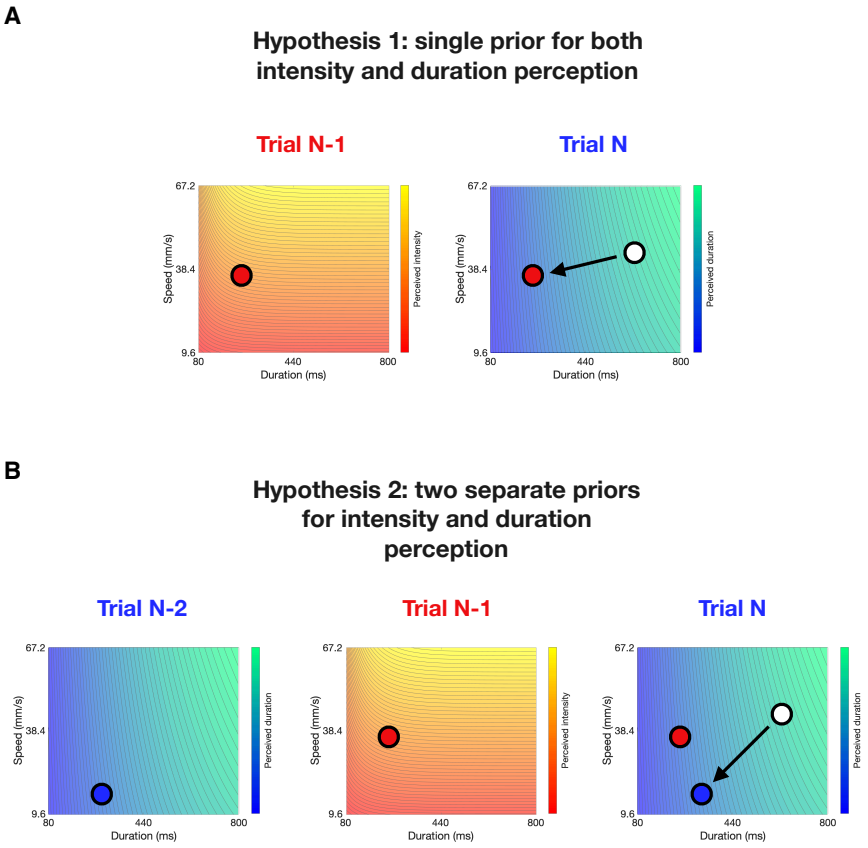

Figure 2. Alternative hypotheses: a single prior or multiple priors for intensity and duration perception.
A) Hypothesis 1: the perceived intensity of a vibration is extracted on trial *N-1*, represented as a single point in the intensity perceptual space (left panel). At trial *N*, the perceived duration of a different vibration is extracted (right panel). If a single prior exists for both perceptual features, the perceived duration extracted at trial *N*, will be attracted toward the final percept generated at trial *N-1* (black arrow), irrespectively of which of the two perceptual features was extracted.
B) Hypothesis 2: the perceived duration of a vibration is extracted at trial *N-2* (left panel), while the perceived intensity of another vibration is extracted at trial *N-1* (middle panel). If two separate priors exist for intensity and duration perception, the perceived duration extracted at trial *N* (right panel), will be attracted toward the final percept of the stimulus presented at trial *N-2* (black arrow), but not the one presented at trial *N-1*. The two perceptual spaces are separated.

A direct estimation task in human subjects, shows that two different priors exist for the history of perceived intensities and perceived durations (Figure 2B). We will discuss the implications that these results have on the debate about how a prior is formed, and the attractive versus repulsive effect of the prior.

Results

Contraction bias in rats and humans: perception is biased towards both prior durations and prior intensities

In parametric working memory tasks, wherein Stimulus 1 is compared, after a delay, to Stimulus 2, small magnitudes of Stimulus 1 tend to be overestimated, while large magnitudes of Stimulus 1 tend to be underestimated (58). This is called "contraction bias" and is believed to occur when a "noisy" neuronal representation of Stimulus 1 is attracted to, or contracts toward, the prior distribution of the previously presented stimuli (51). Our behavioral task offers an opportunity to work out the structure of the contraction bias: since the vibrations are characterized by both duration and speed, and just one feature must be extracted to solve the task, we can ask whether the prior in one task is constructed from only the physical value of the relevant stimulus feature or else the final percept extracted from the stimulus, which depends on both features (Figure 1).

To determine whether the percept of the intensity and the duration of vibrations is affected by the history of both features or by the history of only the task-relevant feature, we carried out a *delayed comparison task* in both rats and humans, similar to the one presented on Chapter I. On each trial, subjects received two vibrations in sequence (Stimulus 1, Stimulus 2), separated by a fixed delay (500 ms for human subjects, 2 s for rats). The experiment was comprised of two distinct tasks (Figure 3A): in the *duration delayed comparison*, the subject had to judge which of the two stimuli was longer according to the relative T values ($T1 > T2$ or else $T2 > T1$). In the *intensity delayed comparison*, the subject had to judge which of the two stimuli was

greater in intensity according to the relative mean speeds ($sp1 > sp2$ or else $sp2 > sp1$). Each of 19 human subjects carried out both tasks, on different days, while individual rats were trained on a single task: 7 were designated *intensity rats* and 7 *duration rats*. Two human subjects were excluded from the analysis after failing to reach the criterion of 65% correct performance in either one of the two tasks.

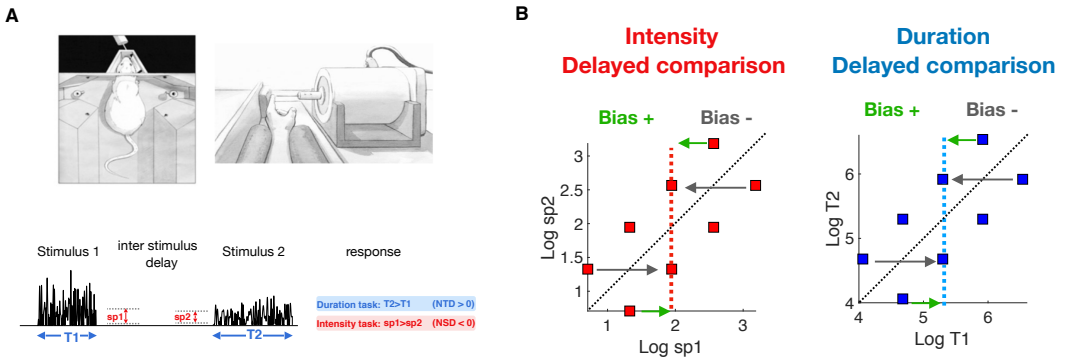

Figure 3. Experimental design and stimulus parameters.
A) Upper panel: setup for the rat (left), and for the human (right). Lower panel: Representation of the delayed comparison trial structure. Each trial consisted of the presentation of two noisy stimuli, with specified durations and mean speeds, separated by an interstimulus delay. The response was deemed correct according to the task rule: compare the two stimuli' relative durations (blue-shaded rule) or relative intensities (red-shaded rule).
B) Representation of all possible stimulus intensities and durations in the delayed comparison task. The Stimulus 1 expected value of the overall stimulus set, the prior, is given by the vertical dashed lines. The contraction bias of the first vibration towards the prior would be expected to increase performance for the Bias + pairs (green arrows), but decrease performance for the Bias – pairs (gray arrows) based on whether the contraction is towards or away from the diagonal.

Figure 3B shows the pairs of *T1, T2* and the pairs of *sp1, sp2* used during the *intensity delayed comparison* and the *duration delayed comparison* sessions, respectively. The impact of the contraction bias (acting on the percept or the memory of Stimulus 1) on trial performance depends on the presented stimuli. If Stimulus 1 is closer to the mean than Stimulus 2 (Bias+ trials), its contraction *increases* the perceived distance between the stimuli and accuracy, consequently, would be expected to increase. Conversely, in trials where Stimulus 1 is farther from the mean (Bias− trials), the contraction of

Stimulus 1 towards this mean *decreases* the perceived difference and accuracy, consequently, would be expected to decrease. Another way to characterize the effects of the bias is to consider whether contraction of the Stimulus 1 percept towards the mean will increase or decrease the distance of the stimulus pair from the diagonal, making it more or less discriminable from Stimulus 2, respectively.

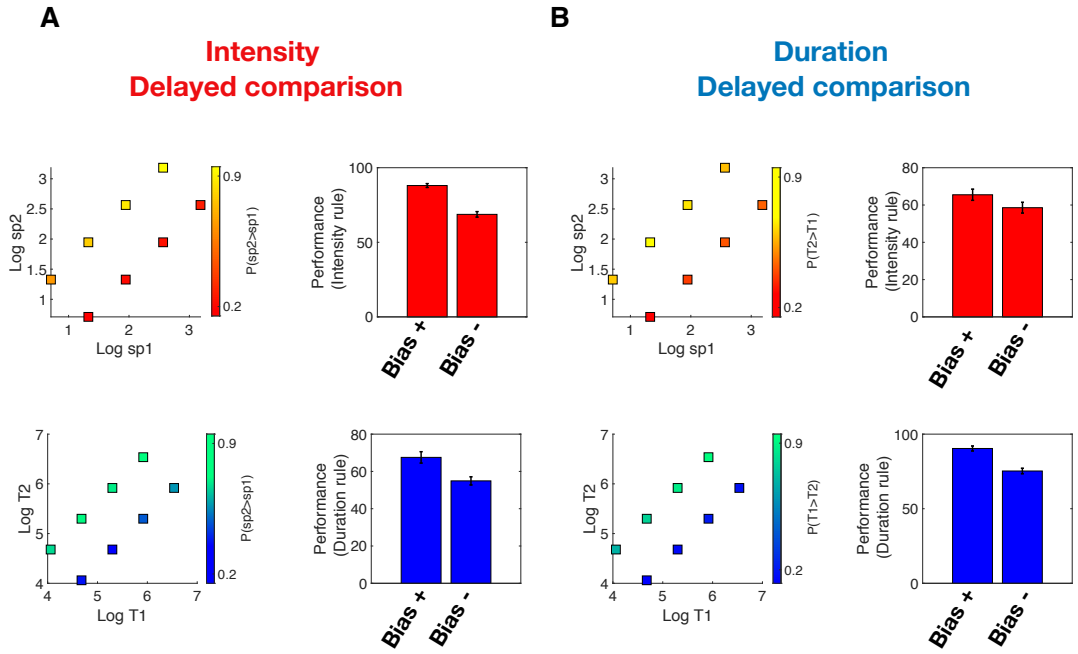

Figure 4. Contraction bias acts on both relevant and irrelevant features in human subjects.
A) Contraction bias acts on both perceived intensity and duration, during intensity delayed comparison task. The left panels show the average probability across subjects of reporting *sp2*>sp1 for each *sp1*, *sp2* and *T1*, *T2* pair. The right panels show the mean performance in comparing intensities and durations for Bias + and Bias – pairs, revealing a contraction bias for both stimulus features. Error bars are S.E.M.
B) Same as A, for duration delayed comparison tasks.

Figure 4A shows the results of the *intensity delayed comparison* task in human subjects. The upper-left panel shows the probability of reporting *sp2>sp1*. Plotting the mean performance obtained on the Bias+ pairs, compared to the Bias- pairs (upper right panel), reveals that subjects were significantly better in the former compared to the latter case (one sample, one-tailed Wilcoxon signed rank test, $p < 0.01$), signifying

that a contraction bias acts upon the perceived intensity of Stimulus 1. The lower-left panel shows how the probability of reporting *sp2>sp1* varied according to the relative durations of the two vibrations. The increase in the probability of reporting *sp2>sp1* for the stimulus pairs in which *T2>T1*, reveals the bias of stimulus duration on perceived intensity, confirming the findings of Chapter I. The lower right panel shows the difference for the Bias+ and Bias- pairs. Performance is calculated according to the "*duration rule*", quantifying how well the subjects would have performed if the task had been to discriminate the difference between the two stimuli durations, instead of their speeds. In other words, for the intensity task, choices are considered correct or incorrect according to comparative durations. The Bias+ pairs were more affected by the duration than the Bias- pairs (one sample, one-tailed Wilcoxon signed rank test, $p < 0.01$). This indicates that the perceived intensity of stimuli is affected by the prior distributions of stimulus durations, even during the *intensity delayed comparison* task. Figure 4B shows the symmetrical analyses for the *duration delayed comparison* task. Again, the contraction bias made the Bias+ pairs more discriminable in duration than the Bias- pairs (upper panel, one sample, one-tailed Wilcoxon signed rank test, $p < 0.01$). The lower left panel shows that stimulus *sp* affected the probability of reporting *T2>T1*, replicating the perceptual confound found in Chapter I. The lower right panel shows that the Bias+ pairs in the intensity domain, were more affected by stimulus *sp*, compared to the Bias- ones (one sample, one-tailed Wilcoxon signed rank test, $p < 0.05$), signifying that the history of previously presented speeds affected the perceived duration of vibrations.

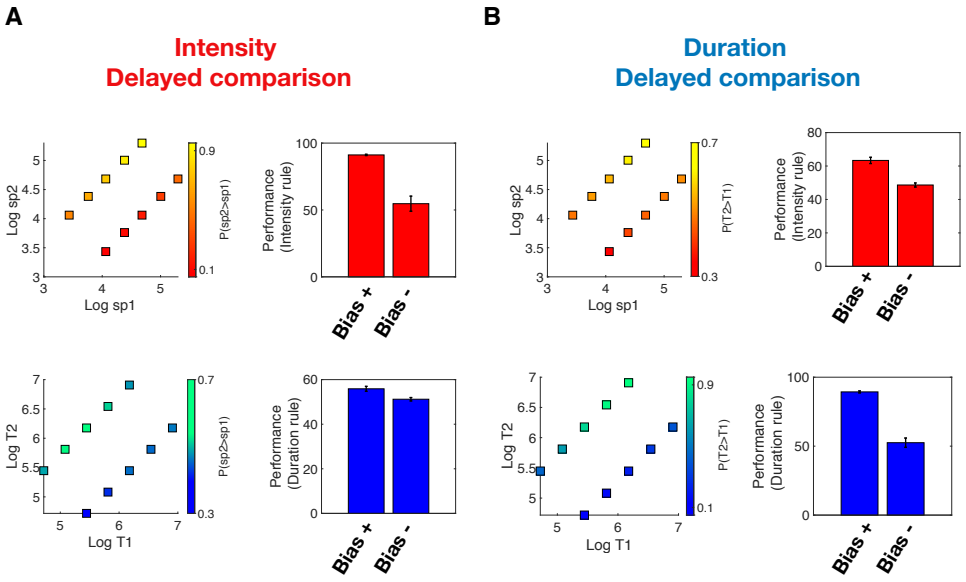

Figure 5. Contraction bias on both relevant and irrelevant features in rats.
A) Contraction bias acts on both perceived intensity and duration, during intensity delayed comparison task. The left panels show the average probability across subjects of reporting *sp2*>sp1 for each s*p1*, *sp2* and *T1*, *T2* pair. The right panels show the mean performance in comparing intensities and durations for Bias + and Bias – pairs, revealing a contraction bias for both stimulus features. Error bars are S.E.M. (difference between Bias+ and Bias- performance, in speed and duration domain: one sample, one-tailed Wilcoxon signed rank test, $p = 0.0156$).
B) Same as A, for duration delayed comparison tasks (difference between Bias+ and Bias- performance, in speed and duration domain: one sample, one-tailed Wilcoxon signed rank test, $p = 0.0078$).

Qualitatively equivalent results were obtained by analyzing rats' behavior during the intensity (Figure 5A) and duration (Figure 5B) delayed comparison task.

Overall these results suggest that, both in rats and in humans, the perceived intensity and the perceived duration of tactile stimuli are affected by two different priors, irrespectively of the relevant feature to be extracted: the distribution of the history of stimulus durations and of stimulus speeds, confirming Hypothesis 2 depicted in Figure 1B.

Serial dependence in rats and humans: the current percept is attracted to the perceived prior, not the physical prior

An advantage of our stimulus design is that a single stimulus is made up of two physical features, and subjects can be instructed (humans) or trained (rats) to judge one or the other feature. We can then distinguish whether the influence of preceding stimuli is accounted for by their physical features or by the extracted percept. A perceptual effect related to history is called positive serial dependence (52): the percept of a stimulus is attracted toward the percept of the preceding stimulus. As the contraction bias analyses revealed that the perception of stimulus duration and the perception of stimulus intensity are affected by the history of both stimulus features, serial dependencies allow us to quantify how much the history of each of the two physical features affects the percept of the current stimulus. In order to quantify serial dependencies of perceived intensity and perceived duration, we designed another delayed comparison task, performed both by humans and by rats.

In Experiment 2, 14 human subjects participated in both an *intensity delayed comparison* session and a *duration delayed comparison* session. The stimulus pairs presented during each session were the same as those of Experiment 1, however we categorized each *N-1* stimulus pair as weak or strong according to speed, and as short or long according to duration (Figure 6A, left panel). When quantifying the effect of the trial *N-1* stimulus on the percept of trial *N*, the number of *N-1* trials of each category in which subjects made opposing choices was balanced. Thus, any motor or decisional carryover from trial *N-1* to trial *N* was averaged out; trial *N-1* was defined only by its stimulus values. We then computed psychometric curves for trial *N*, conditional on *N-1* categorized by speed and on *N-1* categorized by duration.

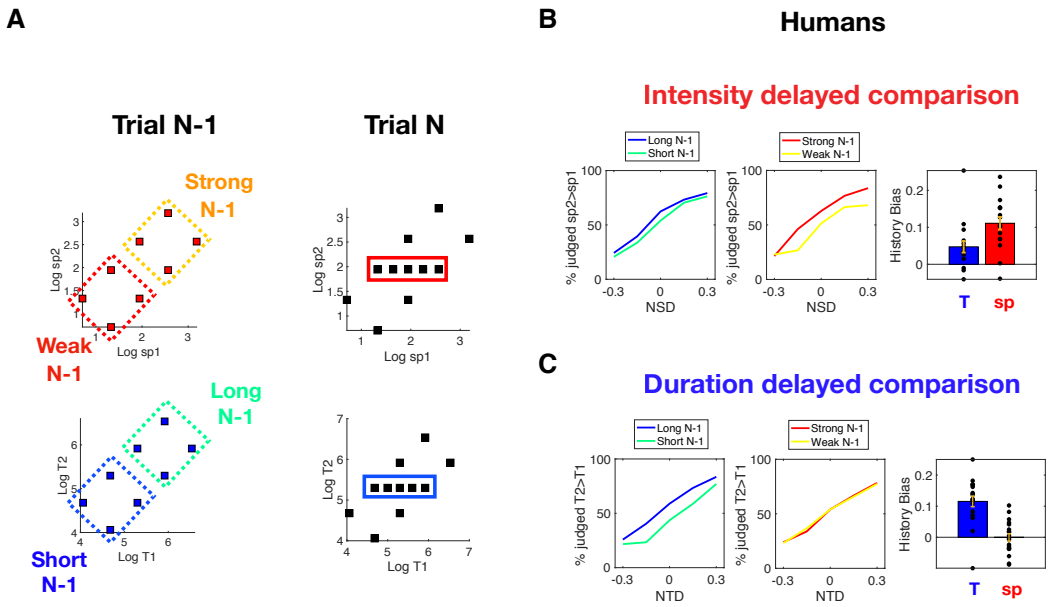

Figure 6. Serial dependencies in delayed comparison in human subjects.
A) Left plots: trial *N-1* speed and duration pairs were defined as weak/strong and short/long. Right plots: duration and intensity pairs on trial *N*. Boxes enclose the stimulus pairs used to compute psychometric curves for the duration discrimination task (in blue) and for the intensity discrimination task (in red).
B) Intensity psychometric curves separated according to the duration category (left panel) and the speed category (middle panel) of trial *N-1*. The right panel shows the *duration history bias* (blue) and *speed history bias* (red) of all subjects. Each dot is a single subject; error bars are S.E.M. Both biases are significantly different from zero (two-tailed Wilcoxon signed rank test, $p < 0.01$).
C) Duration psychometric curves separated according to the duration category (left panel) and the speed category (middle panel) of trial *N-1*. The right panel shows the *duration history bias* (blue) and *speed history bias* (red) of all subjects. Each dot is a single subject; error bars are S.E.M. Duration history bias was significantly different from zero (two-tailed Wilcoxon signed rank test, $p < 0.01$), while speed history bias was not.

Results for the *intensity delayed comparison* session in human subjects are shown in Figure 6B. The left panel shows how the probability of reporting *sp2>sp1* on trial *N* varied in relation to the stimulus pair's normalized speed difference (*NSD*). Psychometric curves are separated according to whether trial *N-1* duration was long (blue) or short (green). The small but significant leftward shift of the curve after long *N-1* duration indicates that the perceived intensity of the trial *N* stimulus is affected by the magnitude of the previous stimulus duration. The middle panel shows, again, how the probability of reporting *sp2>sp1* varied in relation to the stimulus pair's normalized speed difference (*NSD*), however now the psychometric curves are separated according

to whether trial *N-1* speed was strong (red) or weak (yellow). Again, the curve is shifted leftward after strong *N-1* speed, indicating that perceived intensity is affected by the preceding speed. The right panel quantifies the history bias imposed on trial *N* perceived intensity by the two stimulus features (*T* and *sp*) of trial *N-1*, revealing that the percept of trial *N* intensity is mostly attracted towards trial *N-1* speed, and less (but still significantly) attracted towards trial *N-1* duration (see Methods for statistical measures).

Analyses carried out on *duration delayed comparison* sessions are shown in Figure 6C. The perceived duration of the trial *N* stimulus is significantly biased by the magnitude of the duration of the trial *N-1* stimulus (left panel), but trial *N* perceived duration was not systematically biased by the magnitude of trial *N-1* speed (middle panel). The right panel quantifies the history bias imposed on trial *N* perceived duration by the two stimulus features (*T* and *sp*) of trial *N-1*, revealing that the percept of trial *N* duration is strongly attracted towards trial *N-1* duration, and not significantly attracted towards trial *N-1* speed.

The same analyses were done for the 7 rats trained in an *intensity delayed comparison* task, and the 7 rats trained in *a duration delayed comparison* task, used for Experiment 1. Figure 7A shows the presented speed and duration pairs. As for human subjects, we categorized the trial *N-1* stimuli as weak or strong according to speed and as short and long according to duration.

As was done for the analysis of human subjects, when quantifying the effect of the trial *N-1* stimulus on the percept of trial *N*, the number of *N-1* trials of each category in

which subjects made opposing choices was balanced. Thus, any motor or decisional carryover from trial *N-1* to trial *N* was averaged out; trial *N-1* was defined only by its stimulus values. We then computed psychometric curves for trial *N*, conditional on *N-1* categorized by speed and on *N-1* categorized by duration (Figures 7B and 7C).

Results for the *intensity delayed comparison* session in rats are shown in Figure 7B. The left panel shows how the probability of reporting *sp2>sp1* on trial *N* varied in relation to the stimulus pair's normalized speed difference (*NSD*). Psychometric curves are separated according to whether trial *N-1* duration was long (blue) or short (green). A small, but not significant, leftward shift of the curve after long *N-1* duration indicates that the perceived intensity of the trial *N* stimulus is affected by the magnitude of the previous stimulus duration for 4 out of 7 rats. The middle panel shows, again, how the probability of reporting *sp2>sp1* varied in relation to the stimulus pair's normalized speed difference (*NSD*), however now the psychometric curves are separated according to whether trial *N-1* speed was strong (red) or weak (yellow). Again, the curve is shifted leftward after strong *N-1* speed, indicating that perceived intensity is affected by the preceding speed. The right panel quantifies the history bias imposed on trial *N* perceived intensity by the two stimulus features (*T* and *sp*) of trial *N-1*, revealing that the percept of trial *N* intensity is mostly attracted towards trial *N-1* speed, and less (but not significantly) attracted towards trial *N-1* duration (see Methods for statistical measures).

Analyses carried out on *duration delayed comparison* sessions are shown in Figure 7C. The perceived duration of the trial *N* stimulus is significantly biased by the magnitude of the duration of the trial *N-1* stimulus (left panel), while trial *N* perceived duration

was biased by the magnitude of trial *N-1* speed to a lesser extent (middle panel). The right panel quantifies the history bias imposed on trial *N* perceived duration by the two stimulus features (*T* and *sp*) of trial *N-1*, revealing that the percept of trial *N* duration is strongly attracted towards trial *N-1* duration, and less (but still significantly) attracted towards trial *N-1* speed.

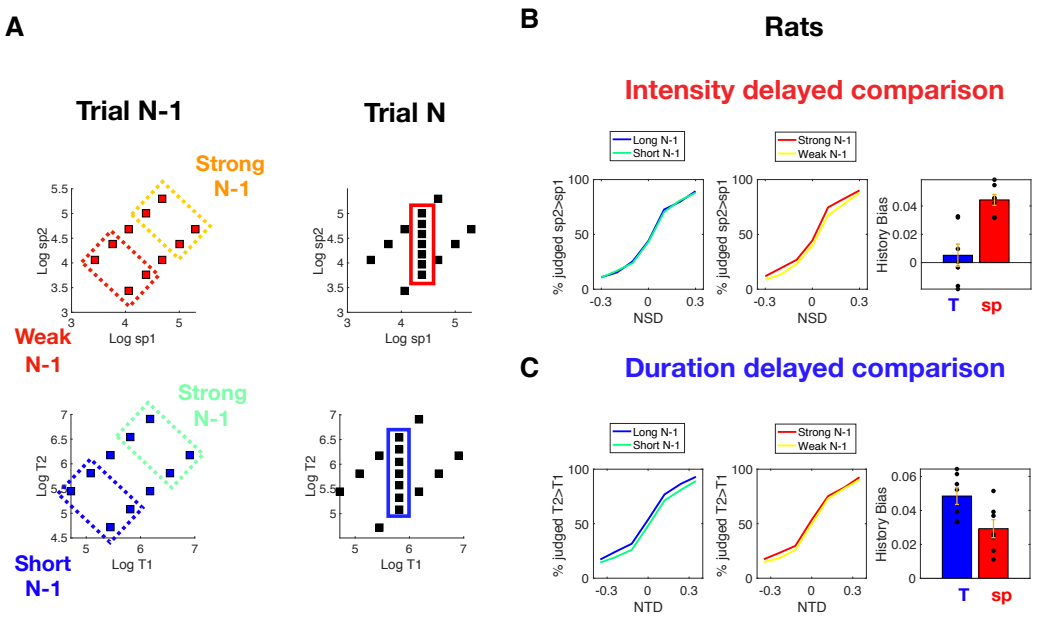

Figure 7. Serial dependencies in delayed comparison tasks in rats.
A) Left plots: trial *N-1* speed and duration pairs were defined as weak/strong and short/long. Right plots: duration and intensity pairs on trial *N*. Boxes enclose the stimulus pairs used to compute psychometric curves for the duration discrimination task (in blue) and for the intensity discrimination task (in red) .
B) Intensity psychometric curves separated according to the duration category (left panel) and the speed category (middle panel) of trial *N-1*. The right panel shows the *duration history bias* (blue) and *speed history bias* (red) of all subjects. Each dot is a single subject; error bars are S.E.M. Speed history bias was significantly different from zero (two-tailed Wilcoxon signed rank test, $p < 0.05$), while duration history bias was not.
C) Duration psychometric curves separated according to the duration category (left panel) and the speed category (middle panel) of trial *N-1*. The right panel shows the *duration history bias* (blue) and *speed history bias* (red) of all subjects. Each dot is a single subject; error bars are S.E.M. Both biases are significantly different from zero (two-tailed Wilcoxon signed rank test, $p < 0.05$).

Overall, the results argue that positive perceptual serial dependency is present in this delayed comparison task. When asked to compare the durations of Stimulus 1 and Stimulus 2, subjects' percept of Stimulus 1 appears to be biased toward the prior duration, and to a lesser extent toward the prior speed. On the other hand, when asked

to compare the intensities of Stimulus 1 and Stimulus 2, subjects' percept of Stimulus 1 appears to be biased toward the prior speed, and to a lesser extent toward the prior duration. These asymmetries of the perceptual bias can be interpreted as the percept of Stimulus 1 of trial *N* being attracted toward the perceived values of the stimuli on trial *N-1*, and not their low-level physical features (Figure 1B). The distinction between low-level physical features and percept was highlighted in Chapter I, where the work suggested that dual percepts, intensity and duration, could be derived from the integration of a low-level sensory drive (with short and long time constants, respectively). The experiments described so far in Chapter II argue that the prior is better approximated as the temporally-integrated stimulus representation rather than the input to the integrator.

Are the priors for intensity and duration fused or else separate?

Previous experiments showed that the percept of stimulus intensity and the percept of stimulus duration are attracted towards, respectively, the perceived duration and the perceived intensity of previously presented stimuli. However, as rats and humans both were asked to extract either duration or intensity within each session, it is not possible to infer whether a single prior is updated with the percept relevant to the ongoing task, or else two separate priors are updated in parallel according to the perceived intensities and the perceived durations of previously presented stimuli (Figure 2).

To answer these questions, we designed a *direct estimation* task, similar to the one presented in Chapter I. An additional benefit of the direct estimation task is that only a single stimulus in trial *N-1* could influence trial *N* (there are of course 2 stimuli within trial *N-1* in the delayed comparison task); likewise, the prior could affect only a single

stimulus in trial *N*. Each trial began when the subject received a colored cue which indicated which of the two stimulus features, intensity (red) or duration (blue), had to be estimated in the current trial. 500 ms after cue presentation, a single vibration, defined by *sp* and *T*, was presented. A slider image appeared on the monitor 500 ms after the end of the vibration (Figure 8A). By choosing the mouse-click position along the slider, the subject reported the perceived intensity of the vibration or else the perceived duration of the vibration, according to the pre-stimulus cue. From trial to trial, the orientation of the slider randomly alternated between vertical and horizontal, independently of task cue. The random switching of slider orientation was intended to separate any perceptual history biases from potential motor carryover effect. The test stimulus set was comprised of 6 durations (linearly spaced from 80 to 800 ms) and 6 mean speed values (linearly spaced from 9.6 mm/s to 67.2 mm/s). All 36 possible combinations of speed and duration were presented in each session (Figure 8B).

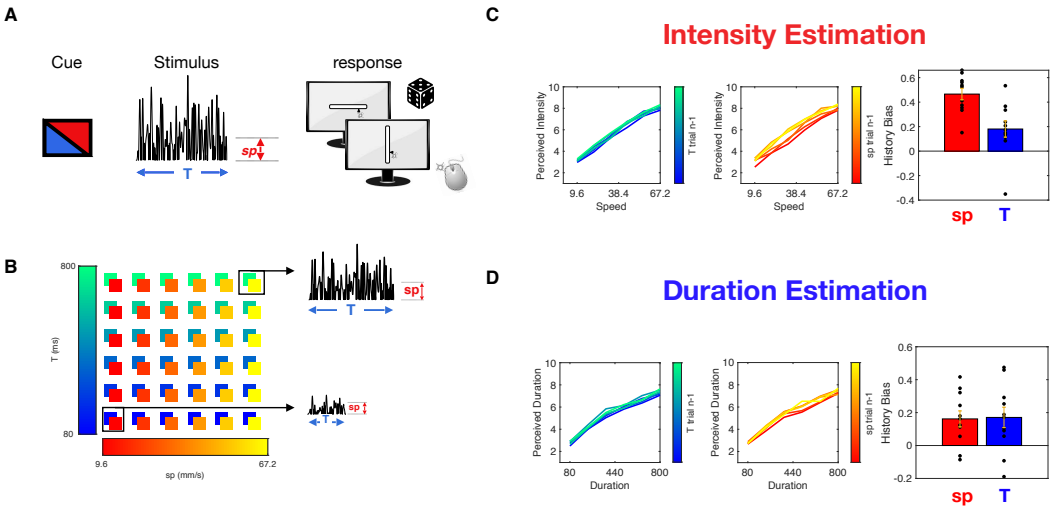

Figure 8. Serial dependencies in the direct estimation task: same task on trials *N-1* and *N*.
A) Experimental setup. Human subjects received a single noisy vibration and reported perceived duration or intensity by mouse-clicking on a computer screen. A colored cue presented at the onset of each trial indicated which feature had to be extracted. Slider orientation was set randomly on each trial.
B) Stimulation matrix. The vibration duration and mean speed was randomly picked from the set of (*T, sp*) combinations represented by the colored squares. Two sample stimuli from the upper right and lower left of the matrix are illustrated.
C) Intensity estimation results: median perceived intensity as a function of stimulus speed, computed separately for each duration (left panel) and speed (middle panel) of the trial *N-1* stimulus. Right panel shows the *duration history bias* in blue and *intensity history bias* in red of all subjects. Each dot is a single subject, while error bars are S.E.M. Both biases are significantly different from zero (two-tailed Wilcoxon signed rank test, $p < 0.05$)
D) Duration estimation results: median perceived duration as a function of stimulus duration, computed separately for each duration (left panel) and speed (middle panel) of the trial *N-1* stimulus. Right panel shows the *duration history bias* in blue and *intensity history bias* in red of all subjects. Each dot is a single subject, while error bars are S.E.M. The duration history bias was significantly different from zero (two-tailed Wilcoxon signed rank test, $p < 0.01$), as was the intensity history bias (two-tailed Wilcoxon signed rank test, $p < 0.05$).

First, we plotted how the perceived intensity and the perceived duration on trial *N* varied according to *T* and *sp* of trial *N-1*, when the stimulus feature to be extracted on trials *N-1* and *N* was the same. Figure 8C shows the case in which *N-1* and *N* were both *intensity estimation* trials. The left panel depicts the perceived intensity on trial *N* in relation to that trial's *sp*, separated according to the value of *T* on trial *N-1*. It is clear that the perceived intensity on trial *N* increases with stimulus *N* speed (as it should) but also increases with the duration of stimulus *N-1*. The middle panel again depicts the perceived intensity on trial *N* in relation to that trial's *sp*, but is now separated according to the value of *T* on trial *N-1*. It is clear that the perceived intensity on trial *N* increases

with stimulus *N* speed (as it should) but also increases with the *sp* of stimulus *N-1*.

Thus, in intensity estimation, the attraction is greater towards the relevant feature, *sp*, of the previous stimulus compared to attraction towards the non-relevant feature, *T* (right panel, see Methods for statistical measures). This finding of attraction towards the prior reinforces the results obtained from the *delayed comparison* task (Figures 6 and 7). Importantly these attractive effects were present both when the orientation of the slider was congruent or incongruent between the two subsequent trials, demonstrating that it cannot be explained purely as a motor carryover effect (see Supplementary Figure 1). Figure 8D, shows the same analysis for *duration estimation*. Again, the perceived duration of stimulus *N*, increases with both *T* and *sp* of stimulus *N-1*. The amount of bias is not symmetric, with a higher impact on perception given by the *T* of the previous vibration, compared to *sp* (right panel).

These results, together with those of Experiments 1 and 2, show that the percept of the stimulus presented on trial *N* is affected by both physical features of the vibration presented on trial *N-1*, making it likely that it is the perceived value extracted on trial *N-1* that influences the percept on trial *N*, and not just the physical properties of the stimulus. To better quantify this effect, we ran a multiple linear regression between the percept extracted on trial *N*, and the speed, the duration and the reported percept on trial *N-1*. As the predictors of the regression are correlated with one another, we used a ridge regularization (see Methods). Figure 9 shows the results obtained for the duration estimation (upper panel) and intensity estimation (lower panel).

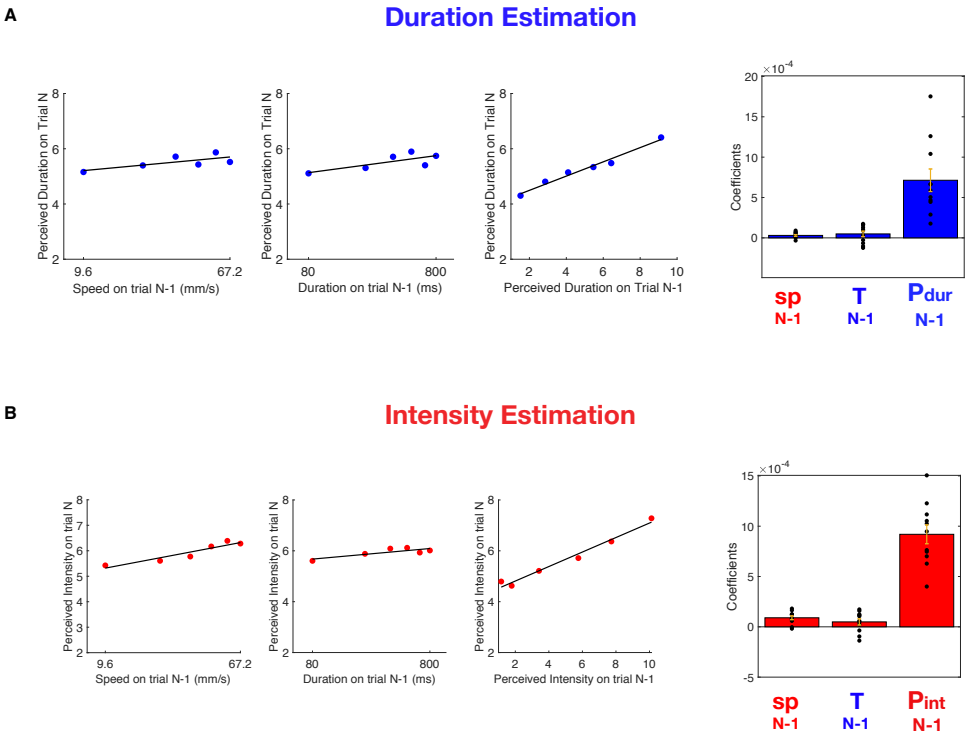

Figure 9. Reported percept on trial *N-1* influences the percept of the stimulus presented on trial *N*.
A) Duration estimation results: median perceived duration reported on trial *N* as a function of the speed (left panel), duration (middle panel) and reported percept (right panel) of the stimulus presented on trial *N-1*. Rightmost panel shows the coefficients obtained from a multiple linear regression between the reported percept on trial *N* and *sp*, *T* and reported percept of the stimulus presented on trial *N-1*.
B) Intensity estimation results: median perceived intensity reported on trial *N* as a function of the speed (left panel), duration (middle panel) and reported percept (right panel) of the stimulus presented on trial *N-1*. Rightmost panel shows the coefficients obtained from a multiple linear regression between the reported percept on trial *N* and *sp*, *T* and reported percept of the stimulus presented on trial *N-1*.

The first three panels on Figure 9A show how the perceived duration reported on trial *N*, changes with the speed (left panel), the duration (middle panel) and the percept reported (right panel) on trial *N-1*. The rightmost panel depicts the coefficients obtained from the multiple linear regression analysis, which confirms that the reported percept on the previous trial influences more the perceived duration of the stimulus presented at the current trial, compared to the physical features of the stimulus alone. Figures 9B shows the same analyses for intensity estimation trials, confirming that the reported percept on trial *N-1* is the most robust predictor of the reported percept on trial *N*.

Next, we examined the effects of *T* and *sp* of trial *N-1* on the perceived intensity and the perceived duration on trial *N*, when the stimulus feature to be extracted on trials *N-1* and *N* was different. As results reported in Figure 9 showed that percept of the stimulus presented on trial *N* is affected by the perceived value of the stimulus presented on trial *N-1*, in the next analyses we focused on how the percept reported on trial *N* is affected by the reported percept on trial *N-1*, instead of the physical features of the stimulus separately, as for previous analyses. Figure 10A, shows how the perceived intensity on trial N is affected by the reported percept of trial *N-1*. The left panel shows that when trial *N-1* required *duration estimation*, the perceived intensity on trial *N* was slightly modified according to the previously reported duration. On the other hand, when the perceived intensity had to be extracted on both trials *N-1* and *N*, the percept reported on trial *N* was strongly attracted towards the previously reported intensity (Figure 10A, middle panel). Thus, in intensity estimation, the attraction is greater towards the perceived intensity of the previous stimulus compared to attraction towards the perceived duration (right panel, see Methods for statistical measures). Figure 9B shows the same analysis for *duration estimation* trials. When both trials *N* and *N-1* were *duration estimation* trials, the percept reported on trial *N* is attracted towards the previously perceived duration. When on trial *N* subjects reported the perceived intensity of the stimulus, the perceived duration on trial *N* was not affected by *N-1*. Supplementary Figure 2 shows that these effects are not dependent on the orientation of the slider in the two subsequent trials.

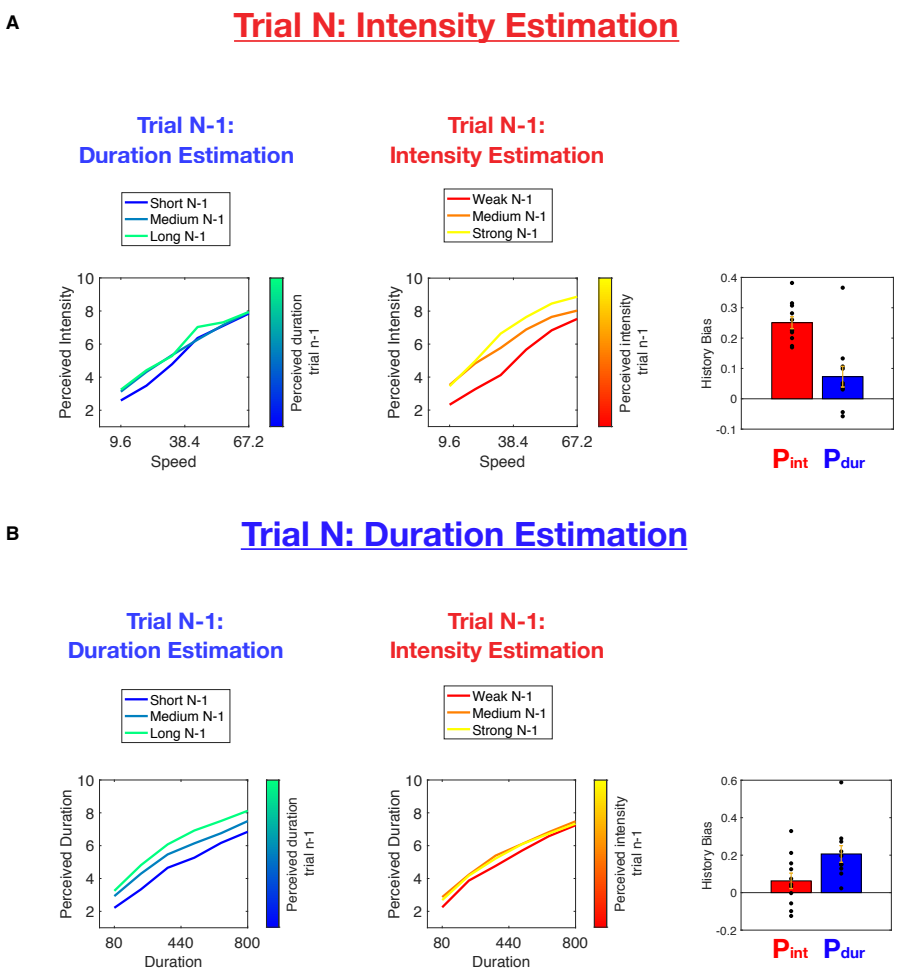

Figure 10. Serial dependencies in the direct estimation task: different task on trials *N-1* and *N*.
A) Intensity estimation results: median perceived intensity as a function of stimulus speed, computed separately for different levels of perceived duration (left panel) and perceived intensity (middle panel) of the trial *N-1* stimulus. Right panel shows the *duration history bias* in blue and *intensity history bias* in red of all subjects. Each dot is a single subject, while error bars are S.E.M. Perceived intensity on trial *N* is significantly attracted towards the *N-1* perceived intensity (two-tailed Wilcoxon signed rank test, $p < 0.01$), and to a lesser extend towards the *N-1* perceived duration (two-tailed Wilcoxon signed rank test, $p = 0.06$).
B) Duration estimation results: median perceived duration as a function of stimulus duration, computed separately for each perceived duration (left panel) and perceived speed (middle panel) of the stimulus presented on Trial N-1. Rightmost panel shows the *duration history bias* in blue and *intensity history bias* of all subjects. Each dot is a single subject, while error bars are S.E.M. Perceived intensity is significantly affected by previous stimulus perceived duration (two-tailed Wilcoxon signed rank test, $p < 0.01$), but not its perceived intensity (two-tailed Wilcoxon signed rank test, $p = 0.2$).

Figure 11 shows that the prior that influences trial *N* extends not only to trial *N-1* but also to trial *N-2*. The upper panel shows that the perceived intensity on trial *N* is not biased by the perceived duration of trial *N-2*, but it is biased by its perceived intensity provided that trial *N-2* is an *intensity estimation* trial. The same relation holds for

duration estimation trials: judgments on trial *N* are biased by the perceived duration of trial *N-2*, but not its perceived intensity.

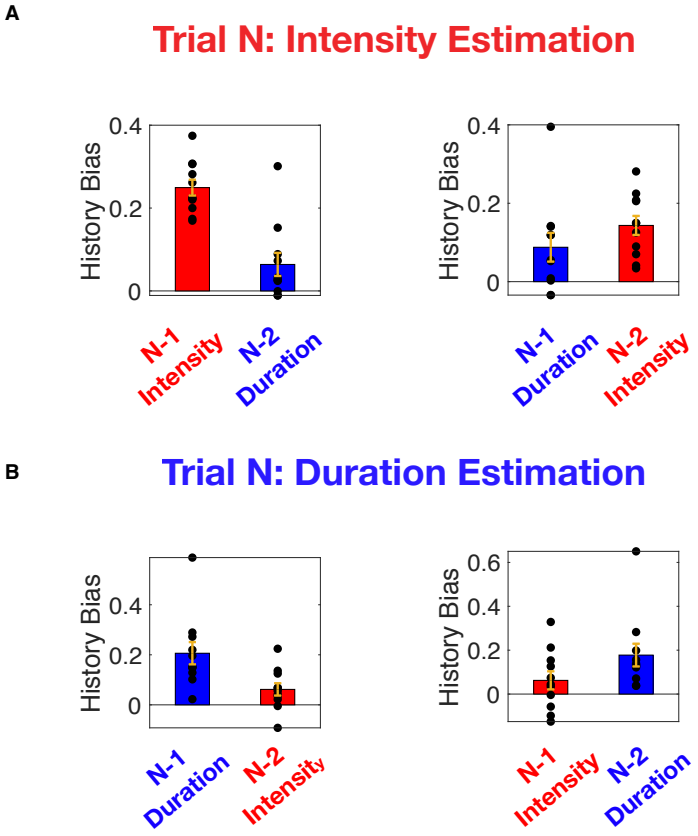

Figure 11. Serial dependencies in the estimation task, for different tasks on trials *N-1* and *N-2*.
A) Intensity estimation results: Left panel shows *history biases* on perceived intensity of stimulus on trial *N*, when an intensity estimation trial was presented on trial *N-1* (in red) and a duration estimation trial was presented on trial *N-2* (in blue). Perceived intensity on trial *N* is significantly more attracted toward the *N-1* perceived intensity compared to the *N-2* perceived duration (one-tailed Wilcoxon signed rank test, $p < 0.05$). Right panel shows same analyses when trial *N-1* was a duration estimation trial and trial *N-2* an intensity estimation trial. Perceived intensity on trial *N* is significantly more attracted toward the *N-2* perceived intensity compared to the *N-1* perceived duration ($p < 0.01$). Each dot is a single subject, while error bars are S.E.M.
B) Duration estimation results: Left panel shows *history biases* on perceived duration of stimulus on trial *N*, when a duration estimation trial was presented on trial *N-1* (in blue) and an intensity estimation trial was presented on trial *N-2* (in red). Perceived duration on trial *N* is significantly more attracted toward the *N-1* perceived duration compared to the *N-2* perceived intensity (one-tailed Wilcoxon signed rank test, $p < 0.01$). Right panel shows same analyses when trial *N-1* was an intensity estimation trial and trial *N-2* a duration estimation trial. Perceived duration on trial *N* is significantly more attracted toward the *N-2* perceived duration compared to the *N-1* perceived intensity ($p < 0.01$). Each dot is a single subject, while error bars are S.E.M.

Overall, these results are in line with the Hypothesis 2, depicted in Figure 2B. Our

findings are best explained by the existence of two separate priors: one for the history of previously perceived intensities, and one for the history of previously perceived durations. Each prior is updated only by its relevant percept. When on trial *N* the subject extracts the perceived intensity of the stimulus, that percept is attracted toward the previously perceived intensities, but not the previously perceived durations, as shown in Figures 8A and 10A. When on trial *N* the subject extracts the perceived duration, that percept is attracted toward the previously perceived durations, but not the previously perceived intensities, as shown in Figures 8B and 10B.

Discussion

By using a *delayed comparison* experimental design, in both humans and rats, and a *direct estimation* design in human subjects, we were able to investigate history effects on the perception of both the intensity and duration of tactile stimuli.

Multiple novel insights arise from the results. The first is that a positive serial dependence, or perceptual hysteresis, was documented for the first time in the perception of the intensity of tactile vibrations. The literature about history effects in intensity perception of vibrotactile stimuli is not rich. Two studies showed after 1 sec presentation of a vibrotactile adapting stimulus on the fingertip, the perceived intensity of the successive vibration was repelled from the intensity of the adaptor, an observation we interpret as a negative aftereffect (59, 60). Positive serial dependencies have not been reported in this sensory modality. Moreover, we were able to show positive aftereffects in intensity perception, for the first time, in rats.

The second one is that, for the first time, positive aftereffect in the perception of tactile stimulus duration was found in both humans and in rats. In time perception, contradictory history effects have been reported. A positive aftereffect was found in a temporal order judgment task and a temporal magnitude estimation task, in which subjects had to estimate the order and the temporal interval between the onsets of an auditory and a visual stimulus, which were presented with an asynchrony of less than 1 second (61). However, a study using a bisection task in which a single stimulus was presented on each trial and had to be classified as either long or short, led to an apparently opposite result. Using both visual and auditory stimuli (durations ranging

from 300 to 800 ms), a negative aftereffect was found (62). This negative aftereffect was interpreted by a Bayesian model, which assumed that each stimulus is compared with the memory of the previously presented durations, that is, the prior. The prior is contracted toward the previously presented stimuli, making the test stimulus judged as repulsed from the previous one.

The third novel insight is that positive aftereffects are towards the previous percepts of intensity and duration, not to the low-level physical features of the preceding stimuli (Figures 1B and 9). These findings have important implications in the debate about what neurophysiological mechanism underlies positive perceptual aftereffects. In the literature, one interpretation is that attraction toward previously presented stimuli can be explained by neural mechanisms taking place at the low-level primary sensory areas. Fischer and Whitney (52) were able to model the positive serial dependence in the perception of oriented visual stimuli using simple neural mechanisms such as neural gain change at the exposed orientation (63), and a tuning shift away from the exposed orientation (54). In fact, phenomenologically contradictory effects such as adaptation and positive aftereffects to visual oriented stimuli, can be interpreted as a balance between two separate mechanisms that take place in V1: neuronal fatigue drives repulsion from previous stimulus orientation, while a shift of orientation selective cells' tuning curves away from the orientation of the adaptor causes an attraction toward previously presented stimuli (55). Some fMRI studies in human subjects showed that the perceptual hysteresis of oriented gratings could be related to changes in V1 activity (56). In contrast, other authors found that the two perceptual opposite effects are generated by different neural populations: while adaptation can be explained by the classical models of neural fatigue (64), positive serial dependence is dependent on

decision-making related cortical areas (53, 65). In humans subjects, fMRI experiments showed that fronto-parietal areas could be involved in perceptual hysteresis of multistable visual stimuli (57), while in an auditory parametric working memory task held in rats, optogenetic inactivation of PPC, decreased contraction bias (66).

The finding that the perceived intensity and duration of a vibration is attracted toward the percept extracted from the previously presented stimulus makes it likely that the neural circuits giving rise to the perceptual serial dependencies we found lie in areas beyond primary somatosensory cortex. Chapter I argued that the perception of stimulus duration and intensity arise form a leaky integration of sensory input from S1, and that the time constants of integration for both percepts are likely to be present in areas higher than S1 in the cortical hierarchy (29). This framework implies that the prior perceived durations and prior perceived intensities of tactile vibrations are stored and represented in areas that lie beyond primary somatosensory cortex, at the output level of the leaky integrators.

Finally, Experiment 3 showed that it is likely that two separate representations of prior perceived intensities and prior perceived durations exist in the brain (Figures 2B, 10 and 11). These findings challenge the theory proposed by some authors, that a global prior exist for all magnitude estimates, including time and intensity (67, 68), already questioned by recent experiments (69). Overall, these results showed that different perceptual priors for stimulus perceived intensity and perceived duration are built in the brain, using the output of a leaky integration of sensory input with a short and long time constant respectively. Future work can shed the light on where in the brain they are represented. Further, it remains to be seen from rat neurophysiology and optogenetics

if the separate priors are held in separate neuronal populations, or else co-exist with a single population.

Methods

Analysis of delayed comparison data

Intensity delayed comparison task:

To characterize how previous stimulus intensity changed the performance of the intensity delayed comparison trials, we computed the proportion of trials in which subjects judged Stimulus 2 greater than Stimulus 1 on stimulus pairs characterized by a fixed $sp1$ ($sp1 = 32$ mm/s for human subjects, $sp1 = 64$ mm/s for rats) and different *sp2* values, separately for each category of intensity (weak/strong) that was presented on trial *N-1*. We fit the data with a four-parameter logistic function using the nonlinear least-squares fit in MATLAB (MathWorks, Natick, MA):

$$P(Stim2 > Stim1) = \gamma + (1 - \gamma - \lambda)\frac{1}{1 + e^{\left(-\frac{NSD-\mu}{\nu}\right)}} \quad (1)$$

where *NSD* is normalized speed difference, (*sp2*-*sp1*) / (*sp2*+*sp1*), γ is the lower asymptote, λ is the upper asymptote, *1/*ν is the maximum slope of the curve and μ is the *NSD* at the curve's inflection point.

The bias of previous stimulus intensity on the percept of current stimulus was calculated by computing a linear correlation between the *PSE* values fitted for different intensity category of stimulus at trial *N-1*, and the category identity (-1 for weak stimuli, +1 for strong stimuli). The additive inverse of the regression coefficient, was defined as *history intensity bias*.

To characterize how previous stimulus duration changed the performance of the intensity delayed comparison trials, we computed the proportion of trials in which subjects judged Stimulus 2 greater than Stimulus 1 on stimulus pairs characterized by a fixed $sp1$ ($sp1 = 32$ mm/s for human subjects, $sp1 = 64$ mm/s for rats) and different *sp2* values, separately for each category of duration (short/long) that was presented on trial *N-1*. We fit the data with a four-parameter logistic function using the nonlinear least-squares fit in MATLAB (MathWorks, Natick, MA):

$$P(Stim2 > Stim1) = \gamma + (1 - \gamma - \lambda)\frac{1}{1 + e^{\left(-\frac{NSD-\mu}{\nu}\right)}} \quad (2)$$

where *NSD* is normalized speed difference, (*sp2-sp1*) / (*sp2+sp1*), γ is the lower asymptote, λ is the upper asymptote, *1/ν* is the maximum slope of the curve and μ is the *NSD* at the curve's inflection point.

In order to quantify the bias of previous stimulus duration on the percept of current stimulus, we then computed a linear correlation between the *PSE* values fitted for different duration category on trial *N-1*, and the category identity (-1 for short stimuli, +1 for long stimuli). The additive inverse of the regression coefficient was defined as *history duration bias*.

Duration delayed comparison task:

To characterize how previous stimulus duration changed the performance of the duration delayed comparison trials, we computed the proportion of trials in which subjects judged $Stimulus\ 2 > Stimulus\ 1$ on stimulus pairs characterized by a fixed

$T1$ ($T1 = 300$ ms for human subjects, $T1 = 334$ ms for rats) and different $T2$ values, separately for each category of duration (short/long) presented on trial N-1, by fitting:

$$P(Stim2 > Stim1) = \gamma + (1 - \gamma - \lambda)\frac{1}{1 + e^{\left(-\frac{NTD-\mu}{\nu}\right)}} \quad (3)$$

where γ is the lower asymptote, λ is the upper asymptote, *1/ν* is the maximum slope of the curve and μ is the NTD at the curve's inflection point.

In order to quantifying the bias of previous stimulus duration on the percept of current stimulus, we then computed a linear correlation between the *PSE* values fitted for different duration category on trial *N-1*, and the category identity (-1 for short stimuli, +1 for long stimuli). The additive inverse of the regression coefficient, was defined as *history duration bias*.

To characterize how previous stimulus intensity changed the performance of the duration delayed comparison trials, we computed the proportion of trials in which subjects judged $Stimulus\ 2\ >\ Stimulus\ 1$ on stimulus pairs characterized by a fixed $T1$ ($T1 = 300$ ms for human subjects, $T1 = 334$ ms for rats) and different $T2$ values, separately for each category of intensity (weak/strong) presented on trial *N-1*, by fitting:

$$P(Stim2 > Stim1) = \gamma + (1 - \gamma - \lambda)\frac{1}{1 + e^{\left(-\frac{NTD-\mu}{\nu}\right)}} \quad (4)$$

s

where γ is the lower asymptote, λ is the upper asymptote, *1/ν* is the maximum slope of the curve and μ is the NTD at the curve's inflection point.

In order to quantifying the bias of previous stimulus intensity on the percept of current stimulus, we then computed a linear correlation between the *PSE* values fitted for different intensity category on trial *N-1*, and the category identity (-1 for weak stimuli, +1 for strong stimuli). The additive inverse of the regression coefficient was defined as *history intensity bias*.

Analysis of estimation task data

In order to make each subject's subjective scale comparable, we used a min-max normalization algorithm:

$$Normalized\ x_n = 9\frac{x_n - min(x)}{max(x)\ - min(x)} + 1 \quad (5)$$

where x_n is the non-normalized response on trial n, x is the range of total responses, and $Normalized\ x_n$ is the normalized response. We then multiplied by 9 and added 1, so that the normalized responses range from 1 to 10.

In order to estimate the bias of previous stimulus intensity on perceived intensity for intensity estimation trials, we first computed the average normalized response across all possible *sp* values of the stimulus presented at trial *N*, for each *sp* presented at trial *N-1*, when trial *N-1* was an intensity estimation task. We then computed a linear regression between the average normalized responses and stimulus *N-1 sp* (in

logarithmic scale), and defined the regression slope as *history intensity bias*. In order to estimate the bias of previous stimulus duration on perceived intensity for intensity estimation trials, we first computed the average normalized response across all possible *sp* values of the stimulus presented at trial *N*, for each *T* presented at trial *N-1* when trial *N-1* was an intensity estimation task. We then computed a linear regression between the average normalized responses and stimulus *N-1 T* (in logarithmic scale) and defined the regression slope as *history duration bias*. Parallel analyses were done for duration estimation trials.

In order to assess the effect of previous stimulus perceived intensity and perceived duration, on the current percept, we divided the perceived values of stimulus presented at trial *N-1* in three categories: short/medium/long if trial *N-1* was a duration estimation trial, weak/medium/strong if trial *N-1* was an intensity estimation trial. The three categories were defined as the lower, central and upper terciles of the whole distribution of responses. To quantify the effect of previous stimulus percept on intensity estimation trials we computed the average normalized response across all possible *sp* values of the stimulus presented at trial *N*, for each category of percept reported at trial *N-1*. We then computed a linear regression between the average normalized responses and the median perceived value of each category and defined the regression slope as *intensity history bias* or *duration history bias*, according to the trial *N-1* task. Similarly, for duration estimation trials we computed the average normalized response across all possible *T* values of the stimulus presented at trial *N*, for each category of percept reported at trial *N-1*. We then computed a linear regression between the average normalized responses and the median perceived value of each category and defined the regression slope as *intensity history bias* or *duration history bias*, according to the trial *N-1* task. The same

type of analysis where done to quantify the effect of trial *N-2*, using the percept reported two trials before the current one.

Multiple linear regressions shown on Figure 9 were done using `fitrlinear` matlab function, with a ridge (L2) regularization. The reported percept a trial *N* was used as the dependent variable, while the mean speed, the duration and the reported percept of the stimulus presented at trial *N-1*, were used as explanatory variables. The lambda parameter for the regularization used, was the one that minimized the loss estimate of a 10 fold cross-validation among all possible lambda values from 1 to 1000. The optimal lambda was 589 and 577 for the intensity and the duration estimation dataset, respectively.

Supplementary figures

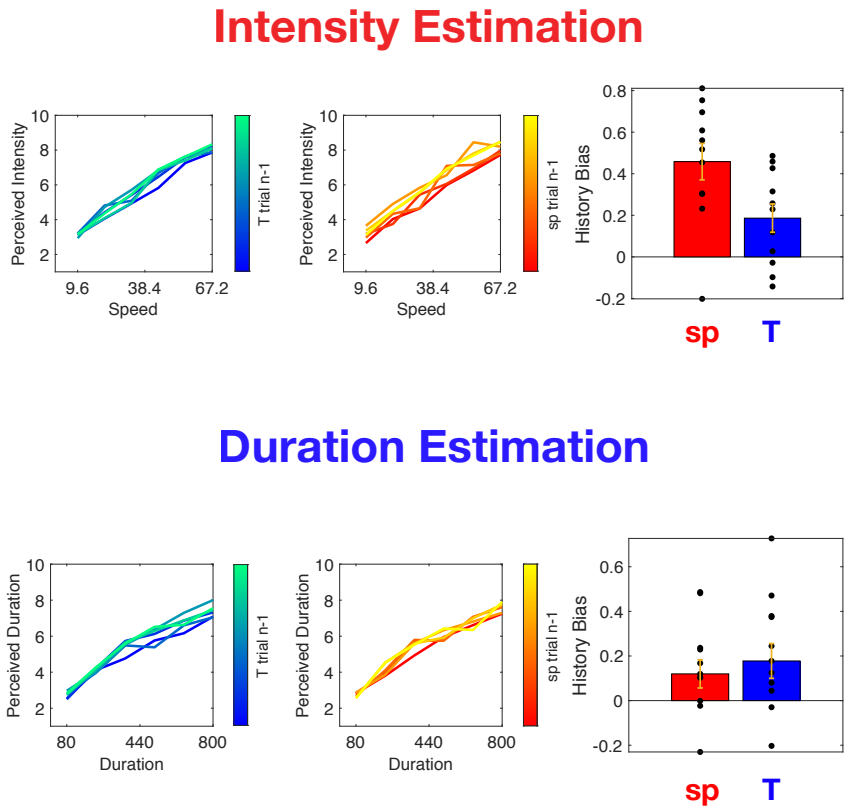

Supplementary Figure 1. Serial dependences in estimation task do not depend on the slider orientation.
A) Intensity estimation results: median perceived intensity as a function of stimulus speed, computed separately for each duration (left panel) and speed (middle panel) of the trial *N-1* stimulus, when the slider had opposite orientation between trial *N* and *N-1*. Right panel shows the *duration history bias* in blue and *intensity history bias* in red of all subjects. Each dot is a single subject, while error bars are S.E.M. Both biases are significantly different from zero (two-tailed Wilcoxon signed rank test, $p < 0.05$)
B) Duration estimation results: median perceived duration as a function of stimulus duration, computed separately for each duration (left panel) and speed (middle panel) of the trial *N-1* stimulus, when the slider had opposite orientation between trial *N* and *N-1*. Right panel shows the *duration history bias* in blue and *intensity history bias* in red of all subjects. Each dot is a single subject, while error bars are S.E.M. The duration history bias was significantly different from zero (two-tailed Wilcoxon signed rank test, $p < 0.05$), as well as the intensity history bias (two-tailed Wilcoxon signed rank test, $p < 0.05$).

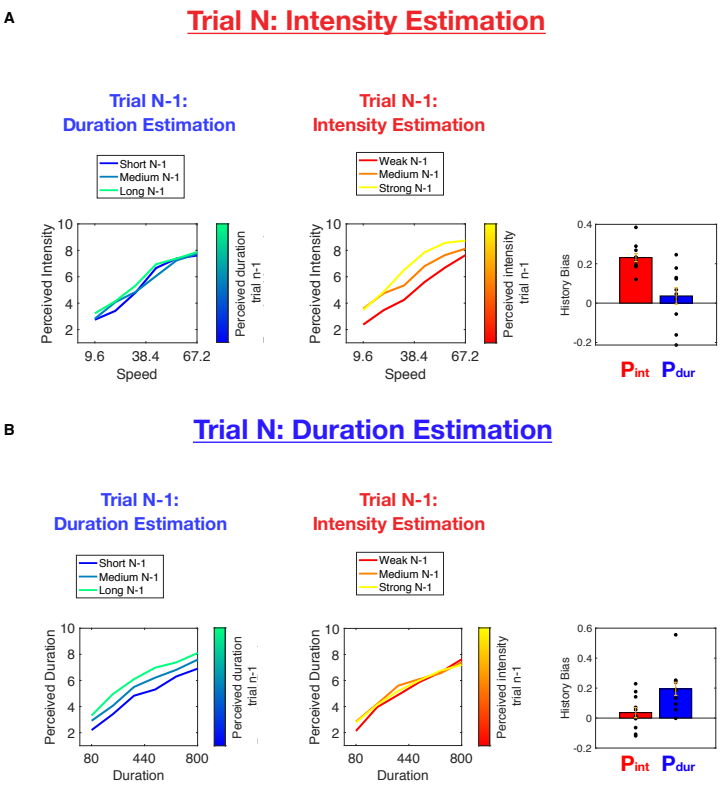

Supplementary Figure 2. Serial dependencies in the direct estimation task do not depend on slider orientation: different task on trials *N-1* and *N*.
A) Intensity estimation results: median perceived intensity as a function of stimulus speed, computed separately for different levels of perceived duration (left panel) and perceived intensity (middle panel) of the trial *N-1* stimulus, when the slider had opposite orientation between trial *N* and *N-1*. Right panel shows the *duration history bias* in blue and *intensity history bias* in red of all subjects. Each dot is a single subject, while error bars are S.E.M. Perceived intensity on trial *N* is significantly attracted towards the *N-1* perceived intensity (two-tailed Wilcoxon signed rank test, $p < 0.01$),), but not its perceived duration (two-tailed Wilcoxon signed rank test, $p = 0.2$).
B) Duration estimation results: median perceived duration as a function of stimulus duration, computed separately for each perceived duration (left panel) and perceived speed (middle panel) of the stimulus presented on trial N-1, when the slider had opposite orientation between trial *N* and *N-1*. Rightmost panel shows the *duration history bias* in blue and *intensity history bias* of all subjects. Each dot is a single subject, while error bars are S.E.M. Perceived intensity is significantly affected by previous stimulus perceived duration (two-tailed Wilcoxon signed rank test, $p < 0.01$), but not its perceived intensity (two-tailed Wilcoxon signed rank test, $p = 0.2$).

Chapter III: Neuronal correlates of perceived stimulus duration in Dorsolateral Striatum

Introduction

Which brain systems, and which mechanisms therein, are responsible for the perception of time remains one of the most intriguing questions in behavioral neuroscience. Many areas have been proposed to be involved in this computation, including prefrontal cortex (70–72), premotor cortical areas (73–75), parietal cortex (76), hippocampus (77, 78), cerebellum (79) and striatum (70, 80, 81). In particular, recent publications give persuasive arguments for the involvement of the basal ganglia in the perception of time, and that will be focus of this chapter. Time can be reliably decoded from the striatal population activity of rats involved in either a reproduction task (81) or a bisection task (80). Optogenetic manipulations of dopaminergic midbrain neurons, many of which project directly to dorso-central striatum, modulate the judgment of time in mice (82). Another recent paper compared the encoding of elapsed time between orbital frontal cortex and striatum, showing that striatum could serve as a more reliable clock (83).

The *duration delayed comparison* task of Chapters I-II offers two novel approaches to the search for the neurophysiological basis of time perception. First, the stimulus matrix used in the task dissociates Stimulus 1 from any decisional process. This means that the neuronal activity that encodes Stimulus 1 duration will not be subject to the cofound of decisional or motor-preparation information. As will be discussed later, temporal overlapping of motor preparation could confound the coding of *perceptual* with the coding of *non-perceptual* (albeit related) functions. Second, the well-documented perceptual bias of stimulus intensity on perceived duration ("stronger feels longer;" see Chapters I-II) implies that a neuronal population code can be a candidate for the

substrate of time perception if, and only if, that neuronal code exhibits the same intensity/duration confound.

Following this rationale, we recorded neuronal activity from the striatum of three rats as they performed the tactile *duration delayed comparison* task. Specifically, we targeted the dorso-lateral part of striatum (DLS), a region found receiving direct input from vS1 (84). The results to be presented here indicate that time information is explicitly encoded within the DLS neuronal population (consistent with recent publications), yet that information does not appear to coincide with the rat's reported percept of vibration duration. By recording neurons from the same striatal region of rats involved in an *intensity* delayed comparison task, we show that the passage of time is present in the striatum independently of the perceptual feature that is extracted from the stimulus.

Results

Dorsolateral striatal activity accompanying duration delayed comparison

To investigate the role of the striatum in time perception, we trained 3 rats in the same *duration delayed comparison* task described in Chapters I and II (Figures 1A and B). Two rats also participated in the experiments described in Chapter I and II, while one was new. Since this chapter focuses on neuronal coding, it reports only studies of rats. Figure 1C shows all the presented combinations of *T1/T2* and *sp1/sp2*. As before, *NSD* (normalized speed difference) was defined as *(sp2-sp1)/(sp2+sp1)* while *NTD* (normalized time difference) was defined as *(T2-T1)/(T2+T1)*. In this experimental design, *NTD* could assume two values (either -0.35 or 0.35), while *NSD* could assume three (-0.3, 0, 0.3). The color code used in Figure 1C highlights the mean probability of reporting *T2>T1* for each stimulus pair among the three rats, showing that they were able to judge stimulus duration, but were biased by stimulus *sp*: confirming earlier chapters, stronger stimuli were more likely to be reported as longer in perceived duration. Figure 1D summarizes the performance of the 3 rats in the *duration delayed comparison* task. The left plot shows how the probability of reporting *T2>T1* varied with *NTD*, while the right plot shows how the probability of reporting *T2>T1* varied with *NSD*; the first measure quantifies task performance while the second measures quantifies the *sp* bias on perceived duration.

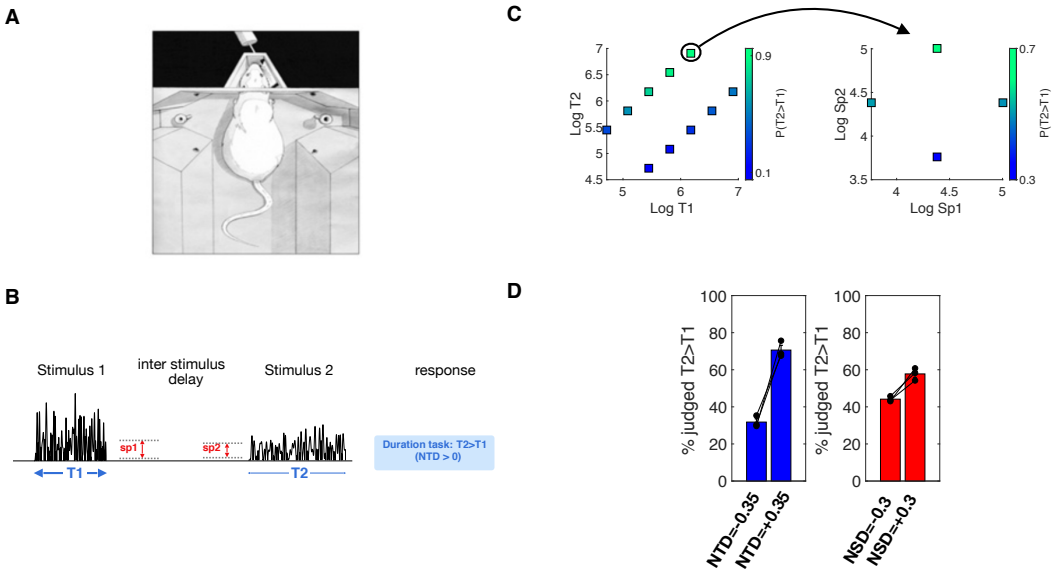

Figure 1. Experiment conditions and behavioral results.
A) Experiment setup for the rat.
B) Representation of delayed comparison trial structure. Each trial consisted of the presentation of two noisy stimuli, with specified durations and mean speeds, separated by an interstimulus delay. The response was deemed correct according to the relative durations (blue-shaded rule) of Stimulus 1 and 2.
C) Average probability across subjects of reporting *T2>T1* for each *T1*/*T2* and *sp1*/*sp2* pair.
D) Mean probability of reporting *T2>T1* according to *NTD* values (left) and *NSD* values (right). Each dot represents a single subject; error bars are S.E.M.

All three rats received a chronic electrode implant in the dorsolateral striatum (DLS). This target was selected because DLS receives direct input from both vS1 and the medial part of the posterior thalamic nucleus (85), and has been proposed to be involved in the sensory processing of tactile information (84). Moreover, this region overlaps with the one found to be involved in the encoding of the passage of time, in rats engaged in a duration categorization task (80). Neuronal activity was collected during the behavioral task through extracellular recordings (see Methods).

A total of 549 neurons were recorded from the three rats (rat 1: n=130, rat 2: n=194, rat 3: n=225). By characterizing the spike shape of each neuron (see 86), we classified each neuron as either a Medium Spiny neuron (MSN, 69% of the population), or a Fast Spiking neuron (FSN, 31%), as depicted in Figure 2A. When temporally aligned to behavioral events, neuronal activity in DLS was heterogeneous; by characterizing firing

profiles in relation to the task time line (see Methods), we identified three functional categories of neurons: action-selective neurons (34% of the recorded population), motor preparation neurons (12%), and ramping neurons (51%). Action-selective neurons fired only after the go-cue sounded, as the rat moved towards one of the two reward spouts (i.e., firing differentially according to left versus right) (Figure 2B). Motor preparation neurons also fired differentially for the two possible choices, but did so before the go cue sounded (Figure 2C). Finally, ramping neurons – which comprised around half the DLS population – exhibited two main characteristics: (i) their firing rate profile was stereotyped across trials, independently of Stimulus 1 or Stimulus 2 duration, and (ii) their firing rate started to ramp either up or down at a specific time point during the trial. The time point at which the neuron started ramping was always fixed in relation to behaviorally-relevant events: nose poke, Stimulus 1 onset or offset, or Stimulus 2 onset or offset (Figure 2D, see Methods).

As no single neuron could be found to clearly encode mean speed (see Methods), as in other cortical areas such as vS1 or vM1 (4), we asked if stimulus duration or mean speed might be represented through a neuronal population code.

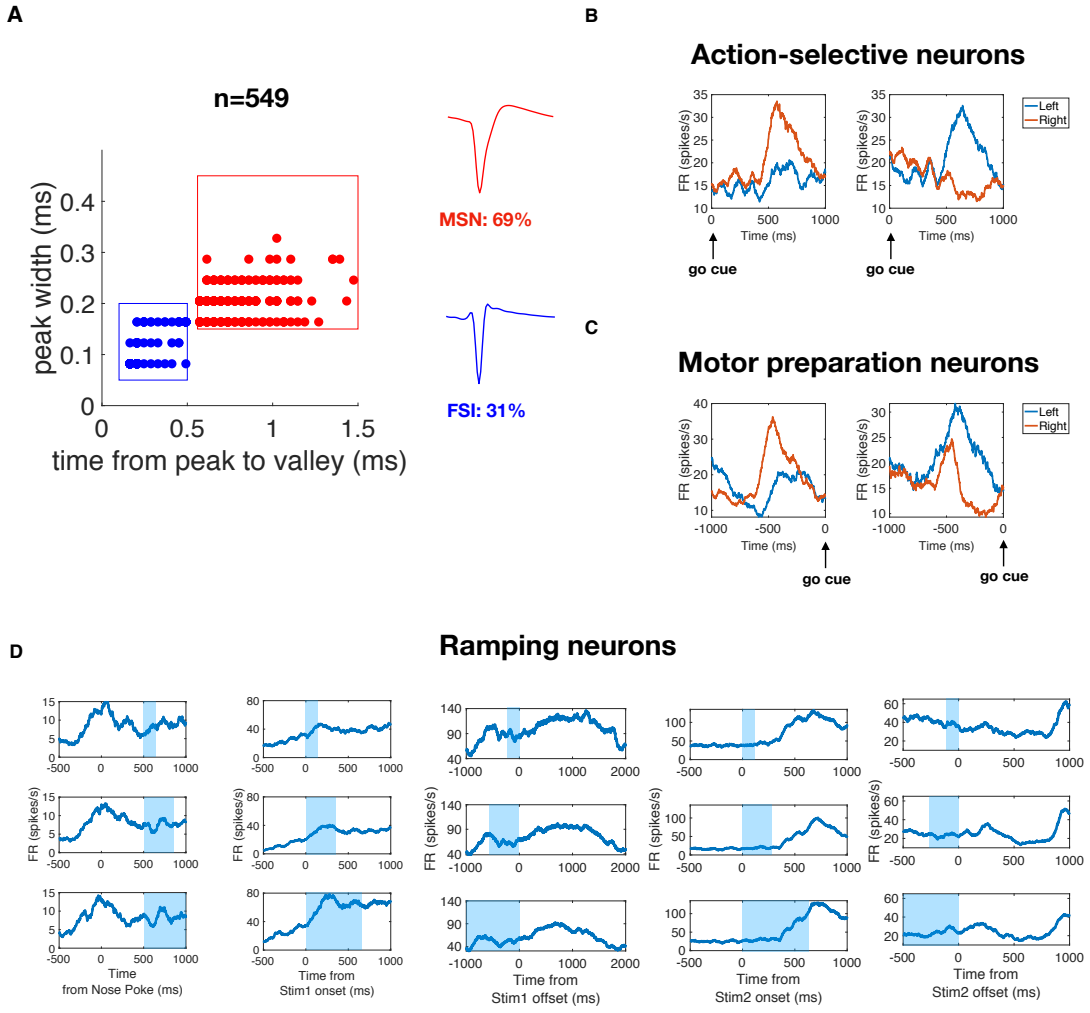

Figure 2. Characteristics of the neuronal population of DLS.
A) Neurons were classified as Medium Spiny (red) or Fast Spiking (blue) according to spike shape. Example spike waveforms are illustrated.
B) Action-selective neurons: two striatal neurons showed a jump in firing rate, selective to turn direction, 500 ms after the go cue.
C) Motor preparation neurons: two striatal neurons showed a jump in firing rate before the go cue, selective to the upcoming turn direction.
D) Ramping neurons: firing profile of ramping neurons, aligned to different trial epochs (nose poke, Stimulus 1 onset, Stimulus 1 offset, Stimulus 2 onset, Stimulus 2 offset). The firing profile is conserved across trials, independently of stimulus duration (blue shadow).

DLS encodes trial time, but not the perceived stimulus duration

Not having detected duration coding in single neurons, we explored population coding. More precisely, we used a Bayesian decoder (see Methods) to evaluate whether information about stimulus duration was encoded within the DLS neuronal population activity patterns. This replicated the analysis methodology used to conclude that DLS

underlies time perception (87). The decoder computes the conditional probability density function $P(t|population_T)$ of being at certain time point *t* during the trial, given the firing patterns of a neuronal population $population_T$, recorded at a specific time window *T*. Window size was 75 ms and was advanced in 1 ms steps. Figure 3A shows the decoded time (defined as the maximum a posteriori of $P(t|population_T)$, for the neuronal activity at each time *T*), using the neuronal activity patterns during the Stimulus 1 and Stimulus 2 presentation. As seen in Figure 3A, the decoder is able to reliably extract the passage of time from DLS activity as the rat receives and, presumably, perceives the vibrations.

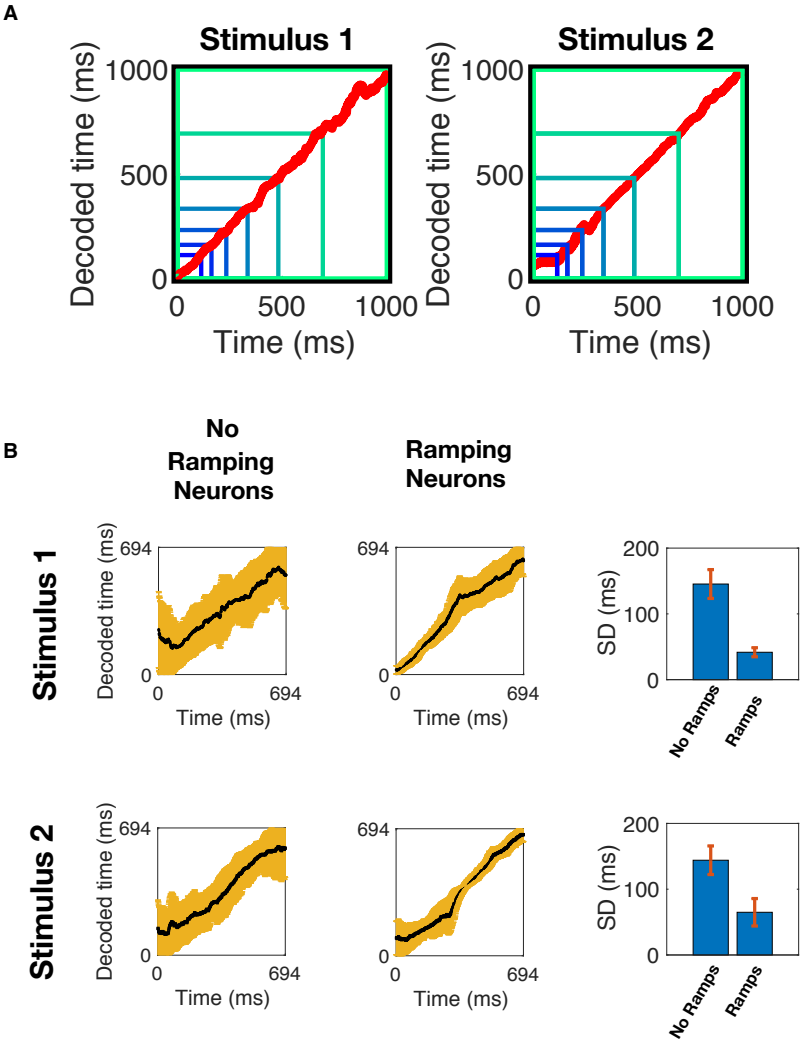

Figure 3. Decoding time from DLS population neuronal activity.
A) Decoded time during Stimulus 1 and Stimulus 2, from the activity of DLS. The squares bordered in blue to green denote the presented vibration durations, from 112 to 1000 ms.
B) Decoded time during Stimulus 1 (upper row) and Stimulus 2 (lower row), in a neuronal population from which ramping neurons have been excluded (left column) and made up of only ramping neurons (right column). Black lines indicate the decoded time, while brown margins indicate the SD of the decoded time. The rightmost plots show the average SD of the decoded time using the two neuronal populations for Stimulus 1 (upper panel) and Stimulus 2 (lower panel). Ramping neurons support the decoder with more precision.

Given the clear evidence that the population encodes the passage of time, we asked if a specific type of neuron, from among those depicted in Figure 2, is more relevant than others in this code. We generated two subpopulations containing equal numbers of neurons: a subpopulation of ramping neurons, and a subpopulation of non-ramping neurons. As shown in Figure 3B, the ramping neuron subpopulation was much more

reliable in encoding time within the stimulus presentation. It is of note that time is most efficiently coded by those neurons whose firing rate profile has a clear, stereotypical temporal profile, yet a profile unrelated to actual stimulus duration (blue shading, Figure 2D). This observation constituted the first hint that the DLS might represent the passage of time but not the rat's percept of stimulus duration. In other words, while the plots of Figure 3A suggest that information about time is present in the temporal dynamics of neuronal firing, the results do not directly demonstrate that DLS underlies the perception of stimulus duration used by the rat to solve the task.

In alternative, time information might be an implicit property of the population dynamics, acting as the neuronal substrate of time-related behaviors distinct from the duration percept. We specified three criteria that should be met to support the hypothesis that the striatal population encodes the rat's *perceived time*, as opposed to the configuration of behavior across absolute time. First, the neuronal population should show the same bias imposed by stimulus intensity on perceived time, a robust, universal bias demonstrated by all preceding experiments (also, in humans). That is, given that the stronger stimulus feels longer, in DLS the stronger stimulus should be encoded and decoded as longer. Second, if DLS is involved in the generation of the perception of time, it should encode stimulus duration differently on trials in which the rat correctly vs incorrectly perceived time, as estimated by choice. Third, DLS should show a privileged representation of the durations that must be perceived and acted on, compared to the durations of other trial epochs.

The first criterion is tested in Figure 4A, which shows the decoded time during Stimulus 1 and Stimulus 2, for different stimulus *sp* values (see Methods). The decoded time from the DLS population does not vary according to *sp*. Moreover, from the probability

density functions $P(t|population_T)$ computed for Stimulus 1 and Stimulus 2, we calculated the probability of the decoder of reporting *T2>T1* for each duration pair, separately for each *sp* pair (see Methods). Figure 4B shows that the choices of the decoder were not influenced by *NSD* values (upper panel), differently from the real animal behavior, where choices were biased by stimulus speed (lower panel).

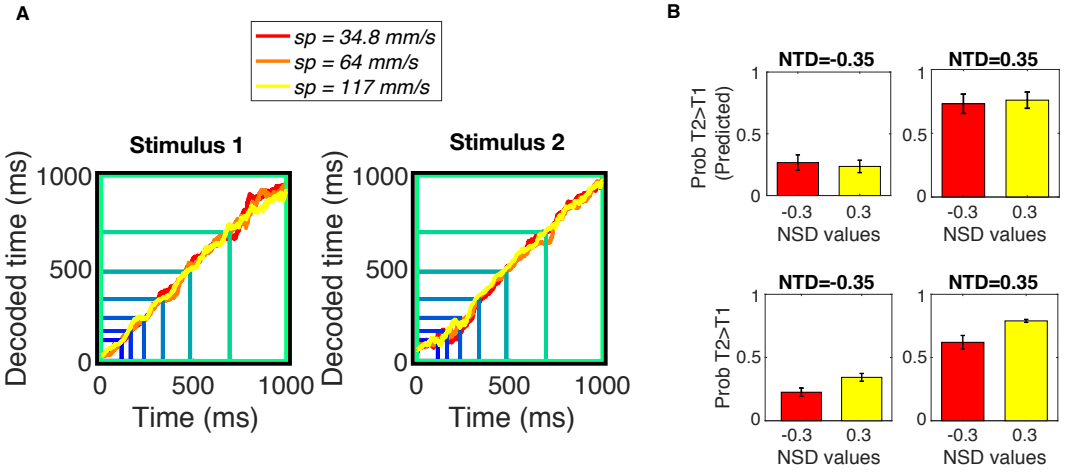

Figure 4. Dependence of DLS time coding time on stimulus mean speed.
A) Decoded time during Stimulus 1 and Stimulus 2 presentation, separated by vibration *sp*. There were no significant differences between decoded times for different speed conditions (one-tailed Wilcoxon signed rank test, $p > 0.05$ between each pair of speed conditions).
B) Upper plots: Decoded probability of *T2>T1* choice from the neuronal population, for different *NTD* and *NSD* values. The value of *NSD* did not bias the neuronal population in favor of either choice (ANOVA, p=0.81 for *NTD*=-0.35, p=0.17 for *NTD*=0.35). Lower plots: Actual probability of *T2>T1* choice seen in rat behavior, for different *NTD* and *NSD* values (ANOVA, p<0.05 for *NTD*=-0.35 and *NTD*=0.35). In the behaving rat, the value of *NSD* biased choices in the direction of "stronger feels longer."

To evaluate the second criterion –DLS must carry time information differently on correct versus incorrect trials – first, we trained the decoder using DLS population firing on correct-only trials, and then decoded the passage of time during both correct and incorrect trials (see Methods). Figure 5A shows that time can be extracted from incorrect trials equally as accurately as from correct trials (the plot for correct is overwritten by incorrect). Secondly, from the probability density functions $P(t|population_T)$ computed for correct and incorrect trials, we calculated the

probability of the decoder reporting *T2>T1* for each duration pair (see Methods). Figure 5B shows that the choices of the decoder were not different for correct and incorrect trials, signifying that the encoding of stimulus durations in DLS was not different when the animal made the wrong choice. In short, there is no apparent choice-predictive signal in DLS, at least in the Bayesian decoder.

Finally, the data obtained from DLS failed to reveal a pronounced and task-specific representation of the stimulus duration, as stated for the third criterion (Figure 5C and 5D). While the passage of time within the stimuli can in fact be decoded (Figures 3-4), it is not a privileged representation, for the DLS population appears to track the elapsed time of the entire trial. Any behaviorally relevant interval – pre stimulus delay, inter stimulus interval, post stimulus delay – could be equally as well decoded.

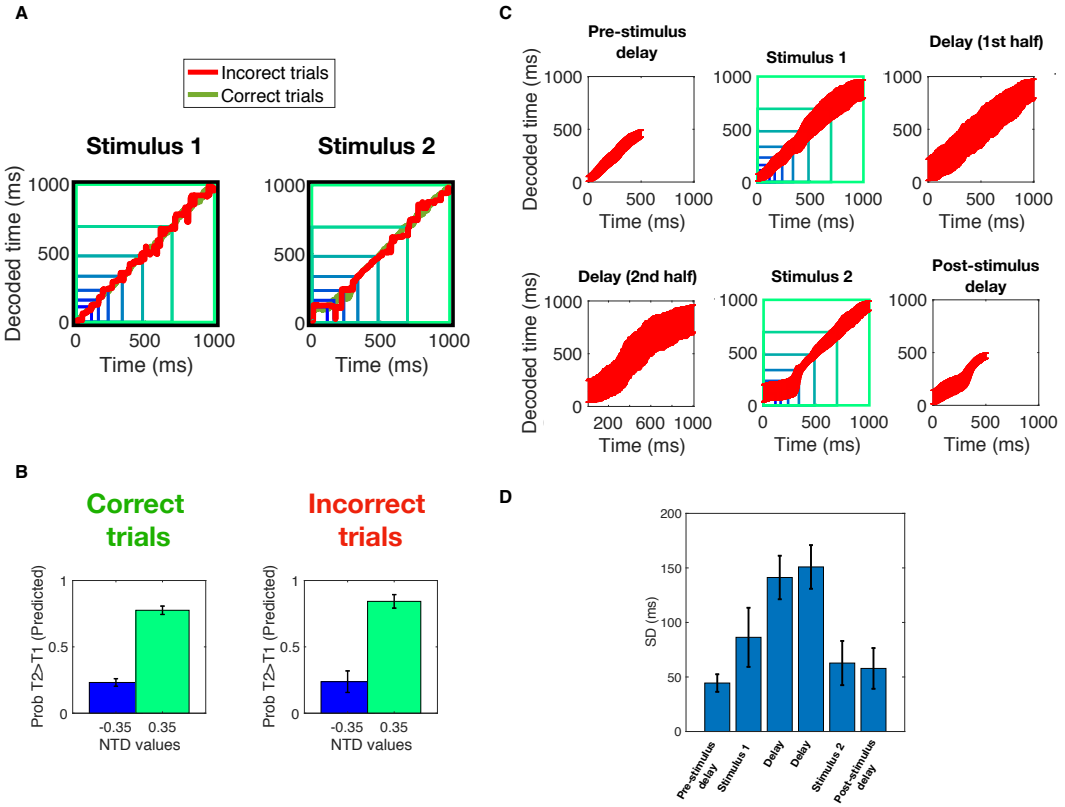

Figure 5. Task-specificity of the coding of time in DLS.
A) Decoded time during Stimulus 1 and Stimulus 2 presentation for correct (green) and incorrect (red) trials.
B) Decoded probability of *T2>T1* choice from the neuronal population, for different *NTD* values for correct (left panel) and incorrect (right panel) trials. The trial type did not bias the neuronal population.
C) Decoded time for different trial epochs.
D) Average standard deviation of the decoded time of each trial epoch. The decoder was able to decode time within the pre stimulus delay, post stimulus delay, and either stimulus duration, with similar accuracy. Accuracy was significantly worse for the time passed during the delay.

Overall our results support the contention that DLS neuronal activity, seen as a population, holds the brain's representation of the unfolding of the trial in time. It does so principally through the temporal dynamics of ramping neurons' activity. In our analyses, DLS neurons failed to satisfy three criteria established *a priori* for the properties of a neuronal population encoding the explicit percept of stimulus duration.

DLS encodes time during an intensity delayed comparison task

The findings described in the preceding section led us to ask whether the encoding of time in DLS was related to the requirement of the behavioral task to judge time. Thus,

as a final control experiment to assess whether time information is inherent to striatal activity irrespectively of the rat's ongoing percept, we recorded neuronal population firing from the same DLS region in two rats that were trained to discriminate stimulus intensities. Indeed, in the intensity task, stimulus duration is a confounding feature that would be discarded by the ideal observer (Chapter I).

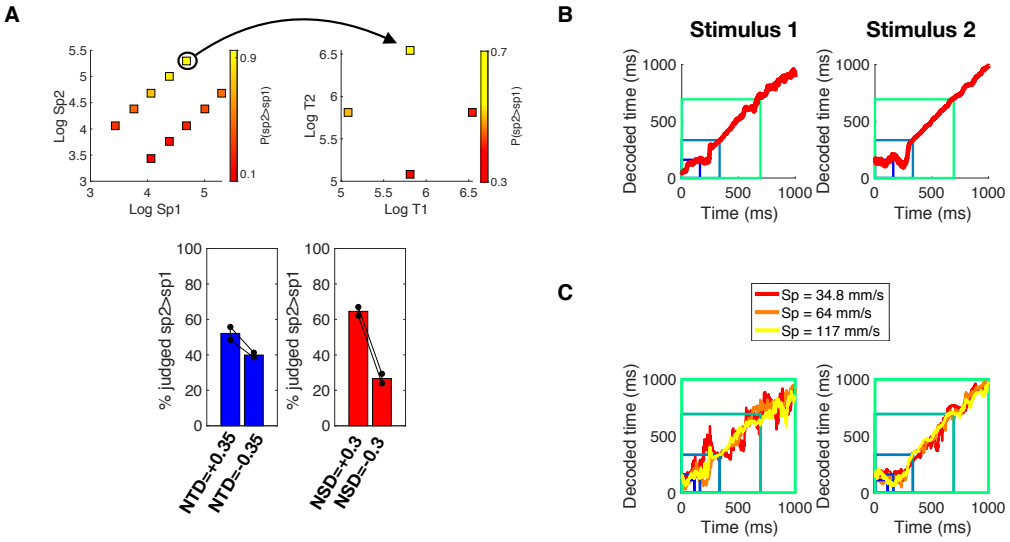

Figure 6. DLS involvement in the *intensity delayed comparison* task.
A) The upper panel shows the average probability across subjects of reporting *sp2>sp1* for each *sp1*/*sp2* and *T1*/*T2* pair. The lower panel shows the mean probability of reporting *sp2>sp1* according to *NTD* values (left) and *NSD* values (right). Each dot represents a single subject; error bars are S.E.M.
B) Decoded time during Stimulus 1 and Stimulus 2, from the activity of DLS of intensity rats. The squares bordered in blue to green denote the presented vibration durations, from 161 to 694 ms.
C) Decoded time during Stimulus 1 and Stimulus 2 presentation, separated by vibration *sp*. There were no significant differences between decoded times for different speed conditions (one-tailed Wilcoxon signed rank test, $p > 0.05$ between each pair of speed conditions).

Figure 6A shows all the combinations of *sp1/sp2* and *T1/T2* pairs, that were presented to the rats, in a manner exactly symmetrical to the *duration delayed comparison* task: *NSD* could assume two values (-0.35 or 0.35), while *NTD* could assume three (-0.3, 0, 0.3). The color code used in the upper panel of Figure 6A highlights the mean probability of reporting *sp2>sp1* for each stimulus pair among the two rats, showing that they were able to judge stimuli intensities, but were biased by stimulus *T*: confirming earlier chapters, longer stimuli were more likely to be reported as stronger

in perceived intensity. The lower panel of Figure 6A summarizes the performance of the 2 rats in the *intensity delayed comparison* task. The left panel shows how the probability of reporting *sp2>sp1* varied with *NSD*, while the right panel shows how the probability of reporting *sp2>sp1* varied with *NTD*; the first measure quantifies task performance while the second measures quantifies the *T* bias on perceived intensity

A total of 419 neurons were recorded from the two rats (rat 1: n=166, rat 2: n=253). Of these, 74% were defined as Medium Spiny neurons, while 26% were defined as Fast Spiking neurons (proportions not different from the duration rats; Fisher's exact test p=0.53). Figure 6B shows that, through the same Bayesian decoder applied to data from the *duration* rats, the passage of time can be extracted from DLS population activity in rats trained in an *intensity delayed comparison* task (Figure 6B). Analogous to the results from *duration delayed comparison* rats, stimulus *sp* did not bias the decoder's estimate of time (Figure 6C).

These results confirm that information about trial time is present in the dynamics of the neuronal activity of the DLS, irrespectively of the importance of stimulus duration for the behavioral task in which the animal is engaged.

Our results are in contradiction with recent work that showing that striatal activity is related to the perception of stimulus duration (80). In that study, not only was the duration of the stimulus to be timed decodable from striatal population, but the decoder was able to capture the over- or under-estimates that the rat made in incorrect trials. We argue that the earlier results can be explained by the overlap of perceptual, decisional and motor computations present in reference memory task. More specifically, the

correlation of stimulus duration with the corresponding motor output could bias the decoder to over- or under-estimate stimulus duration during incorrect choices, simply by using motor-related neuronal activity to decode time. To be more concrete, if the long duration was associated with turning left and short duration associated with turning right, then in a long trial with incorrect choice, the (incorrect) motor program for turning right would be decoded as a short stimulus duration; the decoder might have read out the motor plan, which was in fact highly correlated with the passage of time.

In order to test this hypothesis, we ran additional analyses. We treated the data as if rats were carrying out a reference memory task, in which Stimulus 2, had to be classified as long or short compared to a fixed duration (334 ms; see Methods). We then classified the trials as correct or incorrect, according to this "rule." We trained the classifier to decode stimulus duration using only correct trials, and then tested it using either correct or incorrect trials. When applying these analyses onto the post stimulus delay after Stimulus 2, the classifier tended to overestimate short, incorrect trials and underestimate long, incorrect trials (Figure 7A). This difference in decoded time appeared after Stimulus 2 offset, when neuronal activity linked to motor preparation was present in DLS neurons. The same analyses applied to the DLS neuronal population in rats performing intensity discrimination, revealed the same biases in decoded time, suggesting that the biases are likely independent of the perceptual task (Figure 7B). Moreover, analysis of neuronal firing in the 500 ms after the end of Stimulus 1 – when no decisional or motor information were present – uncovered no over- and underestimations (Supplementary Figure 1).

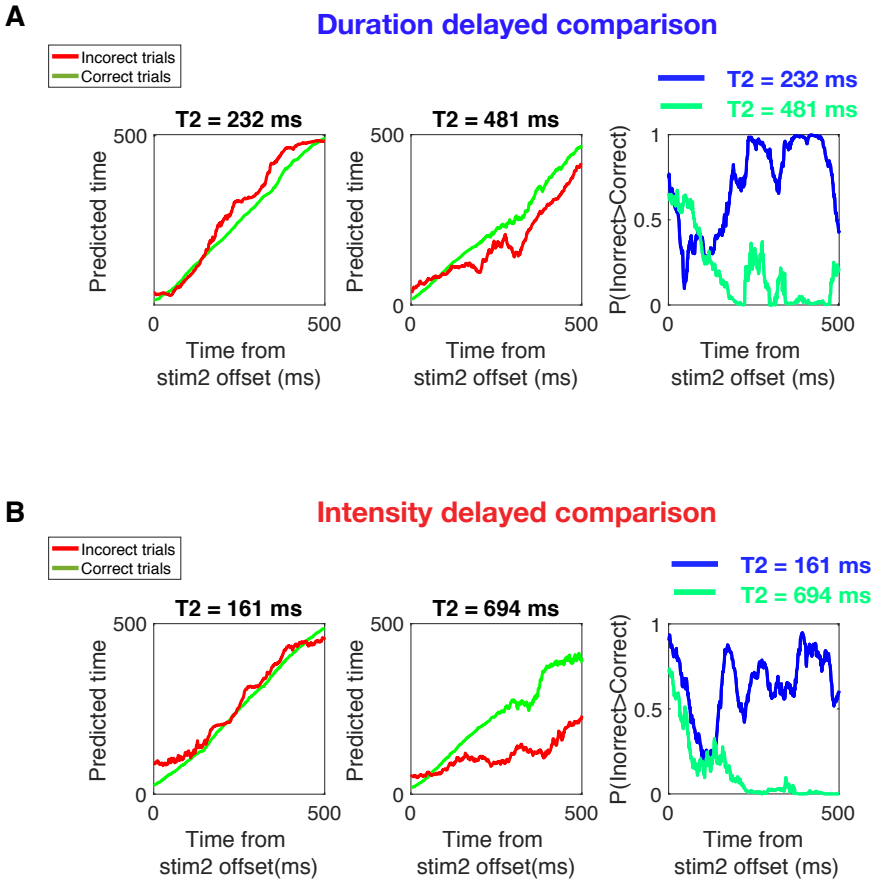

Figure 7. Decoded time from correct and incorrect trials, using a duration reference memory rule.
A) Left panel and middle panel: decoded time during post stimulus delay after Stimulus 2 offset, using correct and incorrect trials, when correctness was labeled as if the rat were classifying Stimulus 2 duration independently of Stimulus 1. The decoder overestimates short *T2* (one-tailed Wilcoxon signed rank test, $p < 0.01$) and underestimates long *T2* (one-tailed Wilcoxon signed rank test, $p < 0.01$) when tested on incorrect trials. Right panel shows the probability that the decoded time in incorrect trials is longer than correct trials, for the two possible *T2* values.
B) Same as A, but using DLS neurons recorded in rats doing an intensity estimation trials.

To confirm that the bias in decoded duration during the post stimulus delay was induced mostly by motor related activities, we conducted the same analyses in the two populations, excluding neurons that showed significant selectivity for the motor action of the rat during the relevant time window. Figures 8A and 8B show that the over- and underestimation of stimulus duration decreases significantly when motor related neuronal activity is excluded from the DLS neurons.

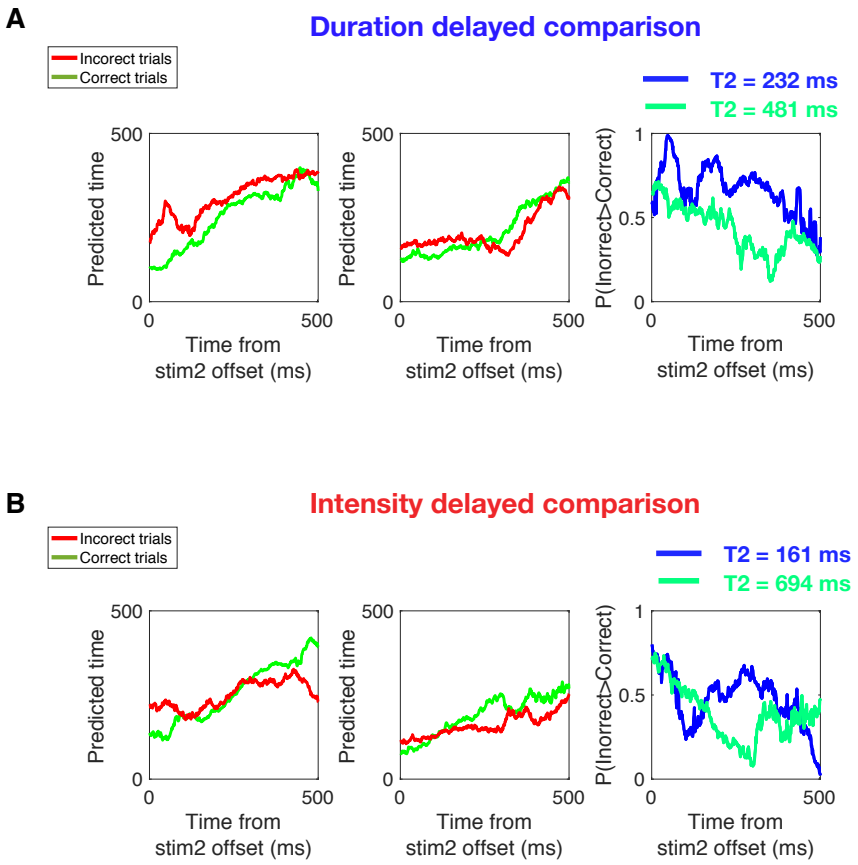

Figure 8. Decoded time from correct and incorrect trials, using a duration reference memory rule, excluding motor related neuronal activities.
A) Same as Figure 7A, when excluding from the DLS population neurons selective for any motor related information. Overestimation of short *T2* is significantly lower than for the full DLS population (one-tailed Wilcoxon signed rank test, $p < 0.01$), as for the underestimation of long *T2* (one-tailed Wilcoxon signed rank test, $p < 0.01$).
B) Same as Figure 7B, when excluding from the DLS population neurons selective for any motor related information. Overestimation of short *T2* is significantly lower than for the full DLS population (one-tailed Wilcoxon signed rank test, $p < 0.01$), as for the underestimation of long *T2* (one-tailed Wilcoxon signed rank test, $p < 0.01$).

Discussion

The neuronal underpinnings of time perception are the object of intensive research. Both neuroimaging and neurophysiological studies have revealed numerous brain regions in which activity correlates with the passage of time. Single-cell recordings from hippocampus of rats showed that the passage of time between the presentation of an object and an odor can be reconstructed from the neuronal activity of so called "time cells" which, taken as a group, fire at sequential moments during the trial (78). Recently, lateral entorhinal cortex of rats was shown to integrate temporal information across different timescales in freely moving rats (77), though the rats were not challenged with any time-dependent task, nor was the temporal information shown to be perceptually accessed by the rats. Time can be decoded from the neuronal activity of prefrontal cortex and striatum of monkeys doing a visuomotor task (70). This decoding, like the case of hippocampus (78), could be done by virtue of neurons whose activity peaked at different time delays after each task event. In all three cases, time was implicitly encoded in the neuronal population, but animals were not asked explicitly to estimate or report the perceived time of an interval or a stimulus.

Other studies recorded the activity of single cells in animals engaged in behavioral tasks which required the extraction of temporal information. Neurons in premotor areas, have been shown to encode the time interval that monkeys have to reproduce either by making a saccade or a button press (74, 88), or the time reproduced in a synchronization-continuation task (73). Similarly, when rats were trained to wait for a specific time interval before licking the reward spout, medial prefrontal cortex neurons exhibited temporal profiles of activity that scaled with the duration to be timed (71).

Similar results were found when recording from striatal neuronal population of rats involved in an interval reproduction task (81).

Another common behavioral task is the reference memory task. In this case the animal is required to categorize a stimulus as short or long, compared to a fixed base duration. Neurons in posterior parietal cortex were found to encode the elapsed time relative to a remembered duration (76) and, similarly, the duration of an empty interval can be decoded from striatal (80) and prefrontal (72) neuronal population in rats involved in categorizing the duration of an interval between two auditory tones, as either short or long.

One of the main limitations of both temporal reproduction and reference memory tasks is that the duration to be perceived is correlated with the decisional and motor processes intrinsic to the tasks. This poses a limit to the interpretability of the neuronal data, for the computations underlying the generation of the perceived duration are overlapping in time at least two other processes – the building up of the decision and the motor preparation for the response. These processes are inseparable within the corresponding neuronal data.

Working memory tasks, like the one we developed, have the advantage of separating the different operations needed to solve the task on each trial: (i) encoding the relevant feature of Stimulus 1, (ii) storing the feature in memory, (iii) encoding the relevant feature of Stimulus 2, (iv) comparing the feature of Stimulus 2 to the one recalled from Stimulus 1, and (v) preparing the motor output to execute the decision. This framework allows a clear interpretation of the neuronal data recorded in behaving animals. While

in the delayed comparison task there are multiple operations underway during Stimulus 2 (like in the reference task), during Stimulus 1 a single operation is at work – time perception.

We recorded from DLS of rats engaged in the *duration delayed comparison* task, in order to investigate whether striatal neurons, previously found to be involved in the encoding of time during a reference memory task (80), would exhibit the same properties. The results show that time can be reliably decoded from neuronal population activity, independently of the stimulus feature to be extracted (whether stimulus duration or intensity), as depicted in Figures 3A and 6B. However, while time information seems to be implicitly present in the temporal dynamics of neuronal activity, it is not related to the perceived duration reported by the rat (Figure 4A and 6C). DLS seems to keep track of the unfolding of "trial time," but not specifically of perceived stimulus duration. The function of the DLS supported by our work – configuring and arranging a sequence of actions (in our case: nose poke, wait across delay, await go cue, withdrawal) – recalls the traditional theories of striatal function (89, 90).

Overall, these results show that time information is inherent in DLS neuronal firing but is not a robust correlate of perceived duration. We think that the ability of the delayed comparison task to separate percept from action, together with the perceptual bias imposed by stimulus speed on perceived duration, can be keys to the future search for the neuronal basis of duration perception. Our upcoming neurophysiological studies will target other areas that may be involved in time perception. Among them, frontal cortex, which has already been shown to represent both the speed and duration of

vibrotactile stimuli (4) and to integrate sensory input with a long enough intrinsic timescale (29), is a good candidate.

Some concluding remarks are given separately (see Appendix).

Methods

Targeting DLS

One rat was used to locate the relevant region of DLS, which receives direct input from vS1. The rat was anesthetized with 2%–2.5% Isoflurane delivered with oxygen under controlled pressure through a plastic snout mask. A single craniotomy was centered 1.25 mm posterior, and 5.75 mm lateral to bregma.

A single electrode was inserted at a depth of 900 um, in order to target layer V of vS1. While recording from vS1, electric stimulation was delivered to DLS (0 mm posterior, and 3.5 lateral to bregma, advanced into the brain at an angle of 30° to the parasagittal plane) through an electrical stimulator. The DLS electrode was stimulated at 200 uA with 0.1 ms pulses, at different depths (from 1500 to 3500 um). The monophasic positive stimulus current was flowing between two paired fhc electrodes (approx. 500um distance) that were located at the same brain depth.

Antidromic spikes were elicited in vS1 around 2 ms after stimulating DLS at 2000 and 3000 um depth (Figure 9), showing that the target area received direct input from somatosensory cortex.

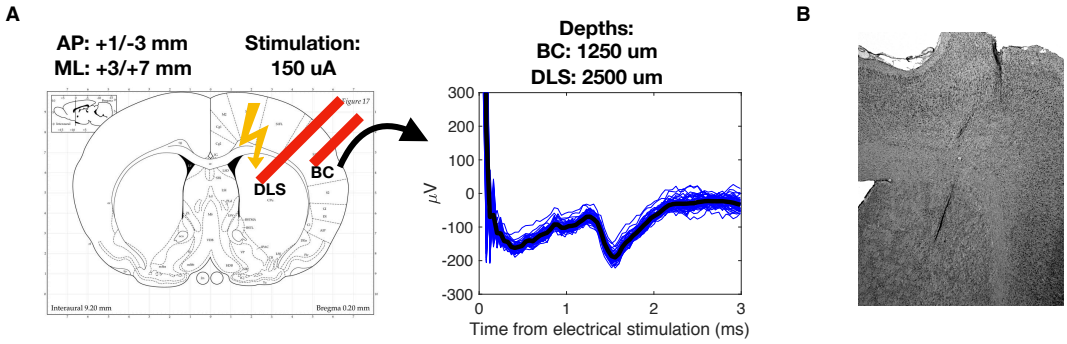

Figure 9. Targeting of DLS which receives direct input from Barrel cortex.
A) Left panel shows a sketch of the areas in which the electrode (BC) and the electrical stimulator (DLS) were inserted. Right panel shows the antidromic spikes elicited in BC by electrically stimulating DLS (150 uA pulses).
B) Example of an electrode tracks (dark tissue) inserted in DLS, in a histologically processed section with Nissl staining, after the conclusion of the experiment.

Extracellular recordings

Rats (n = 5) were anesthetized with 2%–2.5% Isoflurane delivered with oxygen under controlled pressure through a plastic snout mask. They received an implant in dorsolateral striatum. The target region was accessed by craniotomy, using standard stereotaxic technique (centered 1.25 mm posterior, and 5.75 mm lateral to bregma). Dura mater was removed over the entire craniotomy with a small syringe needle. The electrode arrays (Tucker-Davis Technologies (TDT), Alachua FL) were configured as 16 electrodes (2 rows of 8, with 250 µm within-row spacing and 375 µm between-row spacing). Electrodes were sharply tapered and shaft diameter was 50 µm. The electrode array was inserted by slowly advancing a Narashige micromanipulator. After inserting the array(s), the remaining exposed cortex was covered with biocompatible silicon (KwikSil; World Precision Instruments). Two rats were implanted with a novel movable electrode array (SISSA microdrive, Cynexo) in DLS, and re-implanted with a 16 electrodes array, after dis-implantation. In all rats, 5 small screws were fixed in the skull as support for dental cement. All screws served as

a ground and reference electrodes. One hour after the beginning of the anesthesia, atropine (2 mg/kg) was injected (s.c.) to avoid secretions in the respiratory tract and maintain a stable heart rate. They were given the antibiotic (Baytril; 5 mg/kg; i.p.) and analgesic (Rimadyl; 2.5 mg/kg; i.m.) one hour before conclusion of the operation. After surgery, a local antibiotic (Isaderm) was applied around the wound to help the healing. In addition, both the antibiotic and the analgesic were delivered through the water bottle for 24 hr after completion of surgery. During this recovery time, rats had unlimited access to water and food. Recording sessions in the apparatus began thereafter (approx. 1 week).

Extracellular activity was sorted using a MATLAB-based software, WaveClus (91). Two criteria had to be met for a neuron to be included in the analyses. First, overall firing rate within the session was at least 2 Hz. Second, overall firing rate per trial for the entire session, with many different stimulus conditions intermixed across trials, did not show a significant non-zero linear correlation ($p < 0.05$) over time. The second criterion was aimed at excluding unstable recordings.

Striatal cells were further classified as either a putative medium spiny cell (MSN), fast-spiking interneuron (FSI) based on two distinct clusters found in a scatter plot of two measurements of the wide-band spike waveform: (1) the peak width at one-half maximum (FSI: 50–200 ms; MSN: 150–450 ms), and (2) the time from peak to valley (FSI: 100–455 ms; MSN: 560–1500 ms) as shown in previous work (86). Cells that did not show a clear valley were not classified.

Classification of neuronal activity

Neurons were classified in different groups (Figure 2) following different criteria:

Action-selective neurons. To identify neurons that coded for the rat's action, we used a linear regression between the firing rate of each neuron and the movement of the rat on each trial (either left or right):

$$FR(t) = w_a(t) \cdot action + w_c(t) \quad (1)$$

Where *FR(t)* is the firing rate of each neuron calculated in a 100 ms time bin, sliding in 100 ms steps, from the time of go cue to 1 sec after it. $W_a(t)$ is the action regressor, $w_c(t)$ is a constant set according to the neuron's overall excitability at each time time *t*, independently of task variables. Values of the regressors indicate how strongly, at any given moment, the neuron's response varied in relation to the associated variable. A neuron was classified as action-selective, if it showed a significant linear coefficient (t test, $p<0.05$) in at least 5 consecutive bins.

Motor preparation neurons. To identify neurons coding for the rat's action before the presentation of the go cue, we used a linear regression between firing rate and the rat movement on each trial (Equation 1). Differently from action-selective neurons, the firing rate of each neuron was calculated in a 100 ms time bin, sliding in 100 ms steps, from 500 ms before the end of Stimulus 2 to the time of go cue.

Ramping neurons. Ramping neurons satisfied two criteria. First they showed a significant linear regression ($p < 0.05$) between the average firing rate and time in the relevant time period, with a $|r|$-value > 0.5 (where *r* is the Pearson product-moment correlation coefficient, from MATLAB function *corr*) and a $|\beta|$ value > 0.05 (where beta

is the gradient of the least-squares regression line, from MATLAB function *polyfit*). Positive ramping cells were identified as having a positive beta value, whereas negative ramping cells had negative beta values.

The relevant time periods were aligned to different trial events: i) from 500 ms before to 1 sec after nose poke, ii) from stim1 onset to 1 sec after it iii) from stim1 offset to 2 sec after it iv) from stim2 onset, to 1 s after it iv) from stim2 offset, to 1 s after it.

Secondly, their activity had to be stereotyped across trials. In order test this, we measured the average firing rate of each neuron in each relevant time period, grouping trials with same *T1/T2* combination of durations. We then calculated the correlation coefficients between the firing rate profiles for different stimulus duration pairs (using the MATLAB function corrcoef). Ramping neurons had to show a correlation coefficient > 0.5 and a p-value < 0.01.

Stimulus- selective neurons. To identify neurons that coded for stimulus speed, we used a linear regression between the firing rate of each neuron and the mean stimulus speed presented on each trial:

$$FR\ (t) = w_{sp}(t) \cdot sp + w_c(t) \qquad (2)$$

Where *FR(t)* is the firing rate of each neuron calculated in a 100 ms time bin, sliding in 100 ms steps, from either Stimulus 1 or Stimulus 2 onset. $w_{sp}(t)$ is the regressor for either *sp* of Stimulus 1 or Stimulus 2, $w_c(t)$ is a constant set according to the neuron's overall excitability at each time *t*, independently of task variables. Values of the

regressors indicate how strongly, at any given moment, the neuron's response varied in relation to the associated variable. A neuron was classified as stimulus-selective if it showed a significant linear coefficient (t test, $p<0.05$) in at least 5 consecutive bins. The analysis uncovered no neurons that significantly encoded stimulus intensity.

Decoding procedures

In order to decode the passage of time from the DLS neuronal activity, we adapted a decoding procedure from Sanger 1996 (87).

First we assume that the average firing rate of a cell in response to an externally measurable variable *x* can be specified by a tuning curve $\sigma(x)$. In our case the external variable *x* is the time *t*. The firing rate profile of each cell in time is defined as its tuning curve $\sigma(t)$. We assume that the probability of the cell firing *n* times during a short time interval Δt (set at 75 ms in our analysis) for a fixed value of *t* is given by a Poisson statistic with rate $\sigma(t)$:

$$P[n\ spikes \mid t\ ] = (\sigma(t) \cdot \Delta t)^n e^{-\sigma(t)\cdot\Delta t}/n! \quad (3)$$

Assuming that the firing rate of each cell in the population is independent, the conditional distribution for *t*, given the state of the full population of cells is:

$$P[t \mid population\ ] = \frac{1}{N}(P(t) \cdot \prod_{all\ cells} e^{-\sigma_i(t)\cdot\Delta t}) \prod_{all\ cells} \sigma_i(t)^{n_i} \quad (4)$$

Where each cell i has a tuning curve $\sigma_i(t)$, and fired n_i times during Δt . N is a normalization constant calculated so that the total probability is 1. P(t) is the prior probability density, which is a uniform distribution.

The procedure for calculating $\sigma(t)$ and $P[t \mid population]$ was specific to the analyses.

1) Decoding of stimulus duration: in order to decode the passage of time during Stimulus 1 (Figure 3) we first aligned all neuronal activity to Stimulus 1 onset. For each neuron, we selected the same number of trials for each possible Stimulus 1 duration. Half of the trials were randomly selected and used to calculate the tuning curve $\sigma(t)$ for each cell, the other half was used to calculate the number of spikes n during the interval Δt. The matrices of all cells tuning curves and of measured neuronal activity were used to calculate $P[t \mid population]$ from Equation 4. The MAP of the probability distribution $P[t \mid population]$ was taken as decoded time. Same procedure was done for Stimulus 2, a part that activity was aligned to Stimulus 2 onset.

2) Decoding of stimulus duration, for different stimulus speed: in order to decode the passage of time during Stimulus 1 for different stimulus speed values (Figure 4 and 6) we first aligned all neuronal activity to Stimulus 1 onset. For each neuron, we selected the same number of trials for each possible Stimulus 1 duration and Stimulus 1 speed. Half of the trials were randomly selected and used to calculate the tuning curve $\sigma(t)$ for each cell. The other half was used to calculate the number of spikes n measured in the interval Δt, separately for each Stimulus 1 speed. In this way we generated

three separated matrices of population neuronal activity, using trials in which three different *sp1* were presented. The matrix of all cells tuning curves and the matrices of measured neuronal activity for each *sp1* were used to calculate $P[t \mid population]$ from Equation 64 The MAP of the probability distribution $P[t \mid population]$ was taken as decoded time. Same procedure was done for Stimulus 2, a part that activity was aligned to Stimulus 2 onset, and trials were grouped according to *sp2* values.

In this way, $\sigma(t)$ is assumed to be independent to stimulus speed. By testing if the decoder is biased by stimulus speed, we test the hypothesis that the neuronal population is not encoding any information of stimulus speed in its neuronal activity.

3) Decoding of stimulus duration, for different trial correctness: in order to decode the passage of time during Stimulus 1 separately for correct vs incorrect trials (Figure 5) we first aligned all neuronal activity to Stimulus 1 onset. For each neuron, we selected the same number of trials for each possible Stimulus 1 duration. Half of correct trials were randomly selected and used to calculate the tuning curve $\sigma(t)$ for each cell. Then we generated two separated matrices of population neuronal activity depending on correctness, using the other half of correct trials and the incorrect ones. The matrix of all cells tuning curves and the matrices of measured neuronal activity for either correct or incorrect trials were used to calculate $P[t \mid population]$ from Equation 4. The MAP of the probability distribution $P[t \mid population]$ was taken as decoded time. Same procedure was done for Stimulus 2, a part that activity was aligned to Stimulus 2 onset.

4) Decoding of the passage of time during the entire trial: in order to decode the passage of time at different trial epochs (Figure 5) we first aligned all neuronal activity to each epoch onset. For each neuron, we selected the same number of trials for each possible Stimulus 1 and Stimulus 2 duration. Half of the trials were randomly selected and used to calculate the tuning curve $\sigma(t)$ for each cell, the other half was used to calculate the number of spikes n during the interval Δt. The matrix of all cells tuning curves and of measured neuronal activity were used to calculate $P[t \mid population\ ]$ from Equation 4. The expected value of the probability distribution $P[t \mid population\ ]$ was taken as decoded time, and was calculated as:

$$E(t|\ population\ ) = \int_0^T P[t \mid population\ ] \cdot t\ \cdot dt \qquad (5)$$

Where T is the total decoded time.

The error bar plotted in Figure 5 is the standard deviation of the distribution, calculated as:

$$SD(t|population) =$$

$$= \sqrt{\int_0^T (t - E(t|\ population))^2 \cdot P[t \mid population\ ]\ \cdot dt} \qquad (6)$$

The quality of decoding for each trial epoch was assessed by calculating the average SD values across all decoded time: the stimulus epoch was better

encoded by the striatal population compared to the delay period, but not to other trials epochs (Figure 5C).

All $P[t \mid population\,]$ estimations were done by averaging the results of a 50 times bootstrap procedure.

In Figure 4 and 6, to test if the decoded time was significantly higher for bigger speed values, a one-tailed Wilcoxon signed rank test between samples of decoded time for each possible pair of speed condition was done. No significant difference was found.

In Figure 5A, to test statistical significance of the difference in decoded time for correct and incorrect trials, a two-tailed Wilcoxon signed rank test between the samples of decoded time for the two conditions was done. No significant difference was found.

The predicted choices shown in Figure 3 were calculated for each *T1/T2* pairs and *sp1/sp2* pairs as follows:

First we assumed that the perceived value of *T1* and *T2* ($Y_1(T_1)\ and\ Y_2(T_2)$) is equal to the decoded time from the population state at the end of each stimulus. In order to extract the two perceived values, we first calculated the probability density functions $P[t_2 \mid population_{T1}\,]$ and $P[t_1 \mid population_{T2}\,]$ where $population_{T1}$ and $population_{T2}$ are the population states at the end of Stimulus 1 and Stimulus 2. We then fit a gaussian distribution to the two probability density functions (using gaussfit MATLAB function), so that for each stimulus we obtain the perceived value of *T1* and *T2* ($Y_1(T_1)\ and\ Y_2(T_2)$), which follow a normal gaussian distribution. We can now calculate:

$$P\big(Y_2(T_2) > Y_1(T_1)\big) = \int_{-\infty}^{+\infty} \int_{Y_1}^{+\infty} P(Y_2, Y_1)\mathrm{d}Y_2\,\mathrm{d}Y_1 = \frac{1}{2} + \frac{1}{2}\mathrm{erf}(d') \qquad (7)$$

$$d' = \frac{\mathrm{E}[Y_2(T_2)] - \mathrm{E}[Y_1(T_1)]}{\sqrt{2(\mathrm{Var}[Y_2(T_2)] + \mathrm{Var}[Y_1(T_1)])}} \qquad (8)$$

where $\mathrm{erf}(x)$ is the normal error function.

Predicted choices depicted in Figure 5B were calculated for each *T1/T2* pair, separately for correct and incorrect trials.

Simulations of reference memory task

The analyses shown in Figure 7, were done following different steps:

- First, we re-labeled the trials as correct or incorrect, as if the rat had to estimate if the duration of Stimulus 2 was longer or smaller than 334 ms, irrespectively of Stimulus 1 duration. When Stimulus 2 duration was equal to 334 ms , correctness was randomly assigned.

- Secondly, we generated the tuning curve $\sigma(t)$ for each cell, using the same number of correct trials for each of three Stimulus 2 durations (232,334,481 ms for duration rats and 161,334,694 ms for intensity rats). Then we generated two separated matrices of population neuronal activity depending on correctness, using either correct trials or the incorrect ones. Same number of trials was

selected for each duration and each matrix. The matrix of all cells tuning curves and the matrices of measured neuronal activity for either correct or incorrect trials were used to calculate $P[t \mid population\ ]$ from Equation 4, in the 500 ms following Stimulus 2 offset. The expected value of the probability distribution $P[t \mid population\ ]$ was taken as decoded time.

- For each time point we calculated the probability that decoded time was bigger for incorrect trials compared to correct trials, as shown in Equation 7.

- To assess if the decoded time for correct and incorrect trials were significantly different, we used a paired sample, one tailed Wilcoxon test.

Same analyses were done for Figure 8, by excluding neurons which showed any selectivity for rats' action, calculated from Equation 1, in any time window during the post stimulus delay. To assess the difference between the decoded time in the two populations, we:

- Calculated the difference between each decoded time point in incorrect and correct trials, for each Stimulus 2 duration.

- We then tested the hypothesis that this difference was bigger for the full neuronal population, compared to the one without action selective neurons, using a paired sample, one tailed Wilcoxon test

Same analyses were done for Supplementary Figure 1 a part that the labeling of correctness was done according to Stimulus 1 duration, and that the decoder was trained to decode the 500 ms time window after Stimulus 1 offset, instead of Stimulus 2.

Supplementary figures

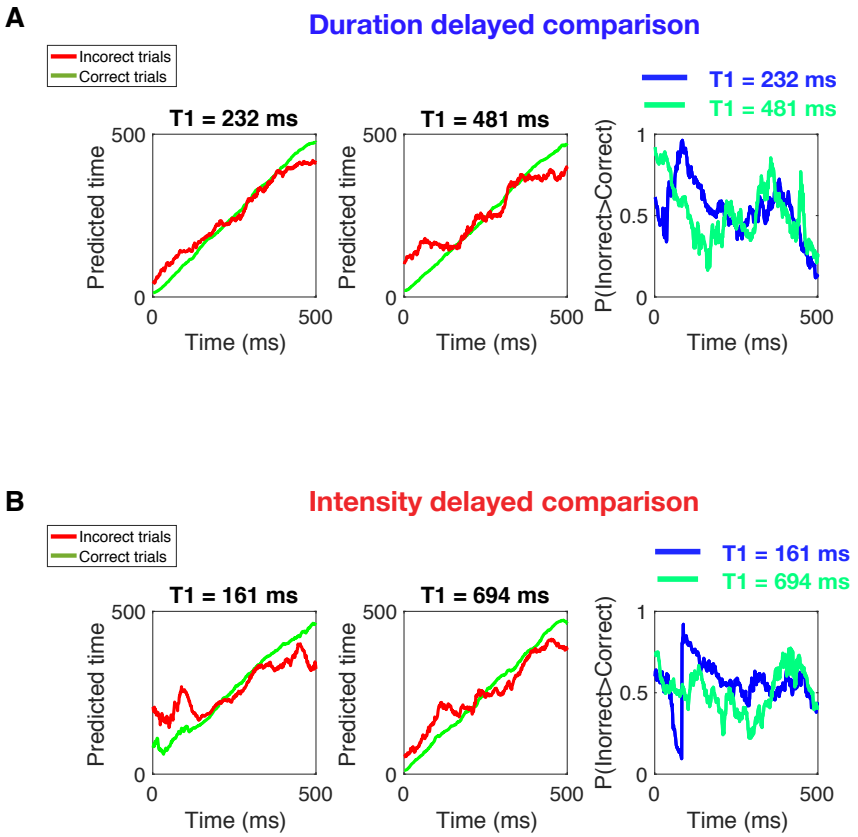

Supplementary Figure 1. Decoded time after Stimulus 1, from correct and incorrect trials, using a duration reference memory rule.
A) Left panel and middle panel: decoded time during post stimulus delay after Stimulus 1 offset, using correct and incorrect trials, when correctness is labeled as if the rat is classifying Stimulus 1 duration independently of Stimulus 2. The decoder does not overestimates short *T1* and underestimates long *T1* (one-tailed Wilcoxon signed rank test), when tested with incorrect trials. Right panel shows the probability that the decoded time in incorrect trials is equal than correct trials, for the two possible *T1* values.
B) Same as A, but using DLS neurons recorded in rats doing an intensity estimation trials.

Appendix

Concluding comments – a look to the past and to the future

In 1840 Muller observed that electrical stimulation of a sensory organ produced a percept specific to the stimulated organ, and thus enunciated the "Law of specific nerve energies" (92). An electrical pulse could be heard, seen, touched, smelled or tasted, according to which nerve is stimulated:

"Sensation is not the conduction of a quality or state of external bodies to consciousness, but the conduction of a quality or state of our nerves to consciousness, excited by an external cause"

Muller laid the foundation for nearly two centuries of investigation of the neural code for perception, stating that our perceptual experience of stimuli is dependent on the structure in the brain to which the nerve carries its message. This idea was confined to the sensations across the five Aristotelian sensory organs, not addressing the different sensations that can be elicited within each sensory system. The idea that different qualities of perception within the same sensory system were dependent on the stimulation of modality-specific fibers, was proposed by Muller's student, Helmholtz, who proposed that different nerves in the visual system were sensitive to three specific colors (red, green, blue-violet) (93), and that the cochlea was made of a graded series of resonators, each tuned to a different frequency (94).

Proof or refutation of such elegant notions required the recording of single nerve fiber activity, first accomplished in the somatosensory system by Adrian. He described the

Pacinian corpuscle's sensitivity to mechanical stimulation, but not to temperature changes (95). Moreover, Adrian work expanded Muller's and Helmholtz's theories, by showing that each nerve responds to its own "preferred stimulus" using a stereotyped language: a discharge of action potentials, whose rate changes with the intensity of stimulation and adapts over time (96). Later on, Mouncastle in monkeys (97) and then Vallbo in humans (98), characterized the specificity of individual cutaneous receptors.

However, not all the possible perceptual experiences elicited by the somatosensory system can be directly mapped to a single fiber type. The idea that each tactile percept is mapped onto a specific receptor type still survives for pain, where the activation of nociceptors sensitive to tissue-damaging events generates a specific perceptual phenomenon (99). The same cannot be said for more complex percepts such as texture perception. When presented with such a complex stimulus, the percept elicited is generated through the convergence of the activity from multiple fibers types (namely rapidly adapting (RA), slowly adapting (SA) and Pacinian (PC) fibers, (100)) and the multiplexing of multiple neural codes within the same sensory pathway such as spiking rate and the temporal pattern of spikes (101). The convergence of inputs from different afferent types and of different neural codes, expands the possible percepts that can be generated from the limited amounts of receptors present in the sensory system, at the cost of increasing ambiguity in the neuronal coding of the stimulus (102). If no "one to one" mapping between fiber types and percepts exist, each fiber type becomes involved in the representation of multiple stimulus features, making each perceptual representation of the stimulus dependent on more than one of its physical characteristics. An example of this ambiguity was recently showed by Delhaye et al (103). In this work a perceptual confound between the perceived speed of a texture

scanned across the skin, and the texture identity was found. The texture properties systematically biased the perceived speed. The firing rate of the Pacinian nerve fibers were found to encode both the speed and the texture identity, generating the ambiguity of neuronal coding discussed above. Another clear example was found in rats, which were shown to be insensitive to the amplitude A and the frequency f of sinusoidal vibrations presented to their whiskers. Instead, rats always extract the product of the two elemental features of the vibration, Af (104). Neurons in rat barrel cortex encode the Af values of each vibrations within their firing rate (26), revealing another ambiguity in the neural coding of tactile perception.

This uncertainty principle highlights a fundamental characteristic of our sensory systems, and helps us understand the neuronal coding problem (102).

One of the most ambiguous percepts that our sensory system can generate is the perception of the passage of time. This is due to two reasons: the first one is that no specific receptors exist for the sensory representation of time – it is a sense without sensory receptors. This implies that, either a neural clock independent of any sensory input exists in the brain, or else the perception of the passage of time relies on the activity of sensory receptors sensitive to other stimulus features. In that case, time is an inherent property of every neural code: for example, rate coding is defined as number of spikes per units of time, or temporal coding relies on the timing at which each spike takes place. This means that time could be reliably decoded from any stream of neuronal activity, but which exact neural code the brain uses to sense time is unknown.

We believe that the work of this thesis reveals another zone of ambiguity of our perceptual systems; we suggest that working out the details of perceptual uncertainty ("longer feels stronger, stronger feels longer") constitutes, ironically, another step towards the understanding of its neuronal codes. The dependence of perceived intensity of a vibration on its duration, and the symmetrical bias of stimulus intensity on its perceive duration, reveals that the neuronal coding of these two percepts is ambiguously dependent on both stimulus features. This is particularly important for the comprehension of the neuronal code of time: the dependency of duration perception on stimulus intensity indicates that the neural representation of duration should depend on the sensory input coming through the neuronal pathways which code the vibration speed. In fact, a separate project in our laboratory has manipulated rats' sense of elapsed time through direct optogenetic manipulation of vibrissal sensory cortex. Moreover, the fact that both humans and rats show the same perceptual biases, suggests that the phenomenon reveals a fundamental limit present within the physiology of the somatosensory system. In Chapter I we showed that this perceptual uncertainty likely arises from a leaky integration of instantaneous speed values, integrated with different time constants according to the perceptual feature sensed by the subject. It is likely that both percepts are generated from a leaky integration of somatosensory cortex activity, computed by a downstream neural population.

The mixed representation of the speed and the duration of vibrations appears to be present in the memory of recent stimuli as well, as showed in Chapter II. Priors, however, are formed by perceived stimuli, not by the mere physical features of stimuli.

Chapter III revealed that the striatum in rats, which is believed by many authors to be the neuronal circuit that generates time perception, encodes the passage of time without any bias of stimulus intensity, making it unlikely to be the neural code used by the animal to generate the percept of stimulus duration. In the coming months, parallel analyses will be done in neuronal populations recorded from the whisker motor cortex (wM1) of rats trained in the same duration discrimination task. This area showed to be involved in the encoding of the perception of the intensity of vibrations (4) and may be involved in the extraction of both percepts.

References

1. Matthews WB *From Neuron to Brain* (Sinauer Associates Sunderland, MA) doi:10.1136/bmj.2.6045.1202-a (1976).
2. Gibbon J, Church RM, Meck WH Scalar Timing in Memory. *Ann N Y Acad Sci* **423**, 52–77 (1984).
3. Fassihi A, Akrami A, Esmaeili V, Diamond ME Tactile perception and working memory in rats and humans. *Proc Natl Acad Sci* doi:10.1073/pnas.1315171111 (2014).
4. Fassihi A, Akrami A, Pulecchi F, Schönfelder V, Diamond ME Transformation of Perception from Sensory to Motor Cortex. *Curr Biol* **27**, 1585-1596.e6 (2017).
5. Bueti D, Bahrami B, Walsh V Sensory and association cortex in time perception. *J Cogn Neurosci* **20**, 1054–1062 (2008).
6. Bueti D The Sensory Representation of Time. *Front Integr Neurosci* **5**, 34 (2011).
7. Buhusi C V., Meck WH What makes us tick? Functional and neural mechanisms of interval timing. *Nat Rev Neurosci* **6**, 755–765 (2005).
8. Merchant H, Harrington DL, Meck WH Neural Basis of the Perception and Estimation of Time. *Annu Rev Neurosci* **36**, 313–336 (2013).
9. Fassihi A, Akrami A, Esmaeili V, Diamond ME Tactile perception and working memory in rats and humans. *Proc Natl Acad Sci* **111**, 2331–2336 (2014).
10. Romo R, Salinas E Cognitive neuroscience: Flutter Discrimination: Neural codes, perception, memory and decision making. *Nat Rev Neurosci* **4**, 203–218 (2003).
11. Mountcastle VB, Talbot WH, Sakata H, Hyvärinen J Cortical neuronal mechanisms in flutter-vibration studied in unanesthetized monkeys. Neuronal periodicity and frequency discrimination. *J Neurophysiol* **32**, 452–484 (1969).
12. Usher M, McClelland JL The time course of perceptual choice: The leaky, competing accumulator model. *Psychol Rev* **108**, 550–592 (2001).
13. Stevens SS Tactile vibration: Dynamics of sensory intensity. *J Exp Psychol* **57**, 210–218 (1959).
14. Kanai R, Lloyd H, Bueti D, Walsh V Modality-independent role of the primary auditory cortex in time estimation. *Exp Brain Res* **209**, 465–471 (2011).
15. Luna R, Hernández A, Brody CD, Romo R Neural codes for perceptual discrimination in primary somatosensory cortex. *Nat Neurosci* **8**, 1210–1219 (2005).
16. Stévens JC, Hall JW Brightness and loudness as functions of stimulus duration. *Percept Psychophys* **1**, 319–327 (1966).
17. Ekman G, Berglund B, Berglund U Loudness As a Function of the Duration of Auditory Stimulation. *Scand J Psychol* **7**, 201–208 (1966).
18. O'Connor KN, Barruel P, Hajalilou R, Sutter ML Auditory temporal integration in the rhesus macaque (Macaca mulatta) . *J Acoust Soc Am* **106**, 954–965 (2002).
19. Ekman G, Frankenhaeuser M, Berglund B, Waszak M Apparent Duration as a Function of Intensity of Vibrotactile Stimulation. *Percept Mot Skills* **28**, 151–156 (2011).
20. Berglund B, Berglund U, Ekman G, Frankehaeuser M the Influence of

Auditory Stimulus Intensity on Apparent Duration. *Scand J Psychol* **10**, 21–26 (1969).
21. Goldstone S, Lhamon WT, Sechzer J Light intensity and judged duration. *Bull Psychon Soc* **12**, 83–84 (1978).
22. Bloch A-M Experiences sur la vision. *Comptes Rendus la Soc Biol* **37**, 493 (1885).
23. Zwislocki J Theory of Temporal Auditory Summation. *J Acoust Soc Am* **32**, 1046–1060 (2005).
24. Treisman M Temporal discrimination and the indifference interval. Implications for a model of the "internal clock". *Psychol Monogr* **77**, 1–31 (1963).
25. Matthews WJ, Stewart N, Wearden JH Stimulus Intensity and the Perception of Duration. *J Exp Psychol Hum Percept Perform* **37**, 303–313 (2011).
26. Arabzadeh E, Petersen RS, Diamond ME Encoding of whisker vibration by rat barrel cortex neurons: implications for texture discrimination. *J Neurosci* (2003).
27. Arabzadeh E Whisker Vibration Information Carried by Rat Barrel Cortex Neurons. *J Neurosci* **24**, 6011–6020 (2004).
28. Protopapa F, et al. Research article chronotopic maps in human supplementary motor area. *PLoS Biol* **17**, doi:10.1371/journal.pbio.3000026 (2019).
29. Murray JD, et al. A hierarchy of intrinsic timescales across primate cortex. *Nat Neurosci* **17**, 1661–1663 (2014).
30. McGuire LM, et al. Short Time-Scale Sensory Coding in S1 during Discrimination of Whisker Vibrotactile Sequences. *PLoS Biol* **14**, doi:10.1371/journal.pbio.1002549 (2016).
31. Simen P, Balci F, deSouza L, Cohen JD, Holmes P A Model of Interval Timing by Neural Integration. *J Neurosci* **31**, 9238–9253 (2011).
32. Sadeghi NG, Pariyadath V, Apte S, Eagleman DM, Cook EP Neural correlates of subsecond time distortion in the middle temporal area of visual cortex. *J Cogn Neurosci* **23**, 3829–3840 (2011).
33. Karmarkar UR, Buonomano D V. Timing in the Absence of Clocks: Encoding Time in Neural Network States. *Neuron* **53**, 427–438 (2007).
34. Matell MS, Meck WH Cortico-striatal circuits and interval timing: Coincidence detection of oscillatory processes. *Cogn Brain Res* **21**, 139–170 (2004).
35. Buonomano D V., Maass W State-dependent computations: Spatiotemporal processing in cortical networks. *Nat Rev Neurosci* **10**, 113–125 (2009).
36. Wang X-J Probabilistic decision making by slow reverberation in cortical circuits. *Neuron* (2002).
37. Machens CK, Romo R, Brody CD Flexible control of mutual inhibition: A neural model of two-interval discrimination. *Science (80-)* **307**, 1121–1124 (2005).
38. Wong K-F A Recurrent Network Mechanism of Time Integration in Perceptual Decisions. *J Neurosci* **26**, 1314–1328 (2006).
39. Deco G, Rolls ET Decision-making and Weber's law: A neurophysiological model. *Eur J Neurosci* **24**, 901–916 (2006).
40. Shadlen MN, Newsome WT Neural Basis of a Perceptual Decision in the Parietal Cortex (Area LIP) of the Rhesus Monkey. *J Neurophysiol* **86**, 1916–1936 (2017).
41. Hernández A, Zainos A, Romo R Temporal evolution of a decision-making process in medial premotor cortex. *Neuron* **33**, 959–972 (2002).

42. Kim JN, Shadlen MN Neural correlates of a decision in the dorsolateral prefrontal cortex of the macaque. *Nat Neurosci* **2**, 176–185 (1999).
43. Ding L, Gold JI Caudate encodes multiple computations for perceptual decisions. *J Neurosci* **30**, 15747–15759 (2010).
44. Yartsev MM, Hanks TD, Yoon AM, Brody CD Causal contribution and dynamical encoding in the striatum during evidence accumulation. *Elife* **7**, doi:10.7554/eLife.34929 (2018).
45. Furman M, Wang XJ Similarity Effect and Optimal Control of Multiple-Choice Decision Making. *Neuron* **60**, 1153–1168 (2008).
46. Paz L, Insabato A, Zylberberg A, Deco G, Sigman M Confidence through consensus: A neural mechanism for uncertainty monitoring. *Sci Rep* **6**, doi:10.1038/srep21830 (2016).
47. Carandini M, Churchland AK Probing perceptual decisions in rodents. *Nat Neurosci* **16**, 824–831 (2013).
48. Salvatier J, Wiecki T V., Fonnesbeck C Probabilistic programming in Python using PyMC3. *PeerJ Comput Sci* **2**, e55 (2016).
49. Watanabe S A widely applicable Bayesian information criterion. *J Mach Learn Res* **14**, 867–897 (2013).
50. Hansen N, Auger A Principled design of continuous stochastic search: From theory to practice. *Natural Computing Series*, pp 145–180. (2014).
51. Raviv O, Ahissar M, Loewenstein Y How Recent History Affects Perception: The Normative Approach and Its Heuristic Approximation. *PLoS Comput Biol* **8**, doi:10.1371/journal.pcbi.1002731 (2012).
52. Fischer J, Whitney D Serial dependence in visual perception. *Nat Neurosci* **17**, 738–743 (2014).
53. Fritsche M, Mostert P, de Lange FP Opposite Effects of Recent History on Perception and Decision. *Curr Biol* **27**, 590–595 (2017).
54. Dragoi V, Sharma J, Sur M Adaptation-induced plasticity of orientation tuning in adult visual cortex. *Neuron* **28**, 287–298 (2000).
55. Jin DZ, Dragoi V, Sur M, Seung HS Tilt aftereffect and adaptation-induced changes in orientation tuning in visual cortex. *J Neurophysiol* **94**, 4038–4050 (2005).
56. St. John-Saaltink E, Kok P, Lau HC, De Lange FP Serial dependence in perceptual decisions is reflected in activity patterns in primary visual cortex. *J Neurosci* **36**, 6186–6192 (2016).
57. Schwiedrzik CM, et al. Untangling perceptual memory: Hysteresis and adaptation map into separate cortical networks. *Cereb Cortex* **24**, 1152–1164 (2014).
58. Hollingworth HL The Central Tendency of Judgment. *J Philos Psychol Sci Methods* **7**, 461 (1910).
59. Hahn JF Vibrotactile adaptation and recovery measured by two methods. *J Exp Psychol* **71**, 655–658 (1966).
60. Lederman SJ, Loomis JM, Williams DA The role of vibration in the tactual perception of roughness. *Percept Psychophys* **32**, 109–116 (1982).
61. Roseboom W Serial dependence in timing perception. *J Exp Psychol Hum Percept Perform* **45**, 100–110 (2019).
62. Wiener M, Thompson JC, Branch Coslett H Continuous carryover of temporal context dissociates response bias from perceptual influence for duration. *PLoS One* **9**, doi:10.1371/journal.pone.0100803 (2014).
63. Maunsell JHR, Treue S Feature-based attention in visual cortex. *Trends*

Neurosci **29**, 317–322 (2006).
64. Kohn A Visual adaptation: Physiology, mechanisms, and functional benefits. *J Neurophysiol* **97**, 3155–3164 (2007).
65. Pascucci D, et al. Laws of concatenated perception: Vision goes for novelty, decisions for perseverance. *PLoS Biol* **17**, doi:10.1371/journal.pbio.3000144 (2019).
66. Akrami A, Kopec CD, Diamond ME, Brody CD Posterior parietal cortex represents sensory history and mediates its effects on behaviour. *Nature* **554**, 368–372 (2018).
67. Petzschner FH, Glasauer S, Stephan KE A Bayesian perspective on magnitude estimation. *Trends Cogn Sci* **19**, 285–293 (2015).
68. Petzschner FH, Glasauer S Iterative Bayesian estimation as an explanation for range and regression effects: A study on human path integration. *J Neurosci* **31**, 17220–17229 (2011).
69. Martin B, Wiener M, Van Wassenhove V A Bayesian Perspective on Accumulation in the Magnitude System. *Sci Rep* **7**, doi:10.1038/s41598-017-00680-0 (2017).
70. Jin DZ, Fujii N, Graybiel AM Neural representation of time in cortico-basal ganglia circuits. *Proc Natl Acad Sci U S A* **106**, 19156–19161 (2009).
71. Xu M, Zhang SY, Dan Y, Poo MM Representation of interval timing by temporally scalable firing patterns in rat prefrontal cortex. *Proc Natl Acad Sci U S A* **111**, 480–485 (2014).
72. Kim J, Ghim JW, Lee JH, Jung MW Neural correlates of interval timing in rodent prefrontal cortex. *J Neurosci* **33**, 13834–13847 (2013).
73. Merchant H, Zarco W, Pérez O, Prado L, Bartolo R Measuring time with different neural chronometers during a synchronization-continuation task. *Proc Natl Acad Sci U S A* **108**, 19784–19789 (2011).
74. Mita A, Mushiake H, Shima K, Matsuzaka Y, Tanji J Interval time coding by neurons in the presupplementary and supplementary motor areas. *Nat Neurosci* **12**, 502–507 (2009).
75. Remington ED, Narain D, Hosseini EA, Jazayeri M Flexible Sensorimotor Computations through Rapid Reconfiguration of Cortical Dynamics. *Neuron* **98**, 1005-1019.e5 (2018).
76. Leon MI, Shadlen MN Representation of time by neurons in the posterior parietal cortex of the Macaque. *Neuron* **38**, 317–327 (2003).
77. Tsao A, et al. Integrating time from experience in the lateral entorhinal cortex. *Nature* **561**, 57–62 (2018).
78. MacDonald CJ, Lepage KQ, Eden UT, Eichenbaum H Hippocampal "time cells" bridge the gap in memory for discontiguous events. *Neuron* **71**, 737–749 (2011).
79. Ashmore RC, Sommer MA Delay activity of saccade-related neurons in the caudal dentate nucleus of the macaque cerebellum. *J Neurophysiol* **109**, 2129–2144 (2013).
80. Gouvêa TS, et al. Striatal dynamics explain duration judgments. *Elife* **4**, doi:10.7554/eLife.11386 (2015).
81. Mello GBM, Soares S, Paton JJ A scalable population code for time in the striatum. *Curr Biol* **25**, 1113–1122 (2015).
82. Soares S, Atallah B V., Paton JJ Midbrain dopamine neurons control judgment of time. *Science (80-)* **354**, 1273–1277 (2016).
83. Bakhurin KI, et al. Differential encoding of time by prefrontal and striatal

network dynamics. *J Neurosci* **37**, 854–870 (2017).
84. Alloway KD, Smith JB, Mowery TM, Watson GDR Sensory processing in the dorsolateral striatum: The contribution of thalamostriatal pathways. *Front Syst Neurosci* **11**, doi:10.3389/fnsys.2017.00053 (2017).
85. Alloway KD, Crist J, Mutic JJ, Roy SA Corticostriatal projections from rat barrel cortrex have an anisotropic organization that correlates with vibrissal whisking behavior. *J Neurosci* **19**, 10908–10922 (1999).
86. Gage GJ, Stoetzner CR, Wiltschko AB, Berke JD Selective Activation of Striatal Fast-Spiking Interneurons during Choice Execution. *Neuron* **67**, 466–479 (2010).
87. Sanger TD Probability density estimation for the interpretation of neural population codes. *J Neurophysiol* **76**, 2790–2793 (1996).
88. Wang J, Narain D, Hosseini EA, Jazayeri M Flexible timing by temporal scaling of cortical responses. *Nat Neurosci* **21**, 102–112 (2018).
89. Jin X, Tecuapetla F, Costa RM Basal ganglia subcircuits distinctively encode the parsing and concatenation of action sequences. *Nat Neurosci* **17**, 423–430 (2014).
90. Kermadi I, Joseph JP Activity in the caudate nucleus of monkey during spatial sequencing. *J Neurophysiol* **74**, 911–933 (1995).
91. Quiroga RQ, Nadasdy Z, Ben-Shaul Y Unsupervised spike detection and sorting with wavelets and superparamagnetic clustering. *Neural Comput* **16**, 1661–1687 (2004).
92. H. CW *Elements of Physiology* (Lea and Blanchard) doi:10.1126/science.26.670.587-a (1907).
93. Helmholtz, von H *Handbuch der physiologischen optik, vol. 3* (Voss) (1860).
94. von Helmholtz H *Die Lehre von den Tonempfindungen als Physiologische Grundlage für die Theorie der Musik* (F. Vieweg und Sohn) doi:10.1007/978-3-663-18653-3 (1913).
95. Adrian ED, Umrath K The impulse discharge from the pacinian corpuscle. *J Physiol* **68**, 139–154 (1929).
96. Adrian ED The basis of sensation: Some recent studies of olfaction. *Br Med J* **1**, 287–290 (1954).
97. WERNER G, MOUNTCASTLE VB Neural Activity in Mechanoreceptive Cutaneous Afferents: Stimulus-Response Relations, Weber Functions, and Information Transmission. *J Neurophysiol* **28**, 359–397 (1965).
98. Vallbo AB, Johansson RS Properties of cutaneous mechanoreceptors in the human hand related to touch sensation. *Hum Neurobiol* **3**, 3–14 (1984).
99. Craig AD (Bud) P AIN M ECHANISMS : Labeled Lines Versus Convergence in Central Processing . *Annu Rev Neurosci* **26**, 1–30 (2003).
100. Weber AI, et al. Spatial and temporal codes mediate the tactile perception of natural textures. *Proc Natl Acad Sci U S A* doi:10.1073/pnas.1305509110 (2013).
101. Zuo Y, et al. Complementary contributions of spike timing and spike rate to perceptual decisions in rat S1 and S2 cortex. *Curr Biol* **25**, 357–363 (2015).
102. Diamond ME Perceptual uncertainty. *PLOS Biol* **17**, e3000430 (2019).
103. Delhaye BP, O'Donnell MK, Lieber JD, McLellan KR, Bensmaia SJ Feeling fooled: Texture contaminates the neural code for tactile speed. *PLOS Biol* **17**, e3000431 (2019).
104. Adibi M, Diamond ME, Arabzadeh E Behavioral study of whisker-mediated vibration sensation in rats. *Proc Natl Acad Sci U S A* **109**, 971–976 (2012).